

Development and Performance of a Miniature, Low Cost Mass Spectrometer

by

Brian D. Hemond

B.S. Massachusetts Institute of Technology (2004)
M.Eng. Massachusetts Institute of Technology (2006)

Submitted to the Department of Mechanical Engineering
in partial fulfillment of the requirements for the degree of

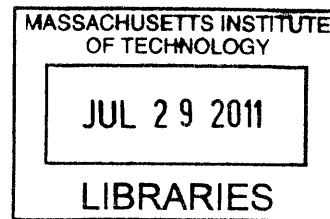
Doctor of Philosophy in Mechanical Engineering

at the

MASSACHUSETTS INSTITUTE OF TECHNOLOGY

June 2011

© Massachusetts Institute of Technology 2011. All rights reserved.



ARCHIVES

Author
Department of Mechanical Engineering
Feb 14, 2011

Certified by
Ian W. Hunter
Hatsopolous Professor of Mechanical Engineering
Thesis Supervisor

Accepted by
David Hardt
Chairman, Department Committee on Graduate Theses

Development and Performance of a Miniature, Low Cost Mass Spectrometer

by

Brian D. Hemond

Submitted to the Department of Mechanical Engineering
on Feb 14, 2011, in partial fulfillment of the
requirements for the degree of
Doctor of Philosophy in Mechanical Engineering

Abstract

A miniature, low cost mass spectrometer has been developed that is capable of unit resolution over a mass range of 10 to 50 AMU. The design of the mass spectrometer incorporates several new features that enhance the performance of the design over comparable instruments. An efficient ion source allows a relatively low power consumption without sacrificing resolution. Variable geometry mechanical filters allow for variable resolution. An onboard ion pump removes the need for an external pumping source. An onboard digital controller allows a large degree of flexibility over the operation of the mass spectrometer while eliminating the need for high voltage electrical feedthroughs. The miniature mass spectrometer is sensitive to fractions of a percentage of inlet gas, and formatted mass spectra are returned digitally to a laptop.

Thesis Supervisor: Ian W. Hunter

Title: Hatsopolous Professor of Mechanical Engineering

Acknowledgments

The author is deeply indebted to his thesis advisor, Professor Ian W. Hunter, for the opportunity and resources to perform innovative research in one of the best laboratories at MIT. The guidance of the author's thesis committee, also including Professors Steven B. Leeb, and Derek Rowell, has been invaluable.

Many others have made important marks on the thesis, in the form of new directions and refinements on old ideas. Dr. Jim Bales at the Edgerton Center and Dr. Barbara Hughey of the 2.671 Undergraduate Teaching Lab are two of these such persons.

The author would like to thank his parents, Professor Harold Hemond, and Dr. Carol Thomson, for their unending support, ideas, and the occasional warm meal.

THIS PAGE INTENTIONALLY LEFT BLANK

Contents

1	Introduction	15
1.1	Motivation	15
1.2	Principles	17
1.3	Mass Spectrometer Types	18
1.3.1	Mass Analyzers	18
1.3.2	Ion Sources	19
1.3.3	Detectors	19
2	Design	21
2.1	Design Overview	21
2.2	Mass Spectrometer Design	24
2.2.1	Vacuum System Design	24
2.2.2	Mass Analyzer Design	26
2.2.3	Ion Source Design	30
2.2.4	Sample Jet	35
2.2.5	Detector Design	36
2.2.6	High Vacuum Pump Design	37
2.2.7	Inlet	38
3	Simulation	41
3.0.8	Dimensioning	41
3.0.9	Ion Flight Simulations	44
3.0.10	Electron Source Simulations	48

4	Construction	51
4.1	Substrate	51
4.2	PCB Design and Construction	53
4.3	Electrodes	55
4.3.1	Mass Analyzer	56
4.3.2	Electrostatic Lens Electrodes	57
4.3.3	Electron Beam Electrodes	59
4.3.4	Electrode Finishing	59
4.3.5	Magnet	60
4.3.6	Ion Pump	61
4.4	Assembly	61
5	Electronics	69
5.1	Power supply	69
5.2	Ion optics drivers	70
5.3	Electrometer	71
5.4	Degas Heater	72
5.5	Digital controller	72
5.6	Control Software	73
5.6.1	Boot	75
5.6.2	Standby	75
5.6.3	Idle	75
5.6.4	Sweep	75
5.7	Known Issues	76
6	Testing	77
6.1	Power and Control Systems	77
6.2	Electron Beam	78
6.3	Degas Heater	79
6.4	Lens Linearization	81
6.5	Ion Pump	83

6.6	Mass Spectra	83
6.7	Introduction of New Species	90
6.8	Ion Source Modulation	90
6.9	Results	95
7	Conclusions	97
7.1	Further Work	98
A	Controller Schematic	99

THIS PAGE INTENTIONALLY LEFT BLANK

List of Figures

2-1	A CAD model of the magnet yoke.	28
2-2	A plot of ion source potential verses ion mass.	30
2-3	A drawing of the optics used in the ion source.	36
2-4	A cutaway drawing of the direct-to-atmosphere membrane inlet.	39
3-1	A simulation of the ion gun with indications of where the elements referred to in the text are placed.	43
3-2	A SIMION simulation of a carbon dioxide molecules transiting the miniature mass spectrometer.	45
3-3	Detailed view of the ion source and first lens.	46
3-4	Isometric view of the potential energy distribution in the mass spectrometer ion source and analyzer. The curvature of the green potential energy surface indicates the effect of the electrostatic lenses. The vertical dimension is potential energy, while the two horizontal dimensions are the plan form of the mass spectrometer.	47
3-5	Side cutaway view of the cylindrical Pierce diode ion source. Electrons are emitted from the surface of a filament in a line. A cathode potential electrode surrounds the filament to screen it from the vacuum chamber. The grid and anode electrodes are shown at the right edge of the simulation.	49
3-6	Side cutaway view of the cylindrical Pierce diode ion source, with the grid biased such as to inhibit electron emission.	50

4-1	A CAD layout of the printed circuit board substrate that underlies the whole mass spectrometer.	54
4-2	A CAD layout of the whole mass spectrometer.	55
4-3	A CAD model of the mass analyzer electrode, with the slits mounted on flexures.	58
4-4	(left) Electrodes are cut from stainless steel plate by wire EDM. (right) Electrodes are etched in nitric acid to remove the oxide layer.	60
4-5	A CAD model of the anode for the miniature ion pump.	62
4-6	A photograph of the completed mass spectrometer, with top cover and magnet yoke removed.	63
4-7	A photograph of the entrance slit to the mass analyzer, showing how it may be adjusted.	64
4-8	A photograph of the completed mass spectrometer, attached to the ConFlat flange used for testing.	66
4-9	A of the vacuum chamber used in the development of the mass spectrometer. The ion gauge is on the left and the turbopump at the bottom.	67
5-1	A block diagram of the digital controller for the mass spectrometer.	74
6-1	A graph of chamber pressure verses time, with the heater transitions indicated.	80
6-2	A series of thermal images taken at 0, 10, 20, 60, 300, and 600 s after the heater is activated. Thermal range is 30 ° C (black) to 60 ° C (white).	81
6-3	A graph of the microprocessor's command voltage verses the actual output of each lens driver.	82
6-4	(top) A graph of the system pressure, ion pump voltage and ion pump current.	84

6-5	A graph of the system pressure, ion pump voltage and ion pump current, in the minutes following segmentation of the vacuum system. Note that the system pressure remained relatively constant at 8×10^{-4} Pa [6×10^{-6} torr], but the pump failed because the power supply voltage collapsed. The supply could provide only 3 W.	85
6-6	A photograph of the plates of the disassembled ion pump. Colored deposits are likely chromium from the stainless steel anode.	86
6-7	A mass spectrograph captured by an early variant of the miniature mass spectrometer prototype.	88
6-8	A mass spectrograph of air captured by the instrument described in this thesis.	89
6-9	A mass spectrograph indicating the value of capturing and using a larger fraction of the ions generated by the electron beam. The signal displayed in the blue curve, in which the electrostatic lenses are active, is nearly an order of magnitude higher than the red curve, in which the lenses were disabled.	91
6-10	A mass spectrograph indicating the effectiveness of narrowing the slits that filter the ion beam. Peaks such as m/z 27 and 26 are invisible with wider slits, as shown in the blue curve, but readily visible in the red curve, with narrow slits.	92
6-11	A mass spectrograph showing the detection of a new species, nitrous oxide or N_2O , and its fragmentary component NO.	93
6-12	A mass spectrum indicating the usefulness of a modulatable grid. In this spectrum, the mass spectrometer's ion source grid was used to generate a trace that could be subtracted from the signal to remove the electrometer offset and drift.	94

THIS PAGE INTENTIONALLY LEFT BLANK

List of Tables

6.1	A table of mass spectrometer supply current in different modes of operation.	78
6.2	A table of trap current as a function of filament voltage.	79

THIS PAGE INTENTIONALLY LEFT BLANK

Chapter 1

Introduction

1.1 Motivation

Mass spectrometry is one of the leading chemical analysis tools. A mass spectrometer, often used as a detector in conjunction with another instrument (e.g., a gas chromatograph), is capable of determining the relative abundances of the chemical species present in a gaseous sample by separating the species by atomic mass.

Mass spectrometry is widely used across many disciplines. Mass spectrometers have been sent aboard unmanned spacecraft; both of the Viking landers carried gas chromatograph/mass spectrometer (GCMS) packages [1], and the Cassini-Huygens probe dropped into Titan's atmosphere carried a GCMS as well [2]. Mass spectrometers are heavily used in the biological sciences; they are one of the commonly used methods of determining protein structure and sequence.

In the medical field of pharmacokinetics, mass spectrometry has been used to track extremely small quantities of drugs through the human body [3].

Mass spectrometers have been designed for chemical and biological defense; the Block II CBMS (chemical biological mass spectrometer) was designed to be a portable, vehicle mounted instrument capable of detecting chemical and biological threats (e.g. nerve agents, bacteria) in the field [4]. More recently, mass spectrometers have been carried aboard unmanned submersibles to aid in the tracking of hydrocarbons released by the Macondo oil well failure in the Gulf of Mexico on April 20, 2010 [5].

Many other fields have employed mass spectrometry as well. As early as 1976 a mass spectrometer was used to continuously analyze the respired gases of patients on ventilators in intensive care for potentially dangerous complications [6]. For various reasons, probably including both the size and cost of the mass spectrometer, this technique has not been widely adopted despite its obvious benefits.

Truly, the mass spectrometer is an extremely versatile instrument, but it is not without some drawbacks. Mass spectrometers are generally large, complex, expensive instruments requiring a substantial amount of electrical power for operation. Progress has been made on the size front, a pair of small instruments, the Mini 10 and Mini 11 [7] developed by Purdue University exist, and small analyzers such as the quadrupole by Microsaic Systems [8] have been built.

To date, none of these instruments incorporate small size, low power consumption, and minimal cost. The applications for such an instrument are wide and varied. Such instruments could be deployed in large quantity to blanket wide areas for air or water quality monitoring, installed in industrial exhaust stacks for combustion process feedback control, or attached to hospital ventilators or used as first response tools in emergency rooms.

However, simply addressing a subset of the issues involved in producing such an instrument, while potentially useful, fails to address the need. A miniature mass spectrometer design must address all of the issues, simultaneously, to be of any value beyond academic. These issues are, in approximate order of importance:

Size: The design must be small enough to be handheld.

Power: The design must be capable of running in remote usage on minimal power for a useful length of time.

Cost and Manufacturability: The design must be inexpensive enough to build and assemble such that it can be widely deployed.

Developing a mass spectrometer that addresses these three issues is the primary objective of this thesis.

1.2 Principles

Many different implementations of mass spectrometers exist, and the configuration often depends on the intended application. Generally, however, they consist of the same basic functional blocks: an inlet, an ion source, a mass analyzer, a detector, and a vacuum system. Samples entering the inlet are ionized, usually by bombardment with an electron beam, then separated by mass using one or more electric and/or magnetic fields, then analyzed for relative abundance.

Ultimately, all of the implementations of the mass spectrometer produce a graph relating the atomic mass-to-charge (m/z) ratios of the components of the ionized sample to the relative abundance of each component. For example, a mass spectrometer measuring a sample of atmosphere would find components at masses 28, 32, 40, and 44, and possibly others depending on the sensitivity of the instrument. These masses correspond to nitrogen, oxygen, argon, and carbon dioxide. The mass spectrometer output will show the highest signal strength for mass 28, nitrogen, which comprises 70% of atmospheric gas, followed by about 1/3 the signal strength of the nitrogen peak for oxygen, at 32 (22% of the atmosphere), and lower signal strengths still for argon and carbon dioxide.

Mass spectrometers are generally designed for specific mass ranges and resolutions, depending on the application. Mass ranges might be 10 to 50 AMU for an instrument designed for environmental gas monitoring, or many tens of thousands of AMU for an instrument used in protein analysis. The mass spectrometer often scans through this mass range by varying one of the electric or magnetic field parameters, producing a spectrum in both mass-to-charge (m/z) ratio and, undesirably, time. The scan will produce peaks in signal intensity where masses are present. The resolution of the mass spectrometer is determined by how narrow these peaks are; some mass spectrometers may only resolve unit masses while some may resolve extremely small fractions of mass (e.g. for distinguishing different species that appear at the same nominal unit mass, such as carbon monoxide at 28.010 and nitrogen at 28.0134). Peaks are often characterized by full-width half-maximum (FWHM) measurements; the width of the

peak at half of its amplitude can help in determining which masses will be visible. In general, mass spectrometers that produce narrower peaks have better resolving power than those with wide peaks.

1.3 Mass Spectrometer Types

Many different types of mass spectrometer exist, generally classified by the method used to separate the different masses. This section briefly covers some of the simpler types of mass spectrometer, and although nowhere near comprehensive, describes those that have potential to be manufactured inexpensively.

1.3.1 Mass Analyzers

The simplest and earliest type of mass spectrometer is the magnetic-sector device that produces a spatial separation in mass. In this design, ionized samples are accelerated in an electric field and injected into a region with a perpendicular magnetic field. The radius of curvature of the ion's trajectory in the magnetic field is proportional to its mass and inversely proportional to its charge state. By scanning either the electric field, and therefore varying the ion's kinetic energy, or scanning the magnetic field and varying the ions trajectory, the various masses can be separated and detected independently. Many variants of this design exist, including some with separate or combined electric and magnetic sectors, producing improved resolution.

A time-of-flight mass spectrometer is another simple design that produces a temporal separation in mass. Ions are injected into a drift region by a fixed electric field; the separation in ultimate ion velocity and therefore arrival time at the far end of the drift region is proportional to ion mass.

A quadrupole mass spectrometer uses two pairs of electrodes parallel to an ion flight path; by applying a variable-frequency RF field using one electrode pair and a DC bias on another, and tuning the RF field for a specific mass, only one mass at any given time has a stable trajectory through the fields.

A similar type of mass spectrometer, the ion trap mass spectrometer, uses principles similar to the quadrupole mass spectrometer to trap clouds of ions in a volume and selectively make the orbits of specific masses unstable. The unstable masses are then ejected from the ion volume and measured.

1.3.2 Ion Sources

In order for any of these mass analyzers to function, samples injected into the mass spectrometer must first be ionized. Only after ionization can the sample molecules be manipulated and separated by magnetic and/or electric fields.

The most common form of ion source uses electron ionization. In this type of source, an electron beam, usually generated thermionically, is aimed into a gaseous sample. Electrons interacting with sample molecules remove electrons from the sample, producing positively charged sample ions, although negative ion mass spectrometry is practical for some electronegative chemical species.

1.3.3 Detectors

Once a sample has been ionized and the resulting ions separated by mass, they must then be detected. The simplest detector is a Faraday cup followed by a high gain transconductance amplifier. Ions striking the Faraday cup produce a tiny but measurable current that is then amplified and recorded. However, since these detectors provide no intrinsic gain, the noise floor is that of the amplifier.

Other types of detectors employ discrete or continuous dynodes, similar to that of a photomultiplier tube without the photocathode. Ions striking the first dynode dislodge electrons, which fall down a series of increasingly higher voltage dynodes, each iteration producing twice or more the number of electrons. This electron cloud is then captured and measured by a transconductance amplifier, but the signal can be many orders of magnitude larger than a simple Faraday cup detector, without a significantly higher noise floor, thus allowing for much more sensitive detection.

THIS PAGE INTENTIONALLY LEFT BLANK

Chapter 2

Design

Many factors were considered in choosing the initial design of the miniature mass spectrometer. Ultimately a simple, robust design, capable of being fabricated without complicated or labor-intensive manufacturing techniques, is preferable to any design that can never be built in quantity.

Ideally, the design should be manufacturable using automated machine tools. Manufacturing can be simplified further by creating a planar design that relies solely on two dimensional machining; any features in the third dimension can be built or approximated by stacking multiple layers of 2D-machined components. Eliminating secondary machining operations is also important. Secondary machine operations invariably involve extra fixturing, time, and waste. Thus, the design incorporates as many cofabricated features as possible.

2.1 Design Overview

Unlike many mass spectrometers, which consist of a number of custom components (e.g. filaments, electrodes, etc.) integrated with standard off-the-shelf components (e.g. vacuum gauges, flanges, fittings), the mass spectrometer presented in this thesis was designed using a system level approach. Every major system of the design was examined and, where possible, designed to be integral to the overall design.

The mass spectrometer presented in this thesis is a single unit that may be op-

erated in a simple, cylindrical vacuum chamber with a port for gas inlet, several low-voltage cables, and a port for a roughing vacuum pump. All of these ports have been successfully implemented with thin tubing or cabling fed through the vacuum chamber wall and embedded in epoxy.

Nearly every choice is a tradeoff among multiple factors, among them performance, size, weight, power consumption, complexity, ease of manufacture, and cost.

This mass spectrometer is designed with a number of potential applications in mind, but for the most part, with common performance requirements. The mass spectrometer is designed for unit resolution (i.e. it can discriminate between ions one or more integer mass units distant) with enough sensitivity to detect species comprising of 0.5% or more of the analyte gas at an operating pressure of 1×10^{-4} Pa [1×10^{-6} torr]. The mass spectrometer must also carry its own high vacuum pump onboard; while slightly less versatile than a design incorporating both the high vacuum and roughing pumps, the substantial savings in cost, weight, and complexity are invaluable so long as the mass spectrometer can run on its own for long periods of time. This in turn places emphasis on low power consumption as well as low maintenance.

Secondly, the production cost of the mass spectrometer is important. An instrument providing this level of performance is of limited utility if the production cost is comparable to that of an existing commercial instrument (e.g. tens of thousands of dollars). The mass spectrometer needs to be quite inexpensive, on the order of \$1000, as it is intended for large-scale deployment in novel applications. Figuring into the cost of the mass spectrometer is ease of manufacture and complexity; difficult or skilled manufacturing techniques and/or large numbers of parts would make the design more expensive.

Thirdly, minimizing power consumption is important. A mass spectrometer meeting the above specifications would be ideally suited for a variety remote or portable applications, in which the mass spectrometer would need to be capable of running for long periods of time off of batteries or perhaps solar power.

Several mass spectrometer configurations were examined and rejected. Designs

requiring complicated 3D electrode geometries, high power RF electric fields, or precise timing abilities were determined to be unsuitable for reasons of manufacturing complexity, power consumption, and scalability. Essentially this rules out designs based on quadrupole and ion trap analyzers (complicated geometries and high power consumption), time of flight designs (precise timing, loss of resolution at small scale), leaving only those designs using magnetic mass analyzers such as the magnetic sector analyzer and cycloid analyzer.

The miniature mass spectrometer detailed in this thesis is a single-focusing 180-degree magnetic sector mass spectrometer. The major reason for this choice is that it was hypothesized that a magnetic sector mass spectrometer could be designed to be constructed using layers of planar components, that could greatly reduce the ultimate cost of the instrument, as most simple manufacturing techniques are 2-dimensional. The geometries involved are simple and no high power RF oscillators or high speed timing abilities are needed, as is the case with a quadrupole or time-of-flight mass spectrometer, respectively. Most other mass spectrometer types such as ion trap or Fourier-transform types tend to be even more demanding in terms of geometry, power, or complexity.

A set of permanent magnets and yoke creates the magnetic field for the mass analyzer. With the ready availability of NdFeB magnets this is an obvious choice; an electromagnet requires too much power for a small instrument. Additionally, a second benefit is available with a permanent magnet. By carefully choosing the sizes of the pole pieces for the yoke, the design can incorporate an ion pump into the same magnetic circuit that encloses the analyzer, thus saving on complexity, size, and parts count. The length of the magnetic sector analyzer was chosen to be 180 degrees, simplifying the layout and minimizing the size of the design by placing the ion source and detector on the same side of the instrument.

The design of each subsystem of the mass spectrometer is detailed in the following sections.

2.2 Mass Spectrometer Design

2.2.1 Vacuum System Design

The entire length of the ion flight path must be kept at high vacuum, i.e. at pressures below 1×10^{-4} Pa [1×10^{-6} torr]. At higher pressures, the mean free path for an ion becomes too short for enough of them to transit the entire length of the flight path. This criterion alone necessitates the use of a vacuum system with very tight tolerances to minimize the leak rate, as well as a vacuum pump capable of producing the high vacuum.

At the same time, the mass spectrometer's vacuum system must contend with a constant influx of gas; the gas entering the system from the inlet must be continuously pumped back out or captured lest the vacuum chamber pressure rise to an unacceptable level. Thus, the vacuum system must also incorporate a one or more vacuum pumps capable of pumping faster than the inlet leak rate.

In most mass spectrometers, the vacuum system is a very expensive part of the design. Compared to the cost of a typical instrument, the vacuum system may not be a large percentage of the overall cost, but for a miniature inexpensive design, the vacuum components alone may easily dominate the budget.

High vacuum components, even standard fittings, are extremely expensive. Nearly every component is constructed of machined or formed stainless steel, typically with welded junctions. Mass spectrometers often use custom vacuum components just due to the geometry of the instrument. For example, a magnetic sector mass spectrometer often has a formed, thin walled, welded section of stainless steel tubing welded to high vacuum flanges for the mass analyzer. This is typically required because the mass analyzers flight path must fit between the poles of the magnet, and the gap is rarely a standard size.

Moreover, electrical signals typically need to be fed into and out of the vacuum system; at a minimum, voltages for every electrode in the system are required. Typically this is anywhere from five to 10 or more separate potentials, and the feedthroughs may be needed at multiple different points in the vacuum system. High voltage elec-

trical feedthroughs are also expensive, due to the need to braze Kovar conductors with ceramic insulators and stainless steel flanges, and minimizing the number of signals penetrating the vacuum chamber is a priority.

The simplest method for minimizing vacuum system cost is to minimize the number of components involved. The design of the vacuum system for the miniature mass spectrometer makes a radical departure from the design of all other existing instruments. The miniature mass spectrometer was designed to fit, in its entirety (including magnets, power and control electronics, high vacuum pump, and ion optics, etc.), within a 100 mm diameter by 150 mm length vacuum chamber. No similar instrument of this size exists.

The mass spectrometer can be mounted on a single vacuum flange through which all of the electrical signals and the inlet pass, and the vacuum chamber can therefore consist of a 100 mm diameter cylindrical pipe for simplicity. Indeed, a simple but smaller vacuum chamber could be constructed that follows the contours of the instrument to minimize size and weight. To minimize the number of electrical feedthroughs, all data will be handled digitally and all control signals will be generated inside the vacuum housing by an onboard control system. In this manner, only two or three low-voltage electrical signals need to be fed through the chamber walls; power and one or two data lines. These three electrical lines may be simple lengths of cable embedded in low-outgassing epoxy, since high isolation is not necessary. Ground reference can be the chamber itself.

A refinement of this design might be capable of transmitting data wirelessly via infrared or RF through the vacuum chamber walls of a glass chamber, making only a single electrical feedthrough for power necessary. Eliminating this might be possible through inductive coupling.

This leaves the issue of maintaining the high vacuum. The miniature mass spectrometer incorporates a cofabricated ion pump, designed to use the same permanent magnet and yoke assembly that the mass analyzer uses. Of course, an ion pump by itself is not sufficient to pump down a mass spectrometer from atmospheric pressure, so a valved port needs to be provided for rough-pumping the chamber to a point at

which the ion pump can start. This port can be mounted on the same flange as the electrical feedthrough and inlet.

2.2.2 Mass Analyzer Design

The mass analyzer is a 180° magnetic sector, with an ion flight centerline radius of 23 mm. This is in part a practical consideration; 50 mm \times 25 mm NdFeB magnets are available without requiring custom fabrication, and some clearance is required between the ion flight radius and the edge of the magnet because the ion flight will never be perfectly circular due to the inevitable nonlinearities of the magnet's field.

The length of the sector, 180° , is a deliberate choice. Primarily, more spatial separation between ion beams of adjacent mass is realizable, as more of each ion's flight is within the sector. Secondly, with a 180° sector, both the ion source and the detector are located on the same side of the mass analyzer, leading to a more compact design and no complications with locating the magnet yoke. This benefit is achievable only in this miniature design; larger instruments typically have separate vacuum compartments for the ion source and detector and the sector length in these instruments is typically limited by the size of the magnet.

The resolution of the mass spectrometer depends heavily on the design of the mass analyzer. Generally speaking, the stronger the magnetic field, the smaller the radius of curvature.

There is a tradeoff between field strength and weight and cost. The maximum magnetic field strength using permanent magnets is in the range of 0.5 to 1 T, using high grade (N52) neodymium-iron-boron magnets. Higher fields require more coercive force: more magnet thickness in the direction parallel to the gap, and more iron in the magnet's return path. This leads to a heavier and larger design.

Likewise there is a tradeoff between resolution and signal strength and cost; narrowing the filter slits leads to higher resolution, but fewer ions complete the flight, requiring a detector with a higher gain for a given noise floor. Furthermore, as the width of the slit is narrowed, alignment of the slit with the axis of the ion beam becomes more critical, leading to tighter tolerances and inevitably, larger cost.

The present design eliminates the need for filter fixturing and alignment by cofabricating the slits with the chassis of the analyzer. Furthermore, the slits are themselves mounted on flexures integral to the analyzer chassis such that the geometry may be varied at assembly; the slit width can be modified to change the operating point on the signal/resolution curve. A further refinement of this design would drive the slit width actively, either by leadscrew or, more likely, by piezo or potentially by shape memory alloy actuators.

A pair of $50 \times 50 \times 10$ mm N52 neodymium-iron-boron magnets in a yoke constructed of 1008 mild steel is used in this design. The yoke increases in cross section from the leading edge of each magnet to 25×50 mm at the trailing edge of each magnet. As shown in Figure 2-1, the cross section of the yoke is approximately constant beyond the magnet. A 10 mm gap is left between the trailing face of the magnet and the yoke to avoid shorting the magnet. The yoke mass, including the magnets, is approximately 1.4 kg.

The yoke also incorporates features for mounting; a pair of holes in the return path allows the magnet, itself the heaviest part of the mass spectrometer, to be bolted to the vacuum flange.

The gap between pole faces is 10 mm, approximately the same air gap as magnet thickness. This configuration produces a field ranging from approximately 0.6 T at the edges of the pole face to about 0.8 T in the center. A CAD model of the magnet yoke is shown in Figure 2-1. The non-uniformity of this field is not ideal; nonuniformity leads to trajectory errors in the ion beam and ultimately, lower resolution.

Given the field strength and ion flight radius, it is a simple matter to calculate the range of ion energies, and therefore the ion acceleration potentials, required to run the mass spectrum sweeps. First is a force balance: in the mass analyzer, the force required to keep an ion on a circular trajectory is equal to the ions mass multiplied by the centripetal acceleration, and is provided by the Lorentz force due to the ions charge and the applied magnetic field,

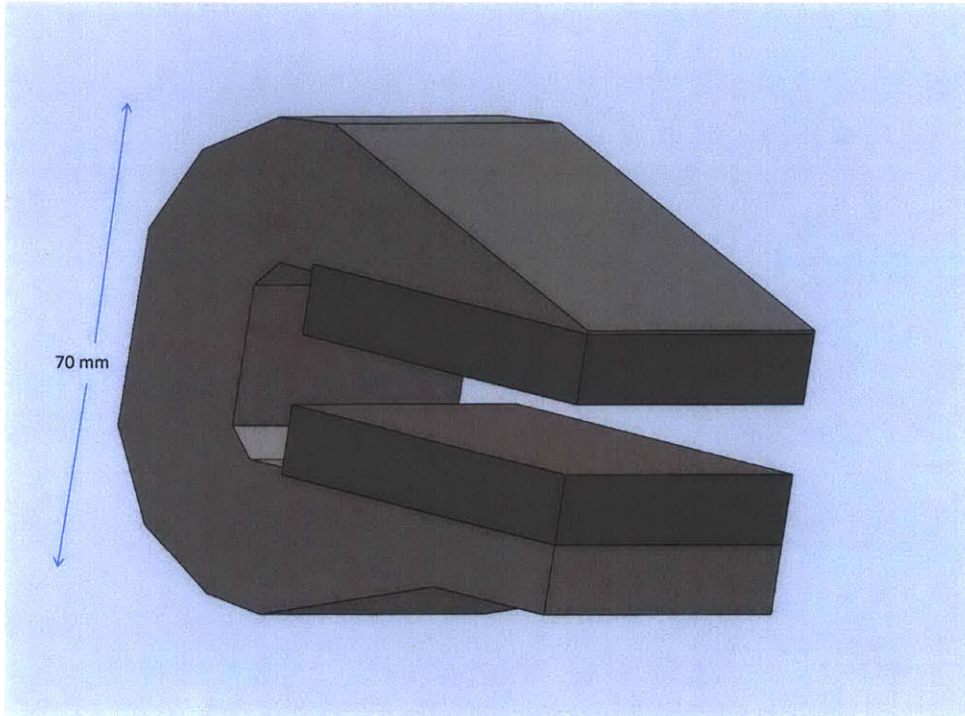


Figure 2-1: A CAD model of the magnet yoke.

$$qvB \sin \theta = \frac{mv^2}{r},$$

where;

B = magnetic field strength in T,

v = ion velocity in $\frac{m}{s}$,

θ = angle between ion beam plane and magnetic field in radians,

m = ion mass in kg,

q = elementary charge in C,

r = ion curvature radius in m.

The velocities give the range of voltages required to accelerate the ions. Final ion velocity, that is, the velocity of the ion as it exits the ion source into the analyzer, is proportional to the voltage E across the electrodes in the ion source,

$$qE = \frac{1}{2}mv^2.$$

These equations can be combined to give the relationship between ion mass and the potential required to accelerate the ion in order for it to reach the detector,

$$E(m) = \frac{qB^2(\sin \theta)^2 r^2}{2m}.$$

So there is an inverse relationship between the required electric field and the mass of the ion, as expected. Heavier ions require more kinetic energy to traverse the analyzer with the proper radius, given constant charge. Assuming each molecule is singly ionized ($q = 1.60 \times 10^{-19}$ C) and within the intended mass range, 10 to 44 AMU ($m = 1.66 \times 10^{-26}$ to 8.3×10^{-26} kg), an analyzer radius r of 23 mm, and a perpendicular B field ($\theta = 0$), the equation can be simplified to,

$$E(m) = 4.23 \times 10^{-23} \frac{B^2}{m}.$$

For an operating point of $B = 0.6$ T and mass range of 10 - 44 AMU, the voltage E required to accelerate the ions must sweep from about 208 V to 915 V. These potentials are attainable, given the dielectric strength of high vacuum. Moreover, there are many methods capable of generating these voltages efficiently. Voltage generation will be discussed in a later section.

Figure 2-2 is a plot of ion source potential verses ion mass for different B field strengths. Note that since this is an inverse power function, resolution will decrease as ion source potential decreases because the same change in ion source potential will span a much larger mass range. This is a feature intrinsic to magnetic sector mass spectrometers, and this design is no different. This issue will be discussed in more detail in Chapter 6.

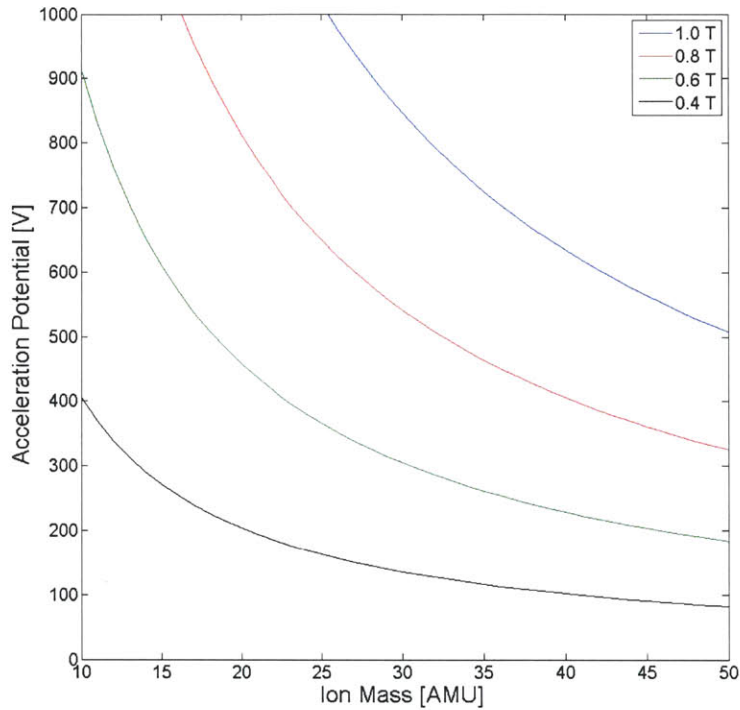


Figure 2-2: A plot of ion source potential verses ion mass.

2.2.3 Ion Source Design

The ion source is of considerable importance to both the efficiency and the performance of the mass spectrometer as a whole. Ions are typically formed by electron ionization; an electron gun generates an electron beam that interacts with the sample gas to form positive ions. This type of ion source has historically been called "electron impact ionization", however, due to the wavelike nature of electrons, the exact mechanism of ionization is not related to particle impact [9].

The ion source must be located far enough from the magnet yoke structure such that the fringing fields from the magnet do not affect the trajectory of the electrons. The distance required, determined empirically, is approximately 30 mm.

Furthermore, the ion source is designed with an electron beam oriented vertically, essentially in parallel with the fringing fields of the magnet. This minimizes the chance that the electron beam will be sent off course by stray fields.

Electron Source Design

The electron beam is typically generated thermionically; a hot wire, usually tungsten or an alloy, is heated to incandescence, adding enough thermal energy to some of the electrons in the wire such that they can overcome the work function of the bulk metal and escape into the surrounding vacuum. The escaped electrons are removed from the area surrounding the wire using electrostatic fields.

This process of generating electrons is typically inefficient; furthermore, the probability of an interaction between an electron in the beam and a molecule in the sample gas resulting in the formation of an ion is also low, on the order of 0.1% [9].

Ideally these ions would emerge from the ion source in a collimated beam of appropriate geometry for subsequent flight through the analyzer. In practice, ionized molecules have a random distribution within the ionization region, and only a small fraction of the ions produced emerge from the ionization region in the appropriate direction to be analyzed.

To improve this last issue, most mass spectrometers have employ a electrostatic field produced by an electrode, typically called the repeller, in the ionization region to sweep ions towards the analyzer; however, the field produced by this electrode is relatively low.

The result is that the ion yield of a mass spectrometer using a thermionic electron gun is extremely low. Thus, a high current electron beam is desirable to maximize the total production of ions, but this requires a large investment in electrical power. For a portable instrument, an improvement in the efficiency of the ion source is required.

There are essentially three methods by which the efficiency of the ion source may be improved. The yield of electrons for a given filament power may be increased, through the use of improved emissive materials. The yield of ions may be improved by increasing the probability of interaction between the electron beam and the sample gas, by changing the trajectories of the electron beam (e.g. a helical instead of straight trajectory). Finally, it might be possible to capture more of the ions that would form but otherwise not be swept into the analyzer. Both high efficiency emissive materials

and methods of increasing ion yield were examined.

The final ion source design focuses mostly on improvements to ion yield, as investigations into high efficiency emission materials proved inconclusive. The ion source in this design operates by ionizing a large volume of ions using a large diameter electron beam, producing an ion beam with a wide dispersion, and then using a series of electrostatic lenses to collect and collimate these ions into a uniform ion beam.

The large, cylindrical electron beam is produced by a simple, low power tungsten filament and a circular aperture in an anode. This structure is called a Pierce diode and well understood; it was studied extensively in the days of vacuum tubes and appears in reference literature [10]. The diameter of the electron beam is quite large, at 3 mm, and is used to ionize a large volume of sample gas. However, instead of directing these resultant ions through an adjacent, narrow mechanical filter, the entire volume is gathered and focused with electrostatic lenses.

In the Pierce diode, the current density of the current emitted from the anode hole is,

$$J_{max} = 2.34 \times 10^4 \frac{r^2}{d^2} V^{1.5},$$

where,

J_{max} = is the current density in $\frac{A}{m^2}$,

V = voltage between anode and cathode in volts,

r = radius of anode hole in m,

d = distance between anode and cathode in m.

For a distance of $d = 5$ mm between the filament and the entrance of the ion source and a potential of $V = 70$ V, the emission current is $120 \mu A$.

The emission angle of the Pierce diode is,

$$\theta = \frac{r}{3d},$$

where,

θ = beam angle in degrees,

r = radius of anode hole in m,

d = distance between anode and cathode in m.

For the Pierce diode used in this electron source, the beam angle is 0.1° .

The emissive material generating the electrons must be capable of producing $120 \mu\text{A}$ of electron current within a 3 mm diameter circle, which is the diameter of the hole in the anode. The space-charge limited emission from an incandescent tungsten filament, as a function of temperature, adapted from [11],

$$i_{max} = 60.2 \times 10^4 T^2 \exp \frac{-52230}{T},$$

where,

i_{max} is emission current density in $\frac{\text{A}}{\text{m}^2}$ of emissive surface,

T = surface temperature in K.

At 2500 K, the current density from a tungsten emitter is $3170 \frac{\text{A}}{\text{m}^2}$. Producing a $120 \mu\text{A}$ electron current therefore requires $4 \times 10^{-6} \text{m}^2$ of emissive surface. The area of the anode hole is $7.1 \times 10^{-6} \text{m}^2$, so this is achievable.

Producing $4 \times 10^{-6} \text{m}^2$ of emissive surface in a $7.1 \times 10^{-6} \text{m}^2$ window is a difficult task. While a tungsten filament 3 mm in length and 0.4 mm in diameter would both fit within the anode aperture with enough surface area, such a filament would be inefficient and difficult to manufacture. The thickness of such a filament would conduct much of the heat out through the supply leads and supporting structure, and require on the order of 10 A according to filament design tables [12], leading to significant losses in connections to the filament and in the filament power supply itself.

Alternatively, the emissive surface area can be produced using a thinner, coiled tungsten wire. Coiled filaments are rarely, if ever, used in mass spectrometers.

The thinner wire of a coiled filament is less thermally conductive, leading to a more efficient system because less of the heat is carried out of the filament power

leads, and for the same power input can be run at a higher voltage and lower current. Fifteen turns of 12 μm diameter tungsten wire, with a turn diameter of 1 mm and pitch of 0.2 mm has a surface area of 4 mm^2 and a length of 3 mm .

These values are not unreasonable; similar filaments exist. A support structure consisting of glass or ceramic insulators and copper conductors could be designed to support such a filament, but alternatives exist. An additional electrical consideration is that of voltage; the voltage drop across the filament directly influences the shape of the electric field surrounding the filament; as such, the filament should operate on as low a voltage as possible. For a given brightness this means more current, and heavier, more thermally conductive supports.

A filament with essentially this ideal configuration is already mass produced as a flashlight bulb, typically designated PR-2. The PR-2 draws 2.4 V at 0.5 A, and has a coiled filament approximately 1 mm in diameter and a length of approximately 3 mm.

The mass spectrometer's ion source was designed to use a PR-2 flashlight bulb with the glass bulb carefully removed. Application of vise jaws allows the bulb to be shattered without damaging the delicate filament structure in the middle.

The electric field across the Pierce diode is set to 70 V. As a result, the electrons emitted from the Pierce diode anode hole are at approximately 70 eV. This value of kinetic energy is a commonly accepted value for maximizing the number of ions produced by electron ionization for a given electron current. This is due to the fact that the de Broglie wavelength of an electron at 70 eV is 14 nm, which is approximately the length of the bonds between atoms in many molecules [9]. At 70 eV, the de Broglie wavelength of the electron is given by,

$$\lambda = \frac{h}{mv},$$

where,

λ = de Broglie wavelength in m,

h = Planck's constant,

m = particle mass in kg,

v = particle velocity in $\frac{m}{s}$.

Ion Lenses

The other half of the ionization source involves capturing the ions generated by this relatively large electron beam. The volume of ions is swept from the ionization region with a weak electrostatic field, then focused on a large slit by a three element symmetric electrostatic lens, also known as an Einzel lens. These ions would subsequently diverge again beyond the filter, but a second two element lens defocuses the beam slightly, changing the focal point to a point infinitely distant from the filter. This beam is then ideally suited for analysis. A diagram of this lens system is shown in Figure 2-3.

Grid

A novel feature not found on existing mass spectrometers is a grid. The grid is an electrode that screens the anode of the Pierce diode from the cathode; potentials on this grid electrode can enhance or prevent the emission of electrons from the cathode. The grid, as an electrostatic element, may be rapidly modulated, operating in much the same way as the control grids in a vacuum tube. The signal used to modulate the thermionic emitter can be used with advanced signal processing techniques such as synchronous detection or stochastic system identification to improve the signal to noise ratio of the mass spectrometer as a whole.

2.2.4 Sample Jet

One of the unknowns is how well the electron beam interacts with the incoming sample gas. To maximize the interaction between the sample gas and electron beam, a hole is provided in the center of the trap electrode. Sample is then directed downward through the trap, while electrons are beamed in the opposite direction.

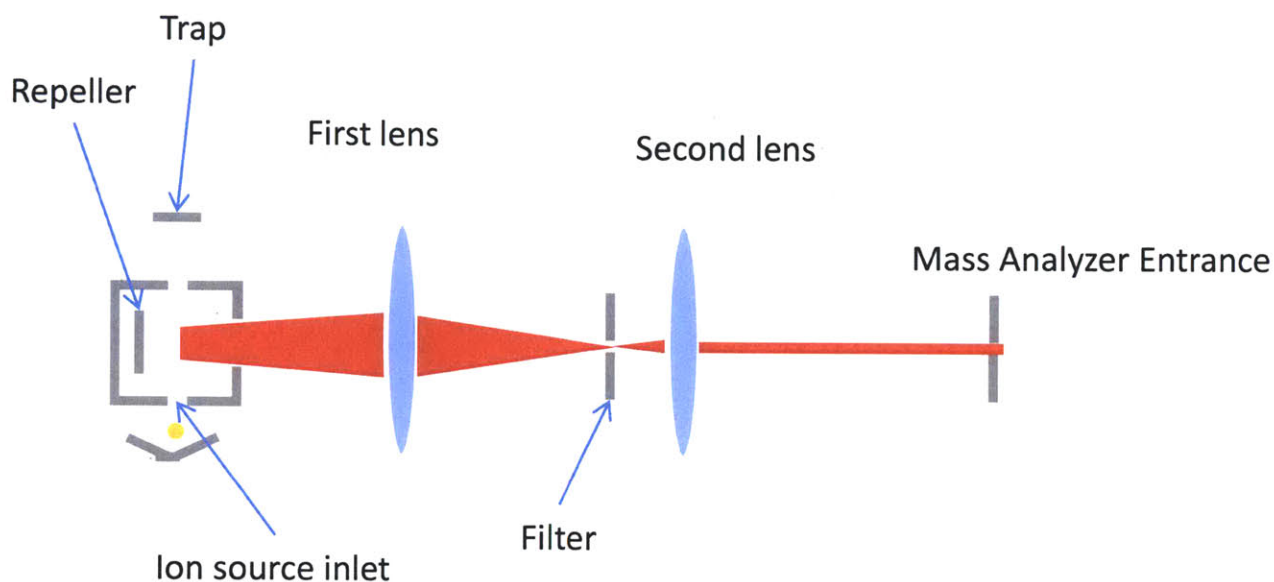


Figure 2-3: A drawing of the optics used in the ion source.

2.2.5 Detector Design

The ion beam that ultimately reaches the detector may be on the order of tens to 100s of fA. The detector at the outlet of the mass analyzer needs to be capable of detecting these minute currents and producing a signal above the noise floor intrinsic to the detector.

The detector of the miniature mass spectrometer is a Faraday cup followed by a transconductance amplifier with a gain of 50×10^9 . The Faraday cup is designed to capture the incident ion beam as well as recapturing any electrons produced by secondary emission. Since the incident ion beam can have quite large energies, on the order of hundreds of eV, secondary emission is a concern. The Faraday cup electrode shape is designed to capture secondary emission by providing a deep cavity into which the incident ion beam travels that recaptures all electrons that are emitted in any direction but perpendicularly back out. However, since the Faraday cup is still within the fringing field produced by the permanent magnet, any secondary emission

electrons will not travel in straight trajectories and will therefore be captured by the cup.

The transconductance amplifier is built around a National Semiconductor LMP7721 (www.national.com) low input bias operational amplifier. Operating with supplies of $\pm 2.5V$, the LMP7721's input bias currents are on the order of 3 fA. A 50 G Ω resistor in parallel with a 5 pF silver-mica capacitor for stability provide the amplifier's feedback path.

The output of this transconductance amplifier drives the front end of a Texas Instruments ADS1278 24-bit analog-to-digital converter. By placing these components in close proximity and under appropriate shielding, the intrinsic noise may be reduced.

2.2.6 High Vacuum Pump Design

The miniature mass spectrometer requires a pump to maintain the high vacuum of the vacuum envelope. While many portable mass spectrometers, such as the Mini 11 [7], use turbomolecular pumps for vacuum maintenance, such pumps represent a significant fraction of the power consumption of the instrument, and must be backed by mechanical pumps.

Another type of high vacuum pump often employed is an ion pump; these pumps are silent, clean, and employ no moving components. In an ion pump, two pumping mechanisms, both capture and sorption, are in operation. While pumping, gases are ionized by high field ionization in cylindrical anodes and accelerated into titanium or sometimes tantalum cathodes. Upon impact, the ions are either buried or cause titanium to sputter back to the anode. This constantly renewed layer of titanium is chemically reactive and captures gases by sorption.

There is relatively little literature on the specific geometries involved in the design of ion pumps. However, several general references exist. Two good but unpublished references by engineers at Duniway Stockroom, Inc. are available online which give general guidelines for the design of ion pumps [13, 14]. Other references give information on the operation of the discharges in the pump [15, 16]. Another unpublished

article provides information on the correlations between ion pump geometries and pumping speed [17].

The electrodes for the ion pump need to be located within a magnetic field, which generally adds mass to the system and complexity to the vacuum chamber. However, the miniature mass spectrometer is already designed with a magnetic circuit located within the vacuum chamber. The size of the pole faces of the magnet can be increased to encompass the footprint of a miniature ion pump as well, adding a pumping capability without a significant increase in complexity.

The ion pump designed is the simplest variety, a diode pump, which consists of a set of stainless steel hollow cylinders, open on each end, suspended between a pair of titanium plates. The pump is designed to produce the maximum pumping speed in the area available. Specific geometries and tradeoffs are discussed in a further section.

The ion pump must keep the system pressure low enough such that the mean free path of the ions is greater than the entire flight length of the mass spectrometer. For this miniature mass spectrometer, the length of the flight path is approximately 200 mm. The mean free path of an ion, adapted from [9], is given by,

$$l = \frac{3.71 \times 10^{-7}}{p},$$

where,

l = mean free path length in m,

p = pressure in Pa.

The intent is to keep the mean free path of an ion an order of magnitude larger than the flight length of the mass spectrometer. For a mean free path of 2 m, the minimum system pressure is 3.3×10^{-3} Pa [2.48×10^{-5} torr].

2.2.7 Inlet

Every mass spectrometer needs an inlet. While this thesis is not about the design of the inlet, as the mass spectrometer as a whole will work with many different types of inlet, this does require some consideration.

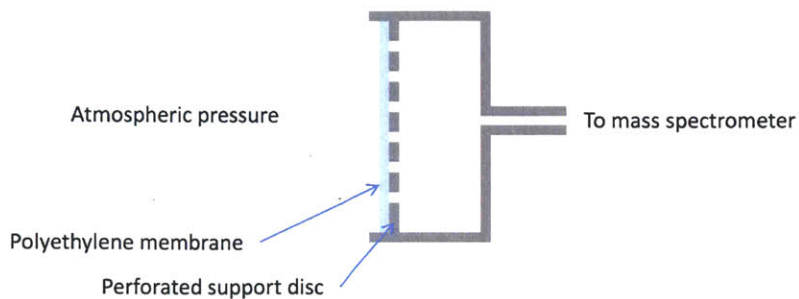


Figure 2-4: A cutaway drawing of the direct-to-atmosphere membrane inlet.

A simple, existing type of inlet was chosen for testing. A semi-permeable hydrophobic plastic membrane supported by a perforated stainless steel plate allows gases to diffuse into the vacuum chamber at a rate proportional to the exposed surface area of the membrane, while preventing the influx of water vapor and liquids. The inlet rate is chosen such that the mass spectrometer's pumping system can handle the inlet gas load at an appropriate vacuum chamber pressure.

A schematic of the inlet is shown in Figure 2-4.

THIS PAGE INTENTIONALLY LEFT BLANK

Chapter 3

Simulation

The miniature mass spectrometer ion optics design was extensively simulated using SIMION 8.0, a commercial ion optics modeling software package [18]. Modeling the ion flight is a crucial verification of the design presented in the previous chapter.

Additionally, the design from Chapter 2 is incomplete insofar as the exact dimensions of the various components are not set. Given the parameters from Chapter 2, as well as some additional guidance, the geometries of the mass spectrometer can be determined. The solution space for a set of dimensions given a set of parameters (e.g. magnet strength, ion radius, etc) is quite large, and some additional information is required to complete the solution.

3.0.8 Dimensioning

The ultimate solution is the result of an iterative process; a few initial choices were revisited due to undesirable simulation results (e.g. the voltages required on the electrodes to properly focus the ion beam were too large, generally those greater than 1 kV).

First, the overall height of the mass spectrometer's analyzer was set. The vertical dimension is somewhat arbitrary. The permanent magnets used are both 10 mm in height, and the gap was chosen to match this figure. Leaving some 1.5 mm for the thickness of each of the top and bottom covers of the mass analyzer, the vertical

dimension was then set to 7 mm.

The radius of the mass analyzer was set to 23 mm in the previous chapter. Using this as a controlling dimension, the remainder of the mass spectrometer ion optics and flight path was designed to be no more than 50 mm in length. The electron beam was placed as far from the magnetic sector as possible, to minimize the influence of the stray magnetic field on the operation of the electron beam.

The next decisions involved the size of the first lens. The first lens collimates the volume of ions created by the electron beam and focuses them on a mechanical filter. This lens is a three element symmetric lens, otherwise known as an Einzel lens, and described as symmetric because the first and third lens elements are at the same potential. This type of lens was chosen because it is a variable focus lens that does not change the energy of the ion that emerges from the other side.

As described in chapter five of *Building Scientific Apparatus* [10], electrostatic lenses should be built with approximately the same width as element length, with an element spacing equal to a tenth of the length. Such lenses typically have focal lengths that are of equal distances on both sides of the lens; hence, the filter following the first lens is the same distance from the lens as the ionization region.

Figure 3-1 is a diagram of the ion source captured from the SIMION simulation of the mass spectrometer.

The second lens, used to defocus the beam slightly (e.g. placing its focal point at infinity), is a two element lens that roughly equally subdivides the region between the first mechanical filter and the second mechanical filter. The longer electrode faces provide a slightly more uniform field; the exact placement of the electrodes is slightly less crucial.

A second mechanical filter after the second lens further limits the beam dispersion to minimize stray ions reaching the detector. This filter was deliberately placed 10 mm from the nominal entrance to the magnetic sector, since the fringing fields from the magnet are quite strong, and may nudge the ion beam off course before it reaches the filter.

Note that all of the electrodes, rather than being simple flat faces along the ion

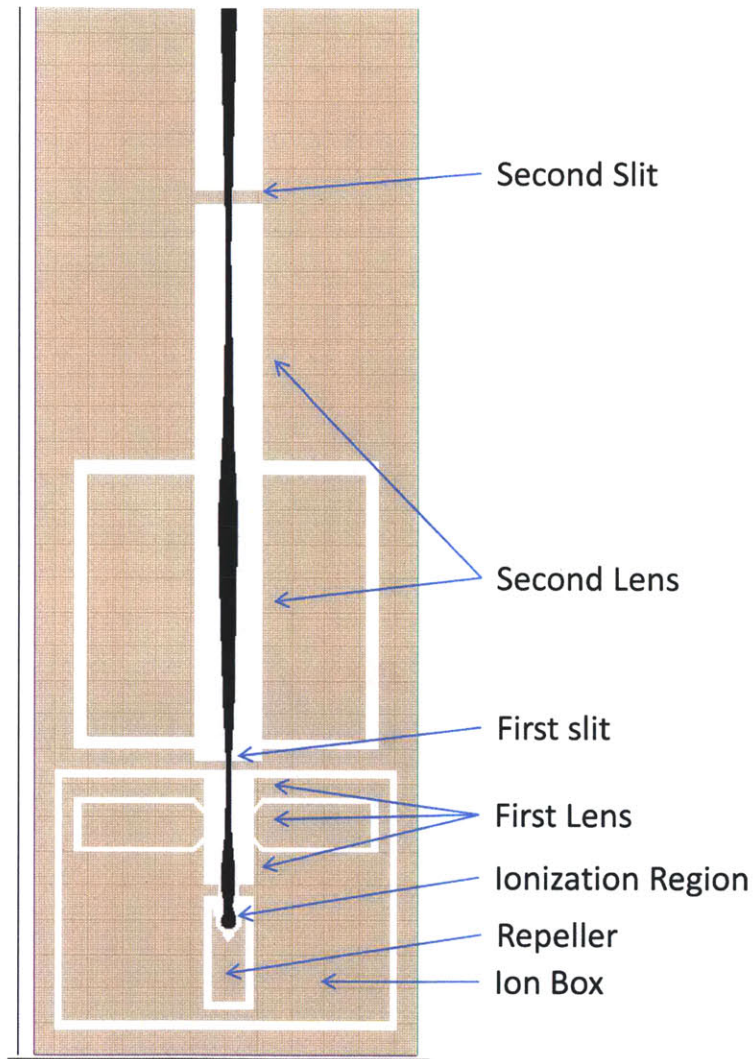


Figure 3-1: A simulation of the ion gun with indications of where the elements referred to in the text are placed.

flight path, extend perpendicularly well away from the flight path. This is also deliberate; although a flat plate would behave identically in this simulation, in practice it would be nearly impossible to fabricate. The depth of the electrodes allows them to be mounted to a common plane; the simulation is done this way as a reminder that the electrodes need to be mounted somehow. The shapes of the back sides of the electrodes are not critical.

3.0.9 Ion Flight Simulations

The entire mass spectrometer design was simulated and found to conform to the initial design work. Simulations were done for ions of mass 10 AMU to 44 AMU. The voltages required on the various electrodes roughly conform to the predictions.

Figure 3-2 is a typical simulation showing the flight of carbon dioxide molecules through the mass analyzer. It is worth remembering that SIMION does not simulate either space charge, ion collisions, or secondary electron emission; the simulations are done on single, isolated ions in the geometry provided. The effects of fringing electric fields are simulated.

It is important to note that the simulation is done under ideal conditions, and one can easily be led off track by improper choice of initial conditions. For example, a simulation done on a stationary ion beginning dead center in the ion beam is likely to behave much more favorably than an ion near the edge of the ionization region with an initial velocity perpendicular to the intended path. An improper choice of initial conditions will lead to a belief that a design will work with much higher ion efficiency and resolution than the design can realistically produce. Thus, the initial conditions for ions in the flight path must be carefully chosen.

Ion initial energies were chosen to have a gaussian spread centered around the thermal energy of a gas molecule at room temperature.

The average translational energy of a gas molecule of an ideal gas is,

$$E = \frac{3}{2}kT,$$

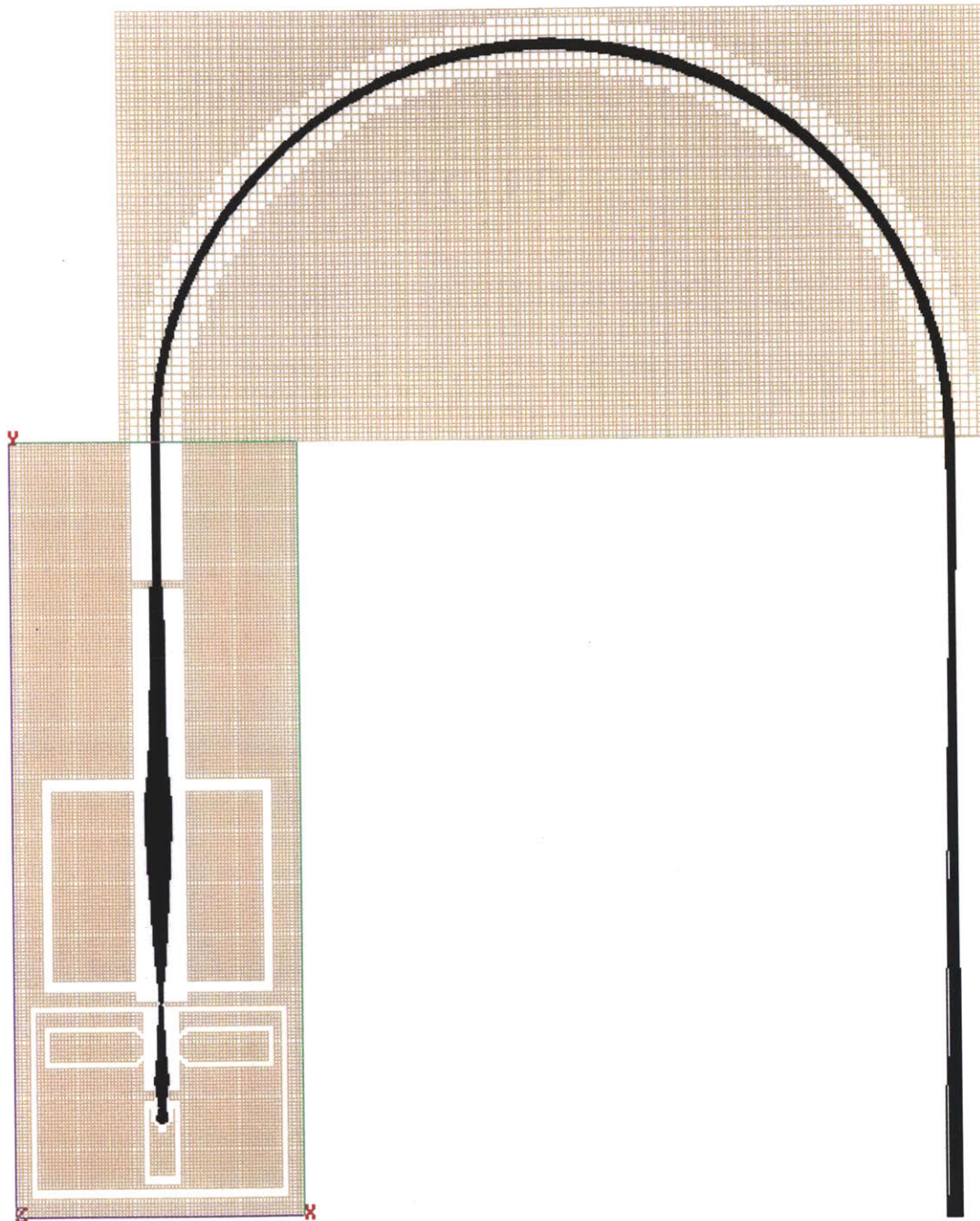


Figure 3-2: A SIMION simulation of a carbon dioxide molecules transiting the miniature mass spectrometer.

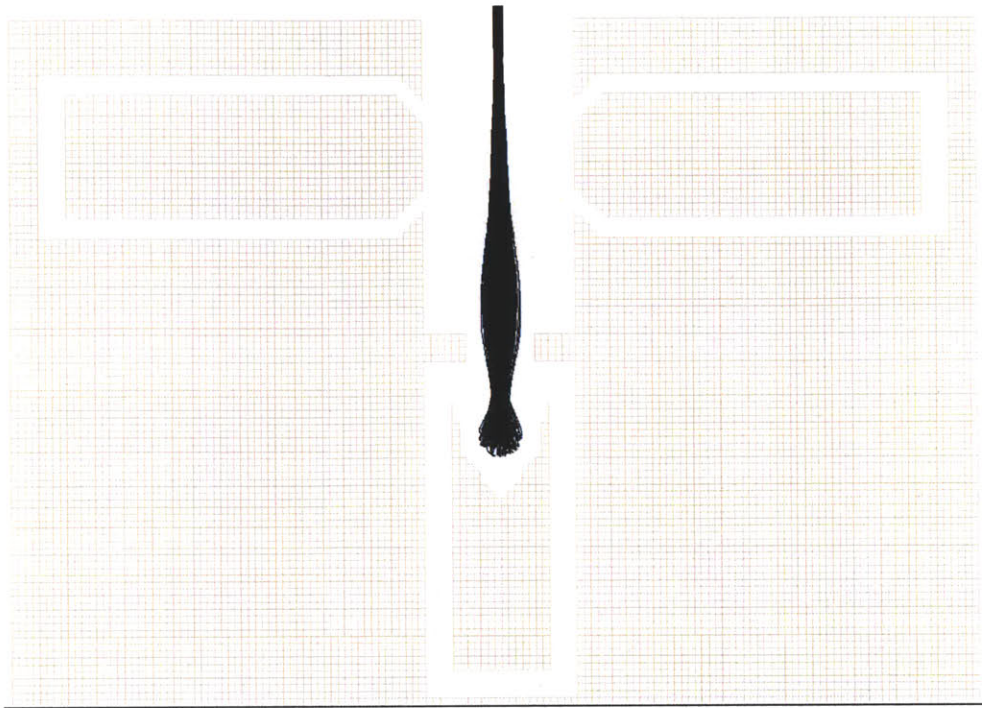


Figure 3-3: Detailed view of the ion source and first lens.

where,

E = kinetic energy in J,

k = Boltzmann constant ($8.617 \times 10^{-5} eV K^{-1}$),

T = temperature in K.

At room temperature, E is approximately equal to 0.015 eV. Therefore all of the later trajectory simulations were done using a gaussian distribution of initial kinetic energy with a mean of 0.015 eV and a standard deviation of 0.005 eV.

Ion initial direction was set using a uniform distribution across 360 degrees radially. Ion initial position was set using a uniform distribution across a cylinder above the projection of the hole through which the electron beam enters the ionization region.

Figure 3-3 is a detailed view of the ion source and first lens of the mass spectrometer. Ions originate in the center, generated by a vertical, cylindrical electron beam, directed vertically out of the page. The initial trajectories of the ions are generated with random direction and random kinetic energy.

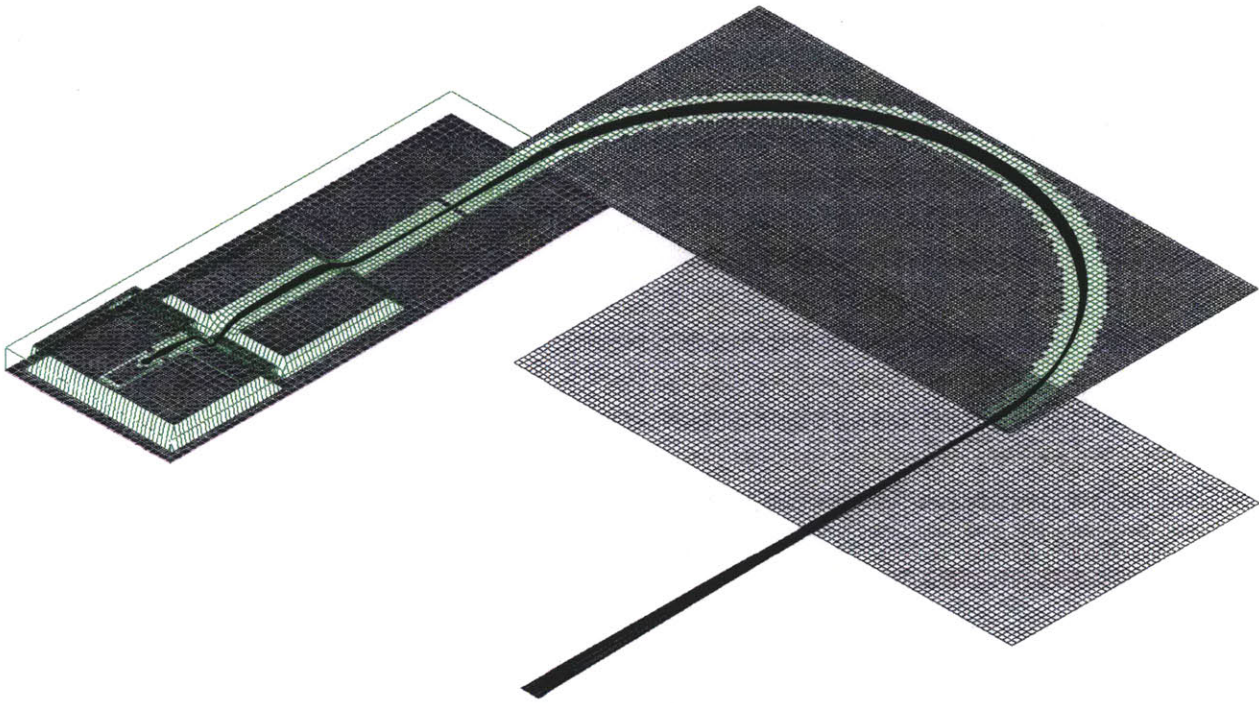


Figure 3-4: Isometric view of the potential energy distribution in the mass spectrometer ion source and analyzer. The curvature of the green potential energy surface indicates the effect of the electrostatic lenses. The vertical dimension is potential energy, while the two horizontal dimensions are the plan form of the mass spectrometer.

The black traces in the simulation diagrams are computed trajectories of ions given a hopefully realistic set of initial conditions. It is reasonable to neglect space charge, due to the low magnitude of the ion current.

Figure 3-4 is an isometric view of the mass spectrometer, with the physical layout represented in two dimensions and potential energy represented in the third, vertical dimension. Here, the wisdom of a longer, lower voltage second lens becomes more apparent; any slight misalignment in a higher voltage lens would cause a much larger trajectory error in the ion beam, as the potential energy 'obstacle' the beam must climb over would be much steeper.

3.0.10 Electron Source Simulations

The electron source, comprising of the Pierce diode and control grid was also simulated. The cathode was simulated as a cylindrical source of electrons 1 mm in diameter and 3 mm in length. The potential between the cathode and anode is 70 V. The results of this simulation are shown Figure 3-5. Note the focusing effect of the anode; the emitted electron beam is collimated with a narrow beam angle.

A second simulation, showing the effect of the control grid, held here at 100 V below anode potential, is shown in Figure 3-6.

In this simulation, an outer electrode is used to simulate the effect of the vacuum chamber as the electron source potential floats to high voltages. The electron beam narrows slightly as the source potential climbs from 150 to 900 V.

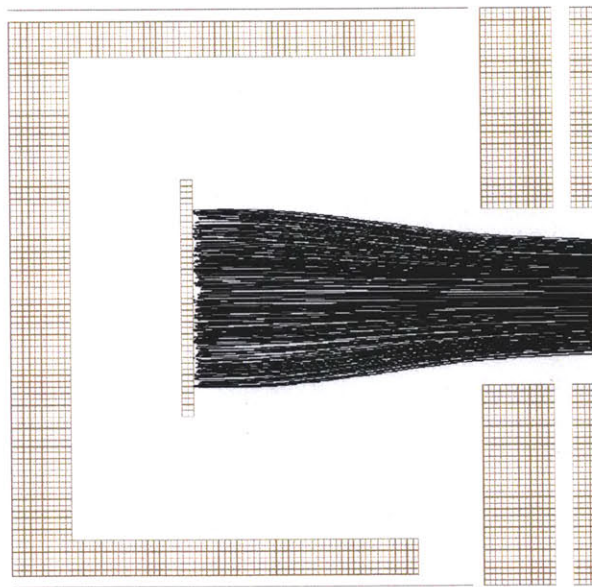


Figure 3-5: Side cutaway view of the cylindrical Pierce diode ion source. Electrons are emitted from the surface of a filament in a line. A cathode potential electrode surrounds the filament to screen it from the vacuum chamber. The grid and anode electrodes are shown at the right edge of the simulation.

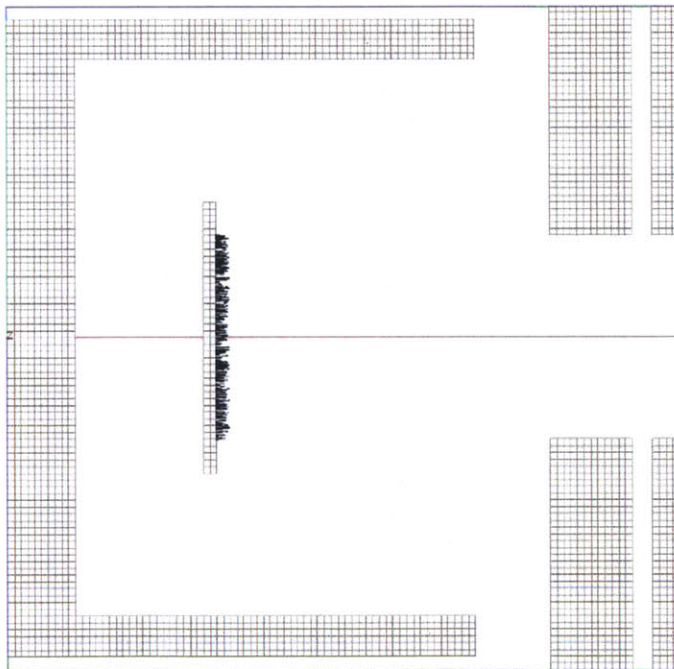


Figure 3-6: Side cutaway view of the cylindrical Pierce diode ion source, with the grid biased such as to inhibit electron emission.

Chapter 4

Construction

The design described in Chapter 2 and simulated in Chapter 3 must be implemented in hardware.

The various electrodes, including those that form the electric field free regions (such as within the magnetic sector) need to be held in precise alignment, while also in electrical isolation.

4.1 Substrate

The mass spectrometer uses a number of electrostatic elements that must be held in alignment while remaining electrically isolated. To minimize parts count, a single, inexpensive substrate was chosen to maintain both alignment and isolation of all of the electrodes.

FR-4 printed circuit board material was chosen as the substrate onto which the mass spectrometer is built. The reasons for this choice are numerous. FR-4 fiberglass printed circuit boards (PCBs) are inexpensive in large quantity, due to the large number of facilities dedicated to producing custom boards and the highly automated processes involved. PCBs can be made with very small feature sizes and extremely high accuracy; typical PCB houses such as Sunstone (www.sunstone.com) can produce feature sizes down to about 0.15 mm in prototype quantities and smaller features in large production quantities, with positioning accuracy to a tenth of that. PCBs,

nominally designed for electrical components, have a very high dielectric strength, on the order of $1 \times 10^7 - 2 \times 10^7$ V per m, which is sufficient for the voltages involved in this mass spectrometer design. Finally, PCBs are mechanically very strong, being primarily composed of woven fiberglass mat and epoxy resin, and are a good choice for keeping electrodes separated.

Since PCBs are in fact designed expressly for the implementation of electrical circuitry, both the electrodes of the mass spectrometer and the circuitry that drives it may be incorporated onto the same substrate. An additional benefit of using PCB material for a substrate is that multiple variants of printed circuit board composition exist, including ceramic printed circuit boards, and the underlying material could be changed relatively easily should the potential drawbacks of FR-4 prevent the design from working properly.

PCBs do have a couple of potential drawbacks, however. FR-4 printed circuit boards are composed of copper over glass-reinforced epoxy sheets. As such, the substrate material has the potential to absorb and adsorb water and gases (diffusion into the bulk material and adhesion to the surface, respectively). These absorbed and adsorbed molecules could then be released slowly into the mass spectrometer's vacuum system, preventing the system pressure from falling low enough such that this background concentration of gas remains visible on top of the inlet gas spectrum. These potential problems are not without solutions. Two primary countermeasures to these problems exist; driving the absorbed and adsorbed gases off the material, or encapsulating the material in a low-outgassing conformal coating.

It is well known that raising the temperature of a material tends to aid in the removal of both absorbed and adsorbed gases in vacuum. Standard procedure when constructing vacuum tubes is to "degas" the tube by heating the elements while the tube is still on the exhaust vacuum manifold. Degassing is usually done either by operating the tube's filament, which heats the tube's electrodes by radiation, or by drawing electron current, which heats the tube's anodes and other electron collecting electrodes, or by "bombing" the tube. Bombing involves heating electrodes by Joule heating using eddy currents induced in the electrodes by an RF coil held external to

the tube envelope [12].

Encapsulating outgassing materials has precedent as well. Outgassing of materials is often a problem on spacecraft, especially satellites, where gases may be emitted by one surface and reabsorbed by other critical surfaces, such as sensors. As such, conformal coatings are often tested for outgassing properties. A standard test method for determining outgassing properties exists, ASTM E595-07. One well known low-outgassing conformal coating is parylene, and parylene coating is a service offered by many job shops.

In this design, a distributed network of resistive heaters was added to the bottom of the PCB substrate, allowing heat to be added at points all across the PCB simultaneously. In a future revision, these resistive heaters might be replaced by a simple network of thin traces, similar to the resistive array on the rear windows of most automobiles.

4.2 PCB Design and Construction

Ultimately, to minimize the overall size of the mass spectrometer, several layers of PCB were used. A bottom layer of printed circuit board carries the electronics package, described in detail in the next chapter, while the two upper PCBs form the bottom and top covers of the mass analyzer. A CAD layout of the printed circuit board, with all of the pieces concatenated (to be cut apart after build to minimize cost) is shown in Figure 4-1.

The boards are mechanically connected by 20 mm long M3 hex standoffs. The M3 screws go through the mounting holes in the analyzer ring, the mass analyzer's lower PCB, and the hex standoff. Cutouts in the mass analyzer's upper PCB allow the screw heads to seat without interference. This allows the top cover of the mass analyzer to be removed for electrode alignment without necessitating the removal of the mounting hardware.

Electrical feedthroughs connect the mass analyzer boards to the electronics boards. The low voltage digital and analog supply pins are carried on two rows of 20 mm tall,

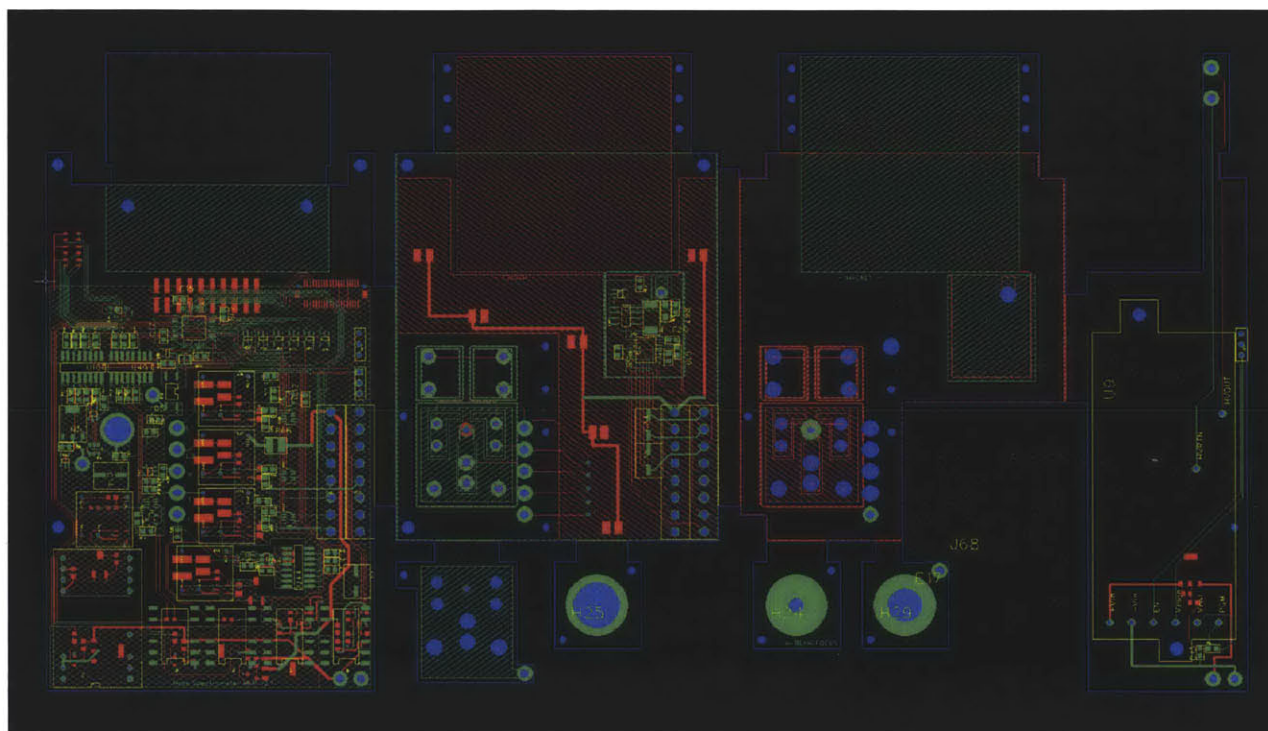


Figure 4-1: A CAD layout of the printed circuit board substrate that underlies the whole mass spectrometer.

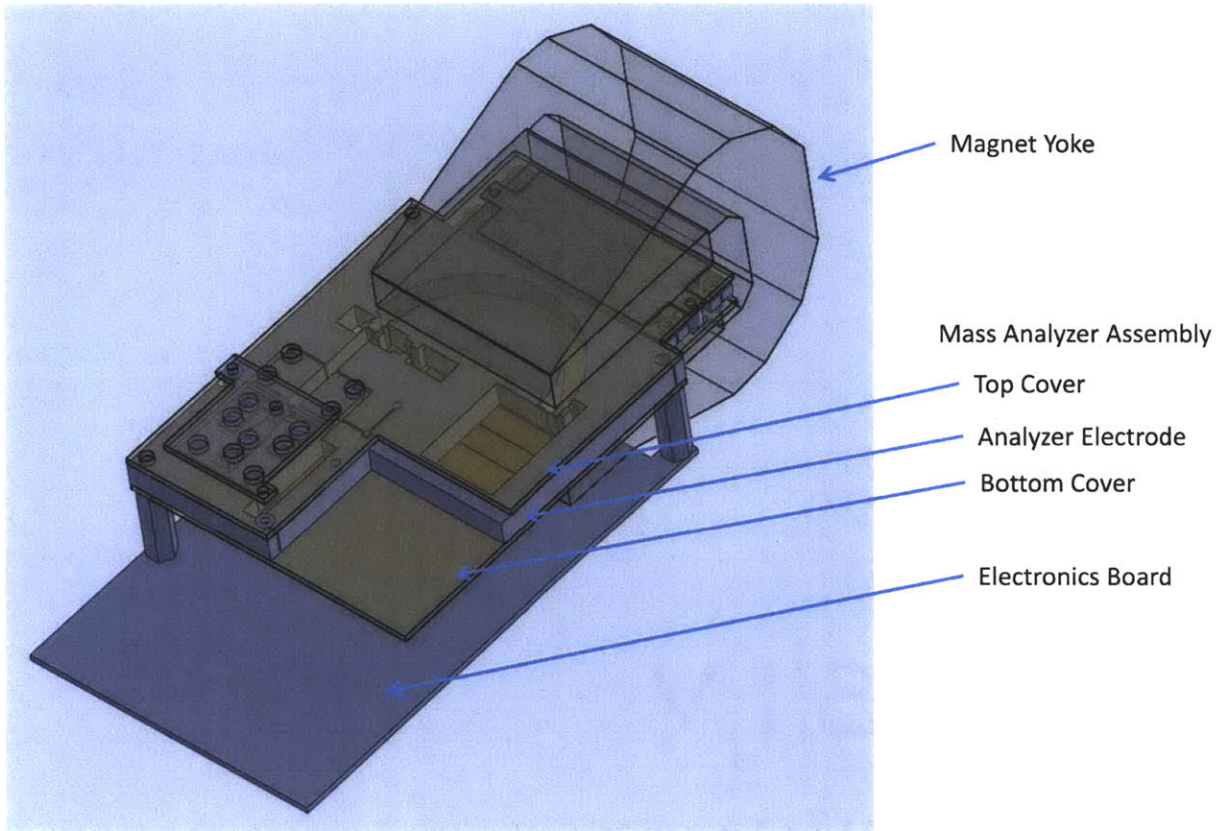


Figure 4-2: A CAD layout of the whole mass spectrometer.

2.54 mm spacing pin header. The high voltages used for electrostatic lenses were more difficult; electrical mezzanine connectors rated for 2 kV do not exist. Instead, a properly spaced row of holes in the mass analyzer board and the electronics board are fitted with 25 mm M2 hardware after the two boards are mechanically mounted together. The copper rings around each hole serve as electrical contacts. A CAD model of the general instrument layout is shown in Figure 4-2.

4.3 Electrodes

Using PCB as a substrate, electrodes must be fabricated and fitted to the PCB. The geometries for these electrodes and their relative spacing can be taken directly from the simulations described in Chapter 3.

The electrodes, as shown in the chapter on simulation, have a symmetry through the vertical axis (the axis out of the plane of the ion flight path). This is not accidental. Most of the simple manufacturing techniques are greatly simplified when carried out in two dimensions; the fixturing or complicated machine required to mount a component to carry out operations on more than two axes adds to the cost of the finished part.

The electrodes are cut from Type 303 stainless steel. This stainless steel has multiple beneficial properties; the bulk metal and its surface oxide are electrically conductive, unreactive, and have a low affinity for gas adsorption. It is a common material used for high vacuum work; most high vacuum components are constructed of 303 stainless steel or similar materials.

Type 303 stainless steel is one of the easiest stainless steels to machine. However, some of the features required to produce these electrodes are quite small, on the order of hundreds of micrometers, and these sorts of features are not conducive to fabrication by cutting tools. Generally, the cutting tool imparts too much force for making thin walled features. Thus, the manufacturing technique chosen for fabrication of mass spectrometer electrodes is wire electrical discharge machining (wire EDM).

All of the electrodes at different potentials must be separate components, but an effort was made to simplify the manufacturing for the mass spectrometer by allowing all of the electrodes that are at the same potential to be cut as one piece from the same stock. Additionally, all of the features necessary for mounting the components were designed into the toolpaths so that each electrode could be cut in a single pass.

4.3.1 Mass Analyzer

Of all the electrodes, the mass analyzer is the most complex and difficult electrode. Since the mass analyzer is at ground potential, its structural loop was designed to encircle all of the other in-plane electrodes in the system for both structural rigidity of itself and of the mass spectrometer, and for electrical shielding. Fields produced by the electrodes within the mass analyzer should be shielded from the outside, thus theoretically preventing some stray fields that might otherwise interfere with the electronics.

The mass analyzer also has a pair of delicate features at the entrance and exit of the magnetic sector. These features are the mechanical filters that limit the width of the detected ion beam, maximizing the likelihood that a detected ion is of the intended mass.

The filters are slits that are tens to 100s of μm wide, and as seen from the simulations, have a direct bearing on the sensitivity and resolution of the mass spectrometer as a whole. Generally, the slits are manufactured and installed separately in most mass spectrometers; here, they are cofabricated with the mass analyzer, both ensuring that they are collinear with the ion optics and minimizing costs by minimizing parts count and eliminating the need for slit alignment.

Another benefit of cofabricating the slits by wire EDM is apparent. The wire EDM is very good at machining thin walled structures, such as flexures. The slits in the mass analyzer are designed such that they are extended from flexures built into the walls of the flight path. Leadscrews, in this version of the mass spectrometer, can be driven in from the sides of the mass analyzer to vary the width of the slits. This gives tremendous control over the resolution and sensitivity of the instrument. A CAD model of the mass analyzer electrode is shown in Figure 4-3.

A future revision will likely include actuated flexures, possibly driven by motorized leadscrews, or more likely, by piezo actuators. This would allow the mass spectrometer to automatically optimize its sensitivity to resolution on the fly, expanding the slits to maximize ion current for weak signals and narrowing them for better resolution when analyzing ions of adjacent mass.

4.3.2 Electrostatic Lens Electrodes

The smaller electrodes used in the ion source, mass analyzer, and detector were also cut from the same stock as the mass analyzer using wire EDM. In addition to the active faces, at least two mounting features were cut into each electrode, corresponding to features in the mass analyzer PCB, thus minimizing the chance of angular misalignment.

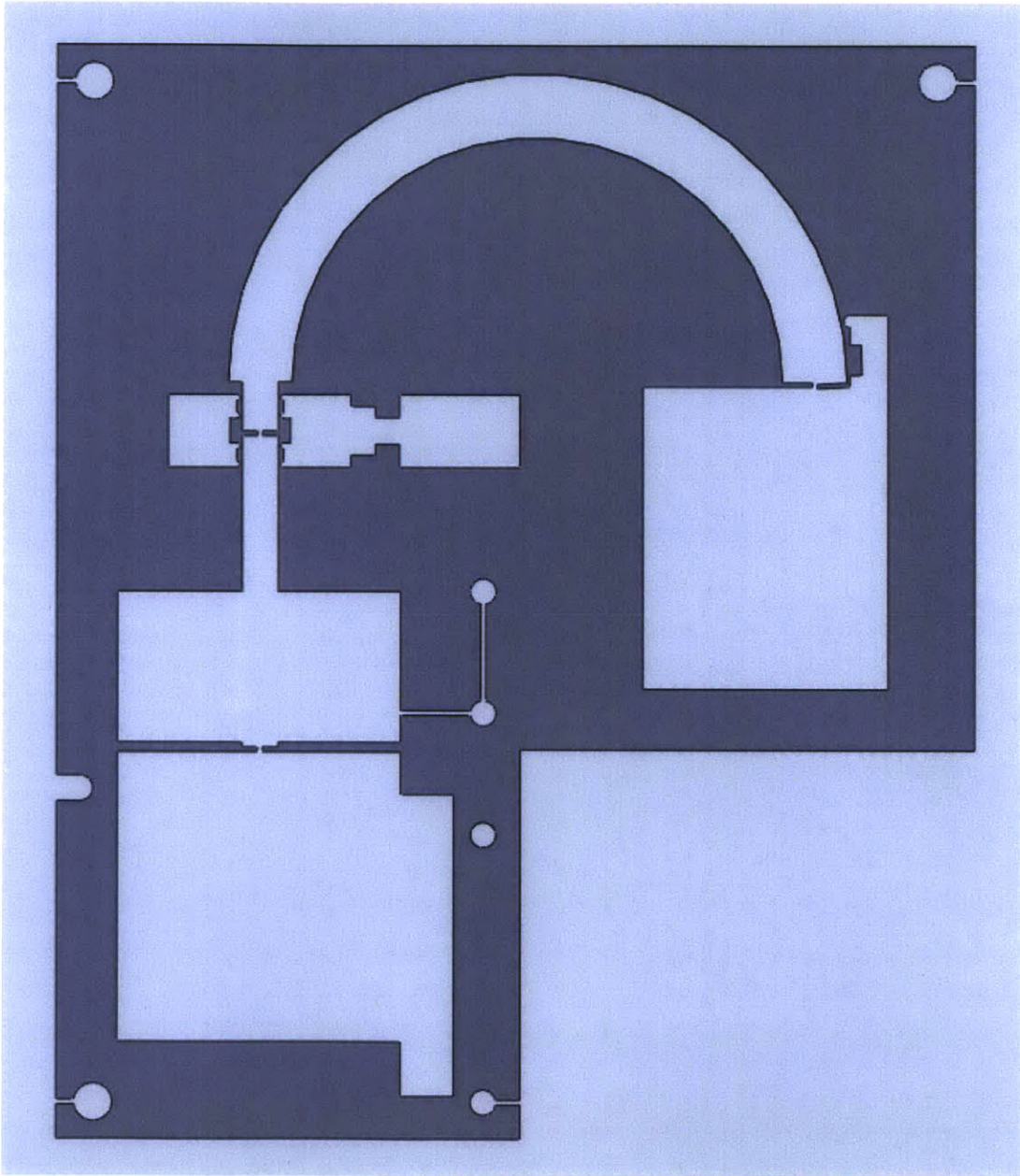


Figure 4-3: A CAD model of the mass analyzer electrode, with the slits mounted on flexures.

4.3.3 Electron Beam Electrodes

The electron beam in the mass spectrometer's ion source requires electrodes for proper function as well, and these electrodes are out of the plane of the ion source electrodes. Since the electron beam runs perpendicularly to the ion beam, from bottom to top, a different fabrication technique is required.

The electron beam electrodes, the trap and the electron focusing ring, are printed on small PCBs and mounted to the main PCBs with M2 hardware.

The electron focusing ring doubles as the physical mounting for the PR-2 flashlight bulb that provides the tungsten filament; the focusing ring allows the filament and its supports to penetrate the electronics PCB while keeping the bulb's mounting flange captive. M2 screws 25 mm in length run through the focusing ring PCB, past the flashlight bulb base and through the electronics PCB. The M2 screws are kept under tension, which fixes the flashlight bulb in place while allowing for alignment; the bulb base can be moved slightly before the mounting screws are tightened.

The trap electrode is mounted above the upper mass analyzer PCB, spaced 200 μm distant by M2 washers, and throughbolted to the mass analyzer. A long M2 screw, constructed of a 30 mm length of M2 threaded rod and jam nuts, electrically connects the trap electrode to the electronics board where the trap potential is generated.

4.3.4 Electrode Finishing

The electrodes of the miniature mass spectrometer were designed to fit to the printed circuit board substrate like standard electrical components. Several variants of mounting were attempted; first, in carrying this analogy to its logical conclusion, notches were cut in each electrode and small stainless steel pins were brazed to the electrode body using a hydrogen flame torch and silver solder.

This approach allowed electrodes to be mounted with no protrusions above the top of the electrode, so that there was no issue of aligning the mounting features of each electrode with the mass analyzer's top PCB cover.

Ultimately this approach, while workable, turned out to be more labor intensive

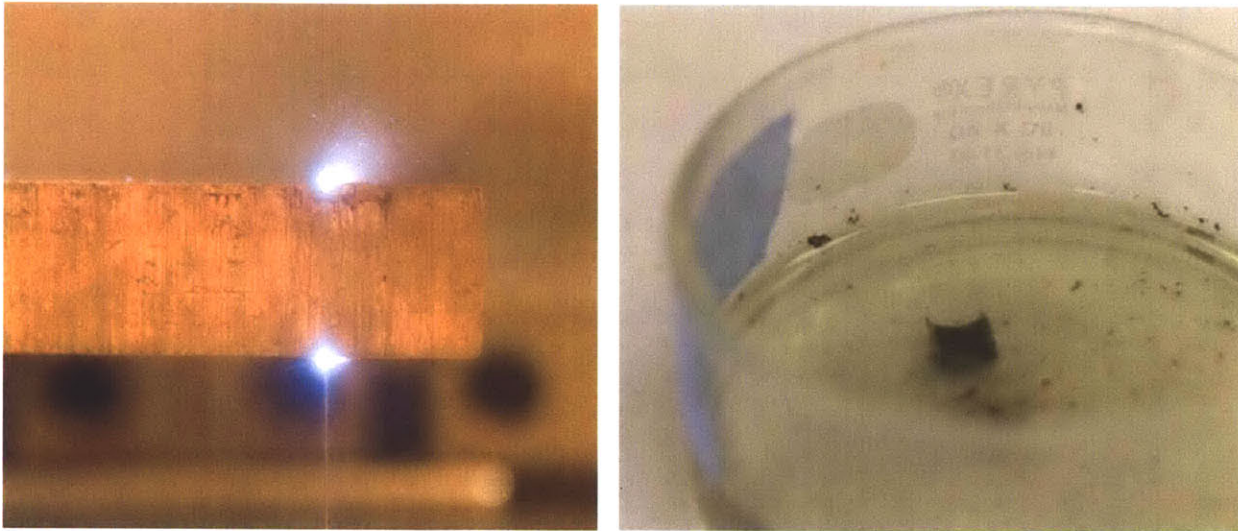


Figure 4-4: (left) Electrodes are cut from stainless steel plate by wire EDM. (right) Electrodes are etched in nitric acid to remove the oxide layer.

than designing the upper PCB cover with cutouts to provide clearance for mounting screw heads. The finished version of the mass spectrometer uses a combination of M2 and M1.6 hardware to affix each electrode to the PCB.

Upon removal from the wire EDM, the cut surfaces of each electrode are covered with a thick oxide layer. Electrodes were bathed in a 30% nitric acid solution for 30 minutes, followed by two changes of anhydrous ethanol for 30 minutes at 50 degrees Celsius in an ultrasonic cleaning bath. This procedure successfully removed the oxide layer, leaving bright metal beneath.

Figure 4-4 shows two steps from the process of assembling the mass spectrometer electrodes.

4.3.5 Magnet

The permanent magnet that provides the B field for the mass analyzer is a pair of NdFeB magnets held in alignment by a soft iron yoke as described in Section 2.

A mounting face is provided on one edge of the magnet yoke, drilled and tapped for M3 hardware. This mounting face is designed to be attached to the electronics

board PCB.

4.3.6 Ion Pump

The volume in which the cofabricated ion pump needs to fit is quite small; it encompasses just the unused half of the magnet face. Since ion pumps operate at high voltage, the printed circuit board is used to insulate the magnet pole faces from the ion pump electrodes. As such, the entire ion pump needs to fit within a $50 \times 25 \times 7$ mm volume.

Typically, ion pumps are designed with bunches of stainless steel tubes bonded together to form the anode. Such a process is costly and labor-intensive; the anode for the miniature ion pump on this mass spectrometer consists of a series of cells cut from stainless steel plate in one pass by wire EDM. Figure 4-5 is a CAD model of the ion pump anode.

Pumping speed is proportional both to diameter and number of cells [13]; increasing these values, to a point, will improve the speed of the ion pump. Given the limited space available, as well as the higher than standard B field strength, more cells were added instead of increasing the diameter of the cells. Another guideline indicates that the length of each cell should be on the order of 1.5 times larger than the diameter of the cell; with a 3.5 mm plate, this is difficult to do without designing extremely small cells.

The ion pump's cathode consists of a pair of titanium plate cathodes, 0.5 mm thick, with mounting tabs located such that they interleave with the four mounting tabs of the anode. The mounting holes in the ion pump electrodes mate with holes in the PCB substrate.

4.4 Assembly

As designed, the mass spectrometer can be assembled without any complicated tools or techniques. All mounting hardware can be attached with a single 1.5 mm slotted screwdriver and long nosed pliers. Alignment features on the printed circuit board in

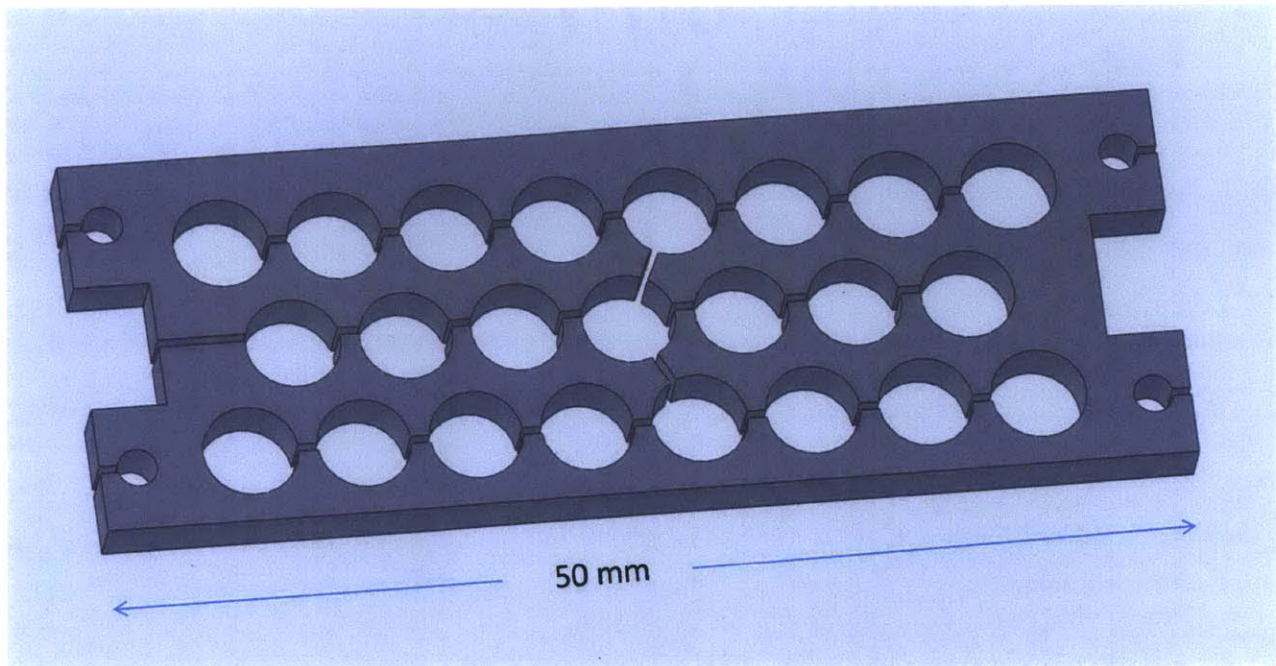


Figure 4-5: A CAD model of the anode for the miniature ion pump.

the form of outlines of each electrode ease the assembly, and a jig can be inserted into the ion flight path upon which the electrodes can be pressed before the screws are fully tightened, ensuring that the electrode faces remain parallel. Other electrodes can be spaced with 0.5 mm shim stock, as all the electrodes were designed with a 0.5mm gap between adjacent features.

A photograph of the complete mass spectrometer, with the top cover and magnet yoke removed, appears in Figure 4-6.

Filament alignment is done optically; a bright flashlight can be shined towards the filament from the side of the partially-assembled mass spectrometer, and the electron focusing ring electrode moved in plane until the center of the filament is clearly visible from above. Due to the large volume ion source and large diameter electron beam, this is a relatively simple procedure as visibility through the electron beam path is good. A photograph of the filament, illuminated from the side with a flashlight, appears in the left photograph in Figure 4-7.

The slits on flexures that form the mechanical filters can be adjusted by tightening or loosening the leadscrews. A macro photograph of the analyzer entrance slit,

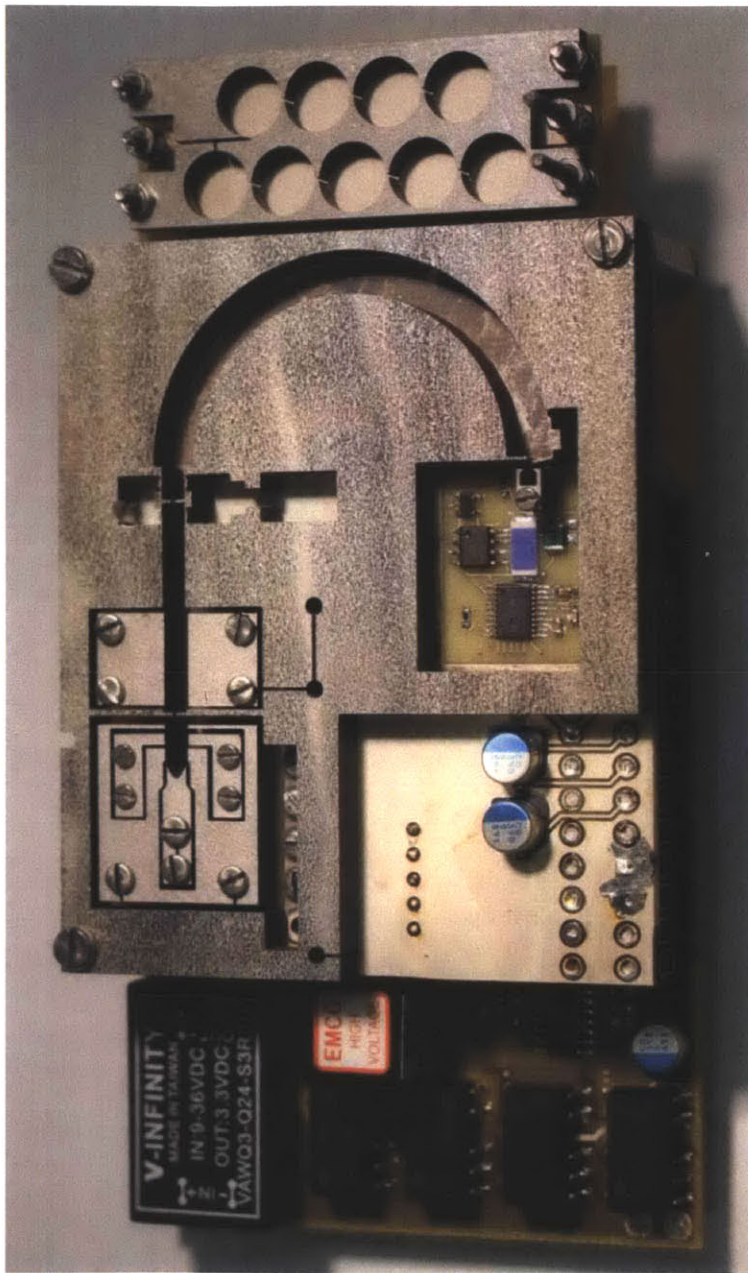


Figure 4-6: A photograph of the completed mass spectrometer, with top cover and magnet yoke removed.

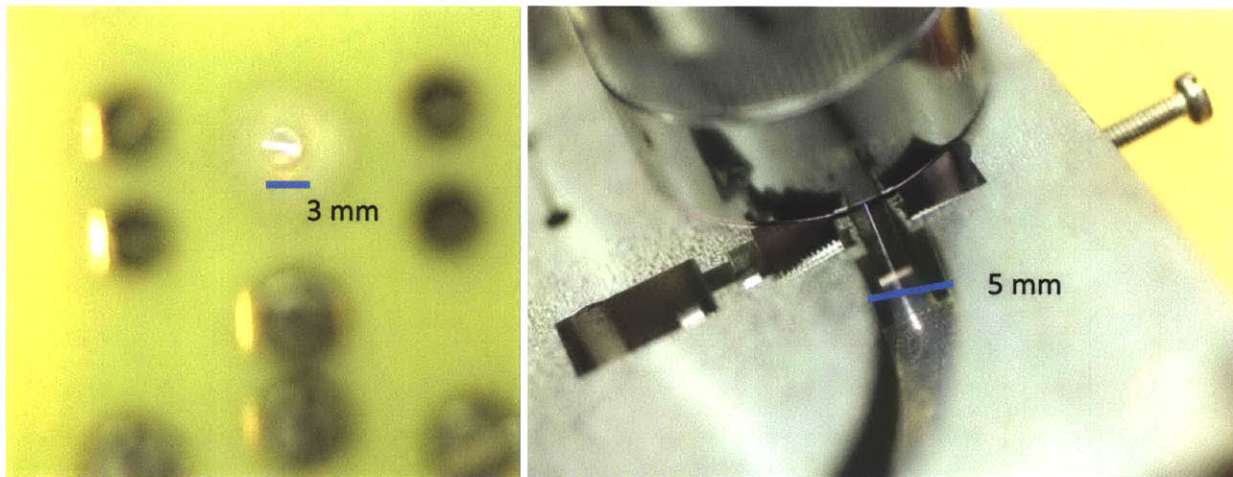


Figure 4-7: A photograph of the entrance slit to the mass analyzer, showing how it may be adjusted.

illuminated from above by a Mag-Lite flashlight, is shown in the right photograph in Figure 4-7.

Once the electrodes are assembled, the mass analyzer's top cover can be fitted and throughbolted with a single M2 screw. The trap electrode is then fitted above the analyzer cover and throughbolted as well.

The whole PCB assembly is then bolted to the magnet yoke; alignment diagrams indicating the relative positions of the magnet poles are etched in the printed circuit board copper layers on the outer sides of the analyzer PCB assembly. Slightly oversized mounting holes allow the magnet to be adjusted slightly to match the diagrams on the outside, thereby ensuring alignment with the now-covered mass analyzer.

The final assembly of the mass spectrometer involves the vacuum chamber. In this prototype, no attempt was made to optimize the vacuum chamber, which need not be any more complicated than a steel or glass cylinder.

The mass spectrometer's magnet yoke was throughbolted to tapped holes in a 6" ConFlat flange. A piece of 1.29 mm outer diameter stainless steel hypodermic tubing for an inlet and a few low voltage wires were fed through holes in the flange and epoxied in place. A photograph of the completed mass spectrometer, attached to the ConFlat flange, is shown in Figure 4-8. The inset photograph is the side of

the vacuum flange opposite the mass spectrometer, showing the electrical and gas connections to the instrument.

In a production version a port for a roughing pump would be needed on this flange; in this case, the roughing port was provided on another end of the vacuum chamber.

The whole mass spectrometer, now mounted on a flange, was inserted into the end of a 6" ConFlat tee. The far face of the tee was fitted with an ion gauge (Duniway Stockroom, www.duniway.com) connected to an ion gauge controller (Varian model 843, www.varianinc.com/vacuum). The third face of the tee was used for the roughing system.

As the initial gas load from this mass spectrometer was expected to be rather high, a powerful roughing system was used. A $0.2 \text{ m}^3/\text{s}$ turbomolecular pump (Varian V-200) was connected to the ConFlat tee, and the turbopump's exhaust connected to a mechanical roughing pump (Welch 1402 www.welchvacuum.com) and cooling provided by a temperature controlled recirculator (VWR Scientific Products www.vwr.com) with distilled water as the working fluid.

A photograph of the vacuum chamber and turbomolecular pump is shown in Figure 4-9.

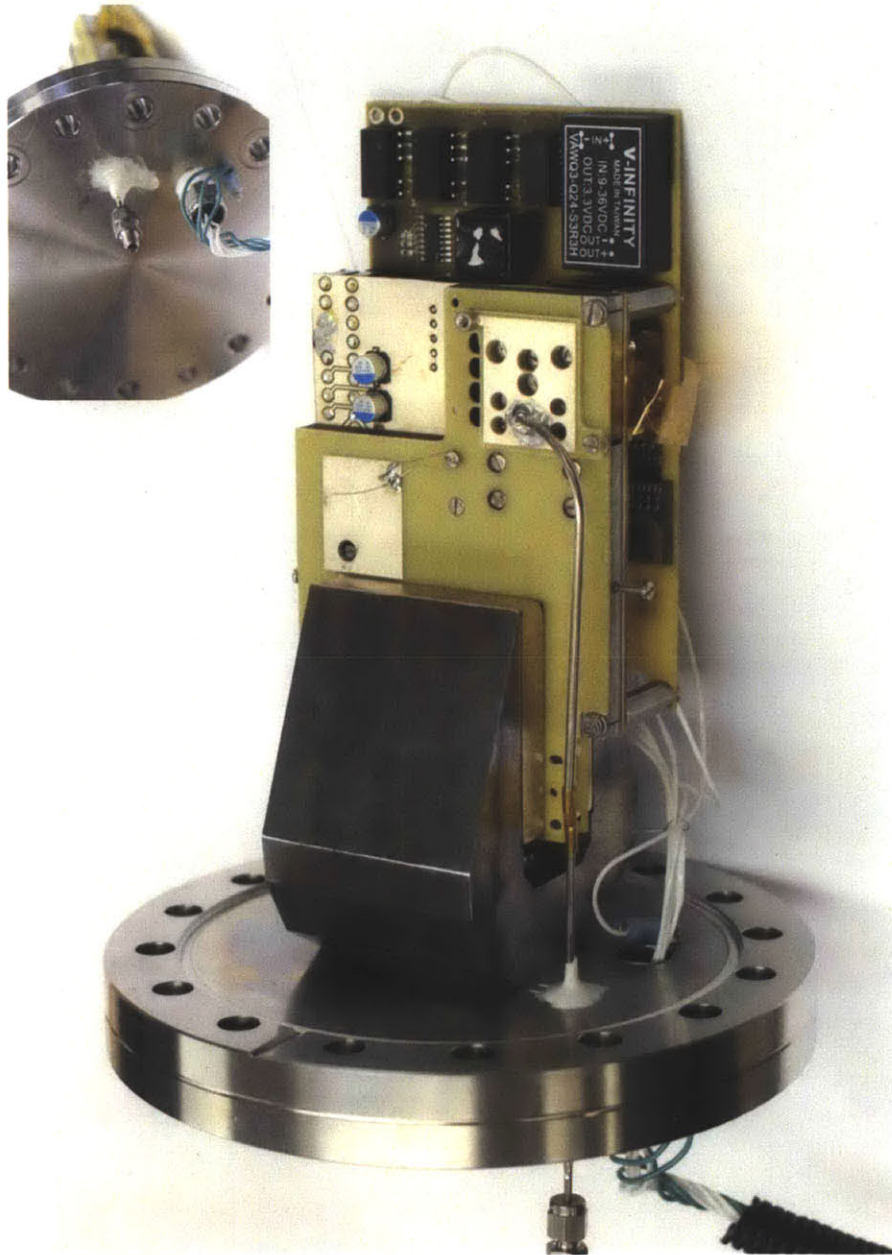


Figure 4-8: A photograph of the completed mass spectrometer, attached to the Con-Flat flange used for testing.

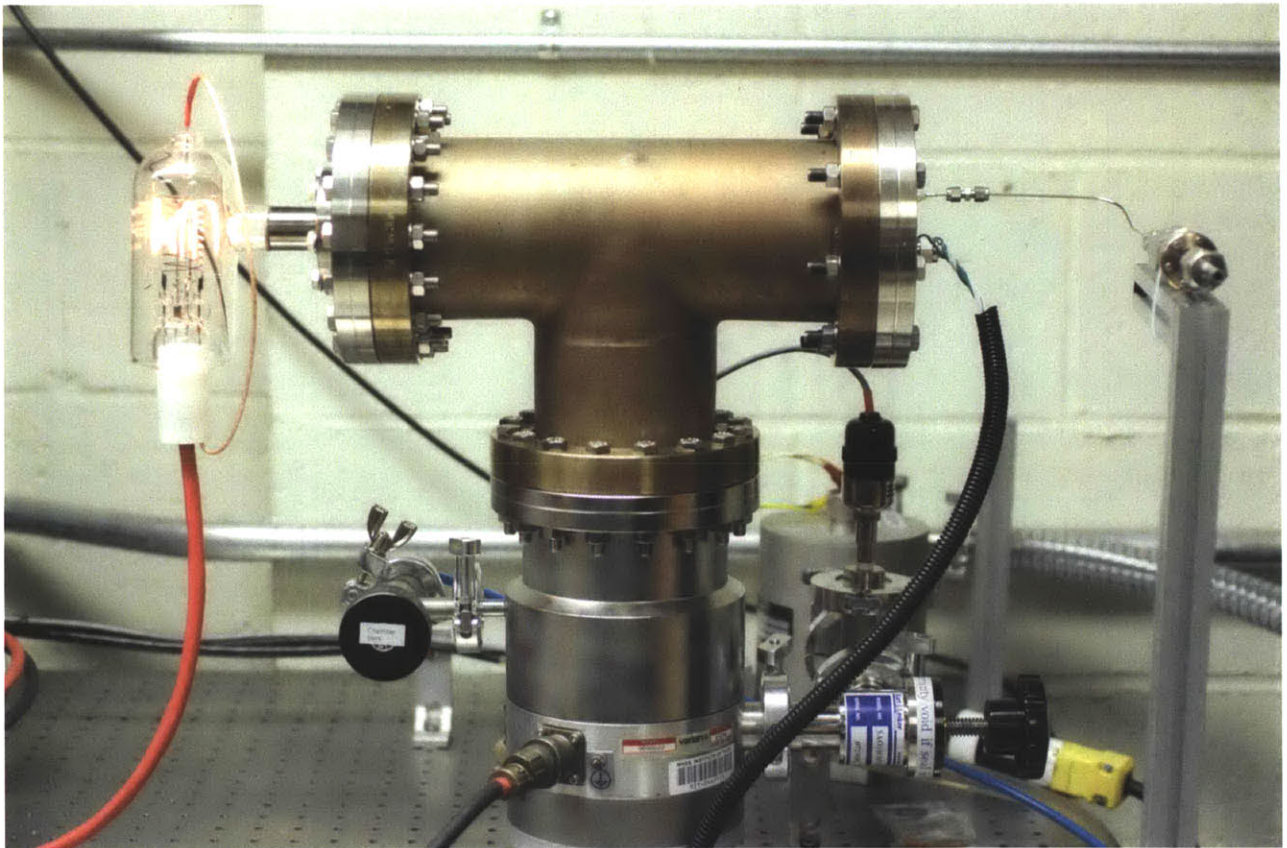


Figure 4-9: A of the vacuum chamber used in the development of the mass spectrometer. The ion gauge is on the left and the turbopump at the bottom.

THIS PAGE INTENTIONALLY LEFT BLANK

Chapter 5

Electronics

The electronics that control the miniature mass spectrometer, aside from the detector, sit on a printed circuit board beneath the mass analyzer board. As with the mass analyzer, the electronics board is fabricated without a solder mask to facilitate outgassing.

Physically, the electronics board is laid out such that 20 mm M3 standoffs can be used to mate it to holes in the analyzer board, and electrical feedthroughs connect the electronics board to the electrostatic elements and detector on the mass analyzer board.

The electronics board consists of two major sections; the power supplies and the digital controller. Multiple independent, isolated supplies are required to operate all of the subsections of the electronics board.

5.1 Power supply

The mass spectrometer operates at a single input supply of +12 VDC, at up to 1.1 A, although typical supply current while operating under normal conditions is 0.5 A. Multiple different supplies are generated internally via dc/dc converters. The +12 V supply also serves as the main supply for the lens drivers, as detailed in a section below. The ground of this supply serves as the system ground and is also tied to the vacuum envelope.

An isolated $+3.3\text{ V} / 1\text{ W}$ dc/dc converter supplies the digital logic. The digital logic includes the microprocessor and the analog I/O modules; these are the DACs and the ADCs that are used to control the mass spectrometer. The digital side of the detector's ADC is also run from the digital logic supply. The ground side of the logic supply is tied to the system ground at a single point.

An isolated $\pm 5\text{ V} / 1\text{ W}$ dc/dc converter followed by a pair of linear regulators provides a $\pm 2.5\text{ VDC}$ supply for the analog stages of the detector. This supply is heavily filtered and lightly loaded, providing supply current for a pair of opamps and the analog half of the detector ADC. The ground of this supply is tied to the system ground right at the detector electrode to minimize noise.

An isolated $+3.3\text{ VDC} / 3\text{ W}$ dc/dc converter provides supply voltage for the filament, which draws nominally a $2.4\text{ V} / 500\text{ mA}$. The ground of this supply is tied to the filament bias supply, which is in turn 70 V below the ion source supply.

An isolated $+3.3\text{ VDC}$ supply, with its ground biased to the trap potential, provides supply voltage for the ADC that measures the mass spectrometer's trap current.

An isolated $+5.0\text{ VDC}$ supply, with its ground biased to the ion source potential, provides the supply voltage for the opamp that drives the repeller electrode.

An isolated $3\text{ kV} / 3\text{ W}$ dc/dc converter provides the anode voltage for the onboard ion pump.

5.2 Ion optics drivers

Five high voltage proportional dc/dc converters provide the electrostatic element potentials. A proportional dc/dc converter generates an output voltage that is linearly proportional to the converter's input voltage, and is useful when a range of output voltages is needed. The input voltage of these dc/dc converters is supplied by operational amplifiers configured such that a fraction of the output voltage of each dc/dc converter is fed back to each opamp, stabilizing the output. The reference for each opamp is provided by a DAC from the digital controller or from a potentiometer for potentials that can be calibrated once and need not change during operation.

These five dc/dc converters supply potentials for the ion source, the ion source's electrostatic lenses, the trap, and the bias for the filament. All of these converters' outputs are referenced to system ground. Although it would have been easier to tie the outputs together appropriately (e.g. reference the trap supply to the ion source supply instead of ground), the output isolation rating of each of these dc/dc converters was not sufficient to do so.

5.3 Electrometer

The electrometer connected to the Faraday cup electrode is a sensitive transconductance amplifier connected to an analog-to-digital converter. The transconductance amplifier is a National Semiconductor LMP7721 operational amplifier in transconductance configuration with a gain of 5×10^{10} . In parallel with the feedback path is a 5 pF silver mica capacitor; the capacitor decreases the amplifier's gain at high frequency, thereby cutting down on the high frequency noise present at the amplifier's output.

Due to the electrometer's high gain, leakage currents can cause drift in the electrometer output. To help minimize this, a guard ring surrounds the junction connecting electrometer's input pin, one end of the feedback resistor and capacitor, and the Faraday cup electrode. This guard ring is driven by a second operational amplifier, a National Semiconductor LMP7715, in unity gain voltage mode whose input is derived from the noninverting and nominally grounded (and slightly offset due to bias currents) input of the electrometer.

The output of the transconductance amplifier is directly digitized by a Texas Instruments ADS1281 24-bit analog-to-digital converter.

The entire electrometer circuit is mounted on the analyzer PCB inside a pocket cut into the mass analyzer electrode. The electrode, in conjunction with copper on the two PCBs, serve to encase the electrometer inside a Faraday cage. The close proximity of the electrometer to the Faraday cup detector electrode minimizes the opportunity for noise to disrupt the signal.

5.4 Degas Heater

The printed circuit boards in the vacuum chamber were expected to carry a fairly large gas load. As such, a network of distributed resistors was added to the printed circuit boards to ensure that the board temperatures could be raised far enough to help remove the gases absorbed and adsorbed by the PCB. Multiple 1 W resistors, operated by the main +12 VDC supply, are placed in strategic locations and gated by a P-channel FET as an on/off or PWM heating control.

5.5 Digital controller

The heart of the mass spectrometer's controller is a 32-bit ARM Cortex-M3 microprocessor manufactured by STMicroelectronics (STM32F103CBT6). The analog data used to operate the mass spectrometer are digitized by Analog Devices AD7680 and AD5662 ADCs and DACs, respectively. These devices are 16-bit serial ADCs and DACs, addressed over a common serial peripheral interface (SPI) bus on the microcontroller. A block diagram of this system is shown in Figure 5-1.

There are three AD5662 DACs, used to set the potentials on the the ion source supply and the two electrostatic lenses.

There are two AD7680 ADCs, used to measure the filament drive current and the trap current. The two ADCs are both operating on supplies biased at high voltage; the SPI bus for these devices is isolated from the logic-level bus by Avago Technologies ACSL-6410 bidirectional (3/1 channel) optoisolators.

The AD5662s and AD7680s, as well as the electrometer ADC, are connected to the microprocessor's SPI bus. Each ADC and DAC has its own dedicated microprocessor GPIO pin for addressing. Additionally, several GPIO lines run to the electrometer ADC for other functions (e.g. data ready, reset).

A Maxim Integrated Products MAX6696 port expander / LED driver is also connected to the SPI bus and three RGB LEDs, used for user feedback.

A pin connected to a hardware timer on the microprocessor is used as the gate

drive for a P-channel FET connected to the filament. The filament is driven in a pulse-width modulated manner for maximum efficiency. Switching frequency is 100 kHz, but can be changed during operation if interference is detected.

Other pins on the STM32F103CBT6 are used to control other peripherals. Several of the power supplies, including the filament and most of the high voltage supplies, and the degas heater, are gated by large P-channel FETs. The FETs are driven by microprocessor pins, such that the filament and HV supplies can be shut down to save power when the mass spectrometer is not being used.

A pair of pins is used to control and monitor the ion pump. One pin enables the ion pump so that the controller can be run at atmospheric pressure without the ion pump arcing. The other pin is used, as an analog input connected to the microprocessor's onboard 12-bit ADC, to monitor the terminal voltage of the ion pump supply.

Two pins connected to a hardware USART transceiver in the microprocessor are the mass spectrometer's means of communication with the outside world. These pins pass through the wall of the vacuum chamber (although the data could be passed optically if the vacuum housing were made of glass).

In this prototype, the three serial wire programming (SWP) pins specific to the Cortex-M3 were also passed through the vacuum housing, so that the microprocessor's code could be reconfigured without requiring venting the vacuum chamber.

5.6 Control Software

The control software for the mass spectrometer is written in the computer language C and compiled for the Cortex-M3 core using the IAR Systems Embedded Workbench IDE and compiler.

The main execution loop is a finite-state machine that controls the basic operations required to produce mass spectra. During each loop cycle, the mass spectrometer reads all of the available data indicating the states of the external variables and then executes code that depends on the state of the instrument. One of the LEDs is tasked with blinking a color depending on the state of the machine. The blinking speed is

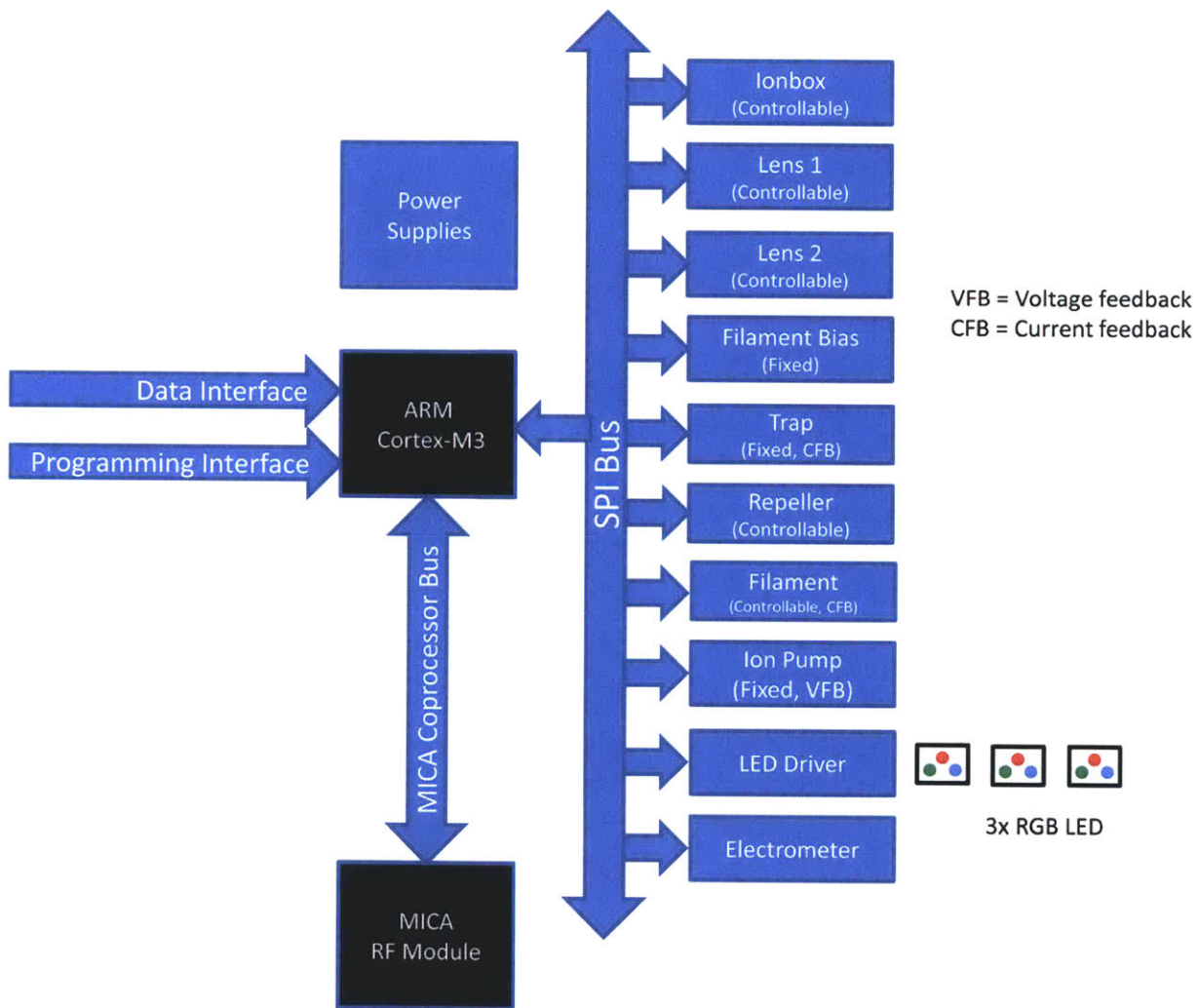


Figure 5-1: A block diagram of the digital controller for the mass spectrometer.

controlled by the main execution loop, providing visual feedback that the code has not locked up. The following sections describe the states in more detail.

5.6.1 Boot

At boot time, the mass spectrometer checks the state of the state of all of the peripherals attached to the buses. Most of the peripherals, the ADCs and the various power supplies, can be checked by interpreting the data they provide. Failure of any of the self checks causes the mass spectrometer to go into fault mode.

5.6.2 Standby

In standby mode, the microprocessor shuts down all of the peripherals except, optionally, the ion pump and degas heaters. In this minimal power consumption mode, the system draws less than 1 W, which is ideal for battery-powered instrumentation not involved in constant measurements.

5.6.3 Idle

In idle mode, the microprocessor brings all of the high voltage supplies and the filament supply online. The filament is operated at reduced voltage to maximize its lifespan. In this mode, the microprocessor can ensure that the HV supplies are functioning properly and that the filament has not burned out. During transitions to idle mode, the filament is brought to temperature slowly to minimize thermal shock. The filament warm-up time is 0.5 s.

5.6.4 Sweep

In sweep mode, the microprocessor is actively driving the electrodes and measuring the ion currents. The ion source supply is brought to the minimum voltage achievable by the hardware, approximately 150 V, and swept through to about 800 V at about 20 V/s. The electrostatic lens voltages are also constantly changed to properly focus the ion beam at each ion source potential.

Electrometer current is sent out the serial port to a laptop connected to the mass spectrometer. Data may be collected with a simple terminal program; when running mass scans, the data are outputted as columns of text which may be captured on the laptop and opened as a comma-separated-variable (.CSV) file in most data analysis programs.

The mass spectrometer is controlled by a serial terminal interface that is accessed via a PC. The terminal program on the mass spectrometer allows commands to be sent and interpreted, mostly for debugging purposes, but also for controlling the state of the machine. The command "mode" with an argument specifying a new state, allows the user to switch between the modes of operation as detailed above. The commands "filament", "repeller", "ionbox", "lens1", and "lens2", with an argument such as a floating point number or on/off (e.g. "filament off" or "ionbox 500.0"), allow the user to directly control the various electrodes in the vacuum chamber. Other commands, "degas", "ionpump" allow the user to turn these peripherals on and off remotely, as the microprocessor can't know when these features should be enabled or not.

5.7 Known Issues

The primary issues with this controller both involve the analog-to-digital converters that measure the filament drive current and trap current. These ADCs both tend to give erratic data due to the fact that they are improperly referenced. Neither ADC was fitted with a dedicated reference supply; instead, they rely on the regulator in the supply bus, which is not stable enough for accurate measurements. This is an oversight and marked for attention in the next version of the controller.

A related issue is the power supply for the filament bias. The -70 V filament bias supply input side is run off of the +3.3 V filament supply. The filament adds enough noise to the rail to make the supply slightly noisy. The next version of the controller will operate the filament bias supply from the +5 V ion source biased supply.

Chapter 6

Testing

The mass spectrometer was subjected to extensive testing of both subassemblies as well as the complete system.

6.1 Power and Control Systems

All of the power supplies were powered on and tested for nominal voltage. Particular attention was paid to the $\pm 2.5\text{V}$ analog electrometer supply, as the noise figure of this supply directly impacts the electrometer noise floor by the CMRR of the electrometer opamp.

The control software was tested by verifying that the mass spectrometer could run in all modes for several days without crashing.

The various modes of operation were examined for power consumption. Below is a table of the power consumption of each mode, Table 6.1. Note that in every mode of operation the instrument draws less power than any other existing miniature mass spectrometer. Currently, the portable mass spectrometer with the lowest published current draw is the Purdue Mini 11, which consumes 70 W.

The ion pump draws 3 W, although this amount of power was not quite enough to sustain the pump.

Table 6.1: A table of mass spectrometer supply current in different modes of operation.

Mode	Current [A]
standby	0.05
idle	0.30
idle, degas on	0.55
sweep	0.60

6.2 Electron Beam

Operation of the electron beam is the first diagnostic of a mass spectrometer. Operation is generally characterized by the trap current. The trap current is the fraction of the electron current that is emitted from the filament, passes entirely through the ionization region, and collected at the trap electrode.

The trap current should be directly proportional to filament brightness, which is itself a strongly nonlinear function of filament power. Above a certain power level, trap current begins to rise rapidly while filament life decreases.

Filament intensity as a function of filament voltage V is proportional to $V^{3.4}$ while filament lifetime is proportional V^{-16} . Thus there is strong incentive not to overdrive the filament.

The filament used in this mass spectrometer is that of a standard PR-2 tungsten flashlight bulb. This type of bulb is rated for a 15 hour lifespan at 2.4 V and 0.5 A. Operating at reduced voltage will increase its lifespan. For example, at 2.3 V the filament will retain 86% of its brightness while doubling its lifespan to 30 hours.

The trap current was measured at two different filament voltages, summarized in Table 6.2.

The trap current was somewhat rather variable during different experiments, dropping to 25 μA during some tests even at an operating voltage of 2.4 V, possibly due to the fact that the mass spectrometer was frequently disassembled and reassembled, changing the exact orientation of the filament with respect to the ionization region.

Table 6.2: A table of trap current as a function of filament voltage.

Filament Voltage [V]	Trap Current [μ A]
2.0	10
2.2	19
2.4	45

6.3 Degas Heater

The degas heater is a network of resistive heaters connected to the various mass spectrometer boards. It is designed to help remove the absorbed and adsorbed gases on the PCB substrate boards by raising the temperature of the boards. This feature is unique to this miniature mass spectrometer.

For the heater to be of use, it should be possible to turn the heater on under vacuum, see a rise in chamber pressure as gas is driven off, then see the pressure fall to a level below the initial level when the heater is turned off again.

An experiment was run to test the degas heater. The mass spectrometer was installed in a vacuum housing and pumped down. When the chamber pressure had stabilized, the heater was switched on, then off again approximately three hours later. This data is shown graphically in Figure 6-1.

Note the relatively slow initial decrease in chamber pressure followed by the rise in chamber pressure when the heater was switched on. The gas is driven off and the chamber pressure begins to fall, at which point the heater is then switched off. At this point the power electronics are activated, which produce their own heat and drive gases off the electronics board.

In the future these two cycles can be run concurrently, however, they currently produce too much heat to operate simultaneously without damage.

A second experiment was run to observe the transient behavior of the heater. The mass analyzer board was placed beneath a FLIR ThermoVision A40 (www.flir.com) thermal imaging camera and the thermal transient behavior observed over time. The result is shown in Figure 6-2.

While the temperature rise is modest in absolute value in this series of frames, this

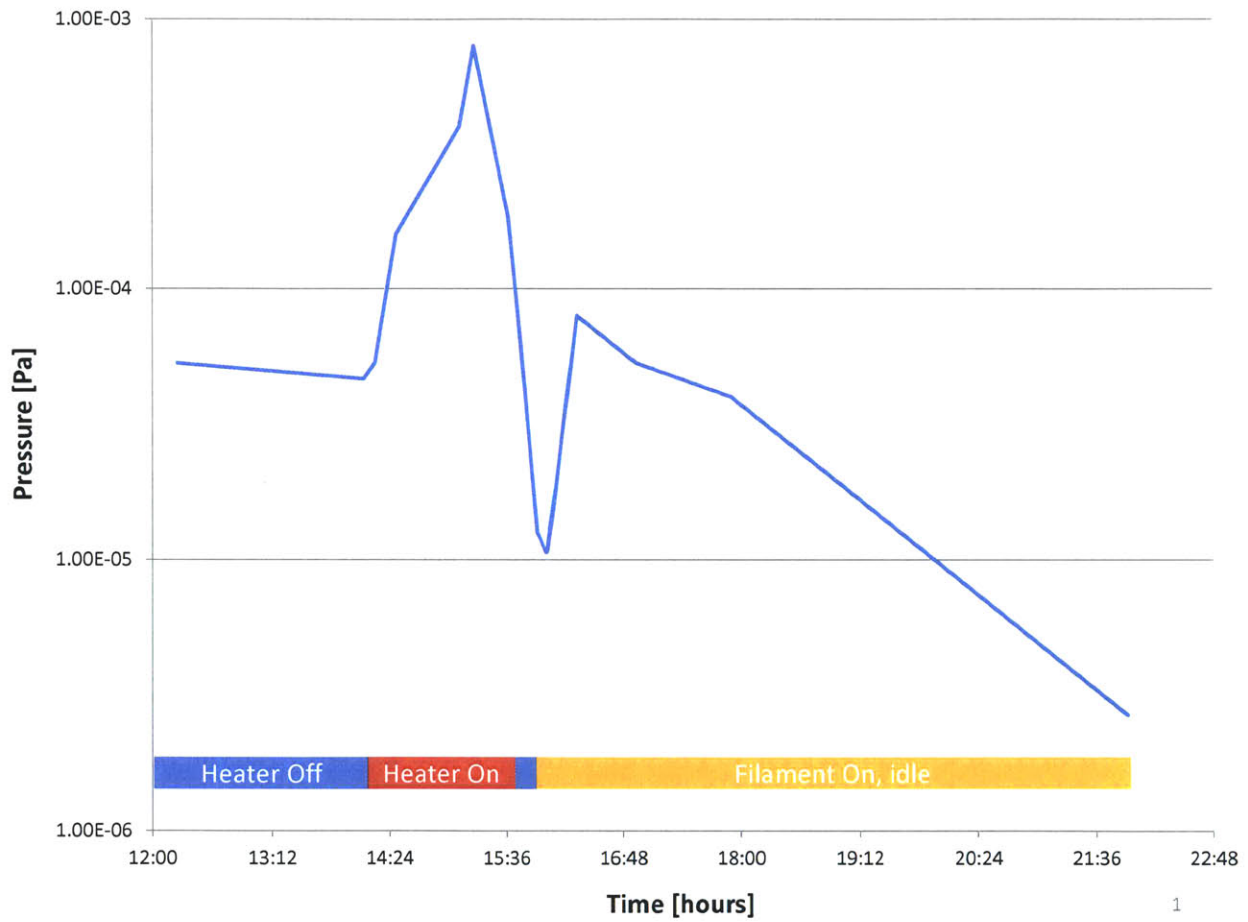


Figure 6-1: A graph of chamber pressure verses time, with the heater transitions indicated.

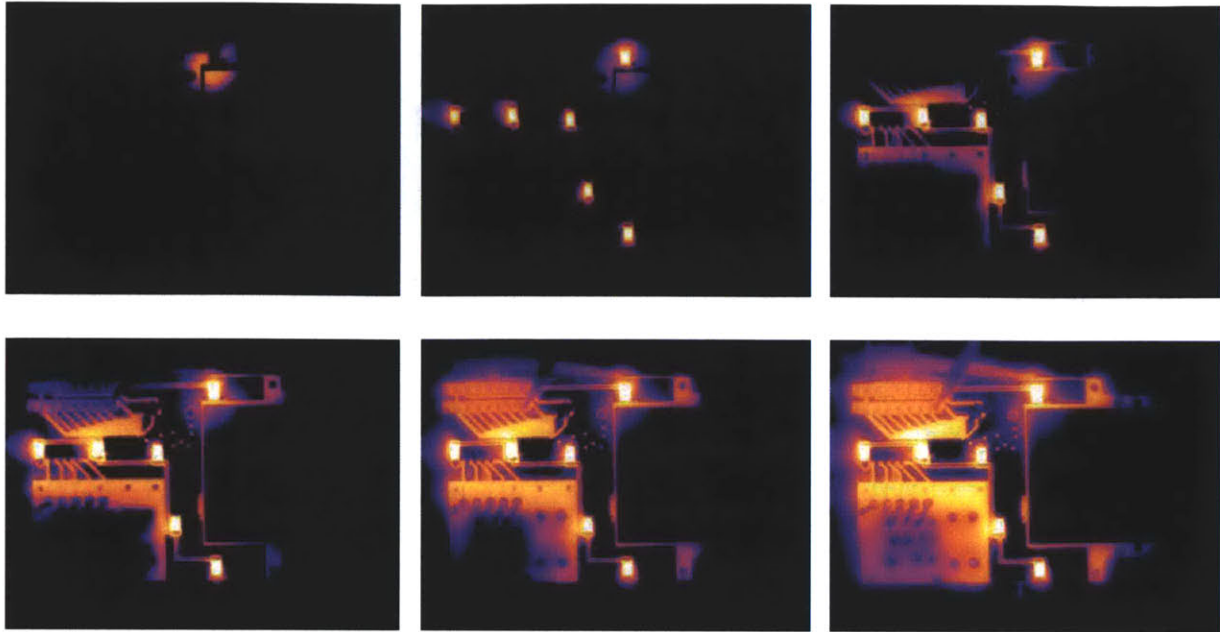


Figure 6-2: A series of thermal images taken at 0, 10, 20, 60, 300, and 600 s after the heater is activated. Thermal range is 30 ° C (black) to 60 ° C (white).

experiment was run in air. In vacuum there is no convection to cool the surfaces and the temperature rise should be substantially faster, though the heat will flow roughly in the pattern observed here.

There is no temperature feedback control on the heater system in this version, however, the temperature the boards reach in vacuum is quite high. One experiment with the degas heater led to the destruction of one dc/dc converter on the lower printed circuit board by thermal damage; the markings on the potting of several dc/dc converter housings had also flowed under the heat.

6.4 Lens Linearization

Despite all attempts to ensure that the feedback control loop wrapped around each of the lens drivers was accurate, there was some variation between lens commands and lens voltages. A calibration was thus run on the ion source potential and the

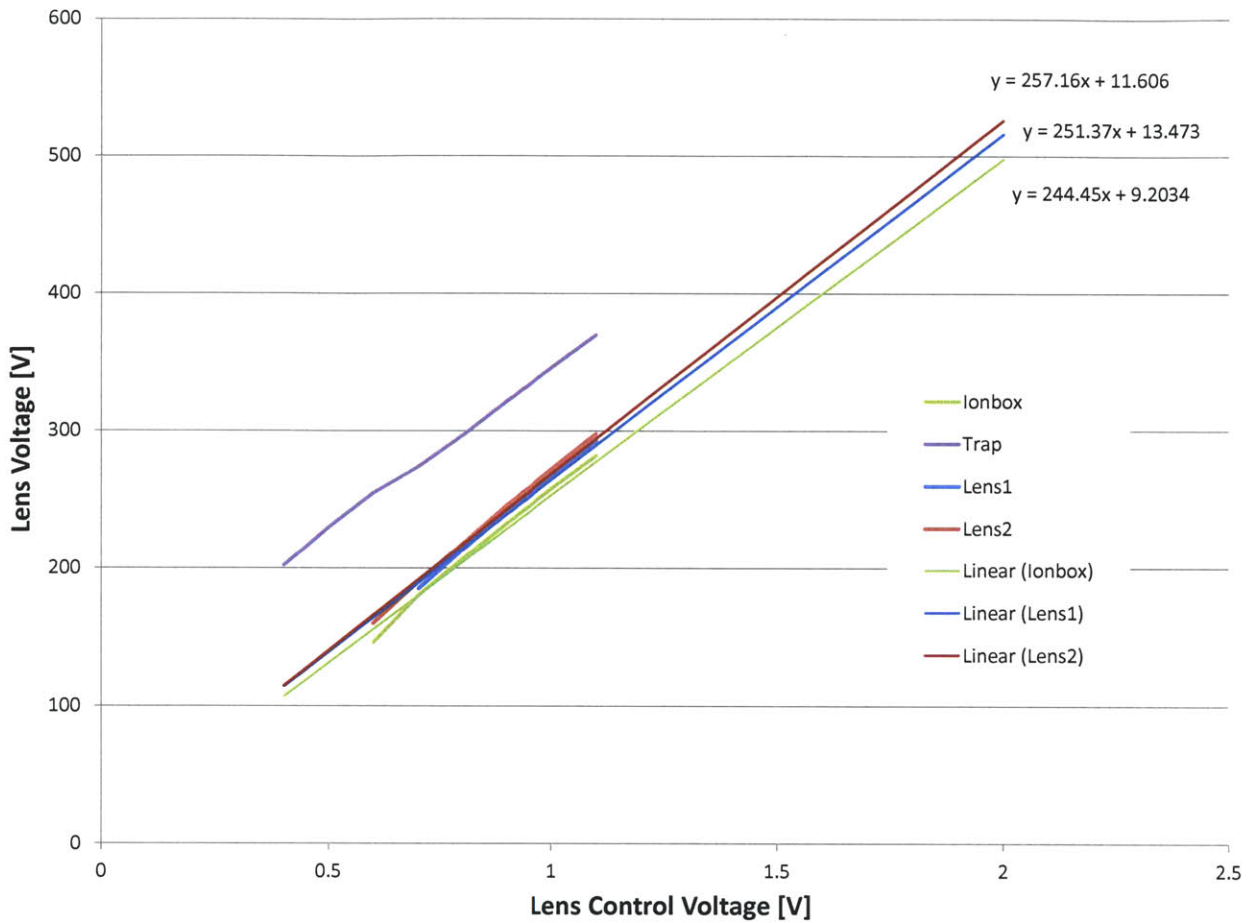


Figure 6-3: A graph of the microprocessor’s command voltage versus the actual output of each lens driver.

two electrostatic lenses. This calibration curve was linearized and programmed into the mass spectrometer controller’s code to ensure that the correct voltages are being output to the lenses. Figure 6-3 shows the relative calibrations of each lens driver.

While the lens drivers were similar, as they should have been given that they were constructed using identical hardware, they varied by a few volts. This may not seem very important, but the potential energy surface in Chapter 3 indicates how carefully some of these voltages must be aligned; a lens tuned incorrectly can severely limit or block the ion beam, eliminating the signal.

6.5 Ion Pump

The miniature cofabricated ion pump was tested on its own after the system had been pumped down to 2.6×10^{-6} Pa [2.0×10^{-8} torr]. The ion pump was started at 2.6×10^{-4} Pa [2.0×10^{-6} torr] and operated in conjunction with the vacuum chamber's turbopump until the pressure reached 2.6×10^{-6} Pa [2.0×10^{-8} torr], at which point a valve inserted between the turbopump and the chamber was closed.

This is the process by which mass spectrometers would be commissioned; at first, the miniature ion pump needs to be heated to drive off the adsorbed gases and will be run in conjunction with a second high vacuum pump until the ion pump is ready carry the gas load.

This process takes approximately 15 hours without using the mass spectrometer's onboard heater. A graph of this commissioning process is shown in Figure 6-4.

An expanded graph of the last few minutes of operation, following the closure of the turbopump valve, is shown in Figure 6-5.

The ion pump was disassembled afterward; the titanium cathode plates were pitted in the center of each pump cell, and the anode was plated with sputtered titanium. See Figure 6-6.

6.6 Mass Spectra

For this mass spectrometer, spectra will appear as ion beam current as a function of ion source potential. While the microprocessor could have been programmed to output ion current versus mass to charge ratio, for this prototype the mapping between ion source potential and m/z is done in post-processing of the data. Large numbers of mass sweep tests were run on the miniature mass spectrometer. Between tests, many optimizations were made based on the resultant data.

Optimizations were generally minor and included adjusting the variable-geometry mass analyzer slits, electrometer hardware (e.g., feedback resistor, capacitor), and modifying the software to optimize filament power, electrostatic lens potentials and

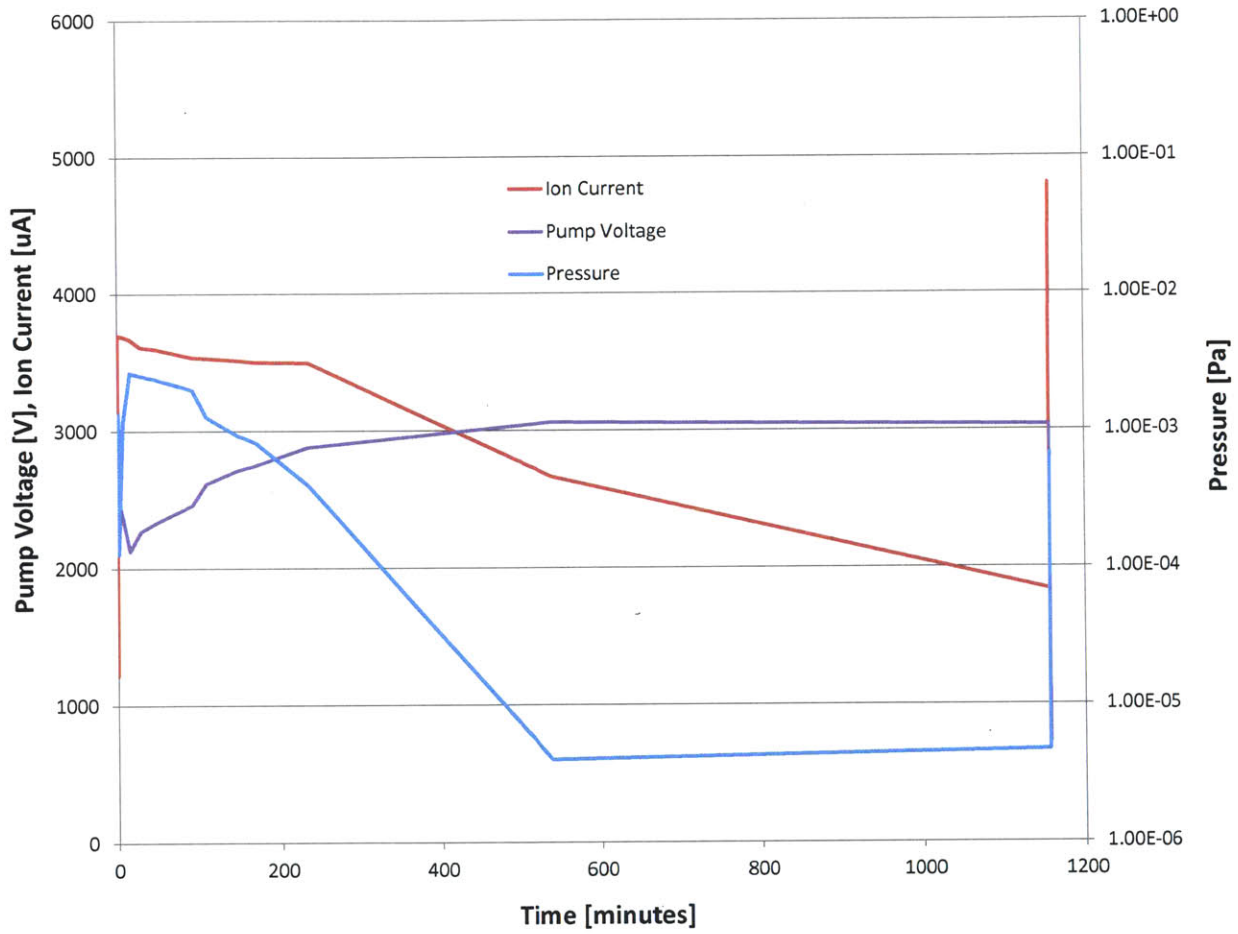


Figure 6-4: (top) A graph of the system pressure, ion pump voltage and ion pump current.

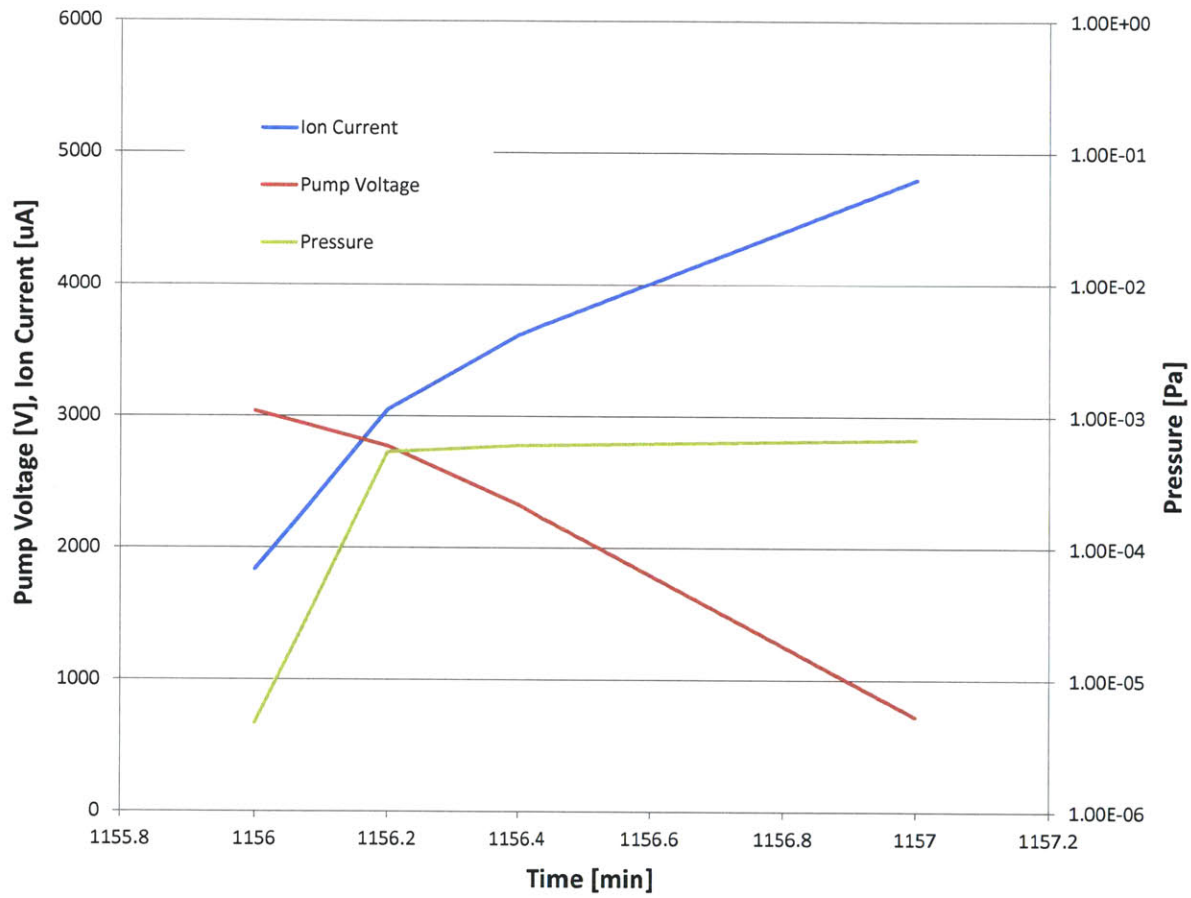


Figure 6-5: A graph of the system pressure, ion pump voltage and ion pump current, in the minutes following segmentation of the vacuum system. Note that the system pressure remained relatively constant at 8×10^{-4} Pa [6×10^{-6} torr], but the pump failed because the power supply voltage collapsed. The supply could provide only 3 W.

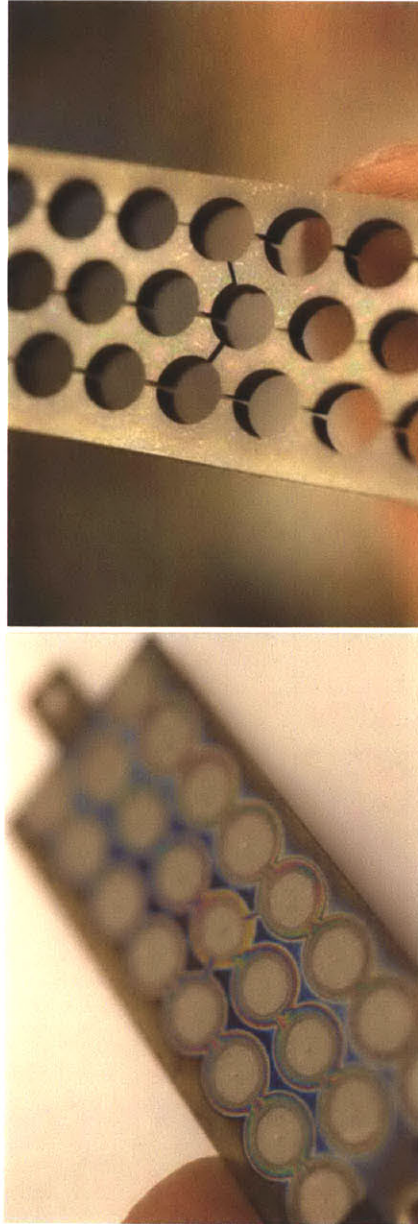


Figure 6-6: A photograph of the plates of the disassembled ion pump. Colored deposits are likely chromium from the stainless steel anode.

ion source voltage sweep rate and range.

Figure 6-7 shows a mass spectrum collected from an early prototype of the miniature mass spectrometer. This is an example of a poor mass spectrum; the resolution is poor, and the noise floor is high relative to the signal strength. The large centered peak is likely nitrogen while the peak on the right side of the graph is water. Oxygen likely appears, as a peak protruding from the left shoulder of the nitrogen peak; this early prototype mass spectrometer did not have sufficient resolution to separate masses that were distant by 4 AMU.

However, this spectrum does show an interesting feature; the ion beam has been chopped using the digital controller to modulate one of the electrodes. While not entirely successful (ideally, the chopping would bring the signal to zero, not just reduce its intensity), the concept of actively modulating an ion beam is sound.

Subsequent generations refined the concept through small changes, arriving at the instrument discussed in this thesis. The subsequent data presented here have been corrected for the inverse relationship between acceleration potential and mass/charge ratio.

Figure 6-8 is a mass spectrum captured by the latest version of the mass spectrometer, with prominent peaks highlighted. Note the peak at m/z of 29, this is likely an isotope of nitrogen, $^{15}\text{N}^{14}\text{N}$, which is present in air with a 0.36% abundance relative to $^{14}\text{N}^{14}\text{N}$.

One interesting feature observed is that the mass spectrometer functions, albeit with a lower signal to noise ratio, even if the electrostatic lenses are disabled (e.g. the lens is programmed not to alter the beam). This result was used to characterize the effect of the electrostatic lenses. Figure 6-9 is a pair of spectra, one run with the lenses off, and another run with the lenses on. The lenses give nearly a factor of ten increase in signal strength without increasing the noise floor. This is extremely valuable in mass spectrometry, and shows how attention to capturing and analyzing a larger fraction of the ions generated can produce a stronger signal.

The lenses were tuned initially by hand; the ion source was set to a potential with a known ion species, and the lenses were then tuned for maximum signal. Several

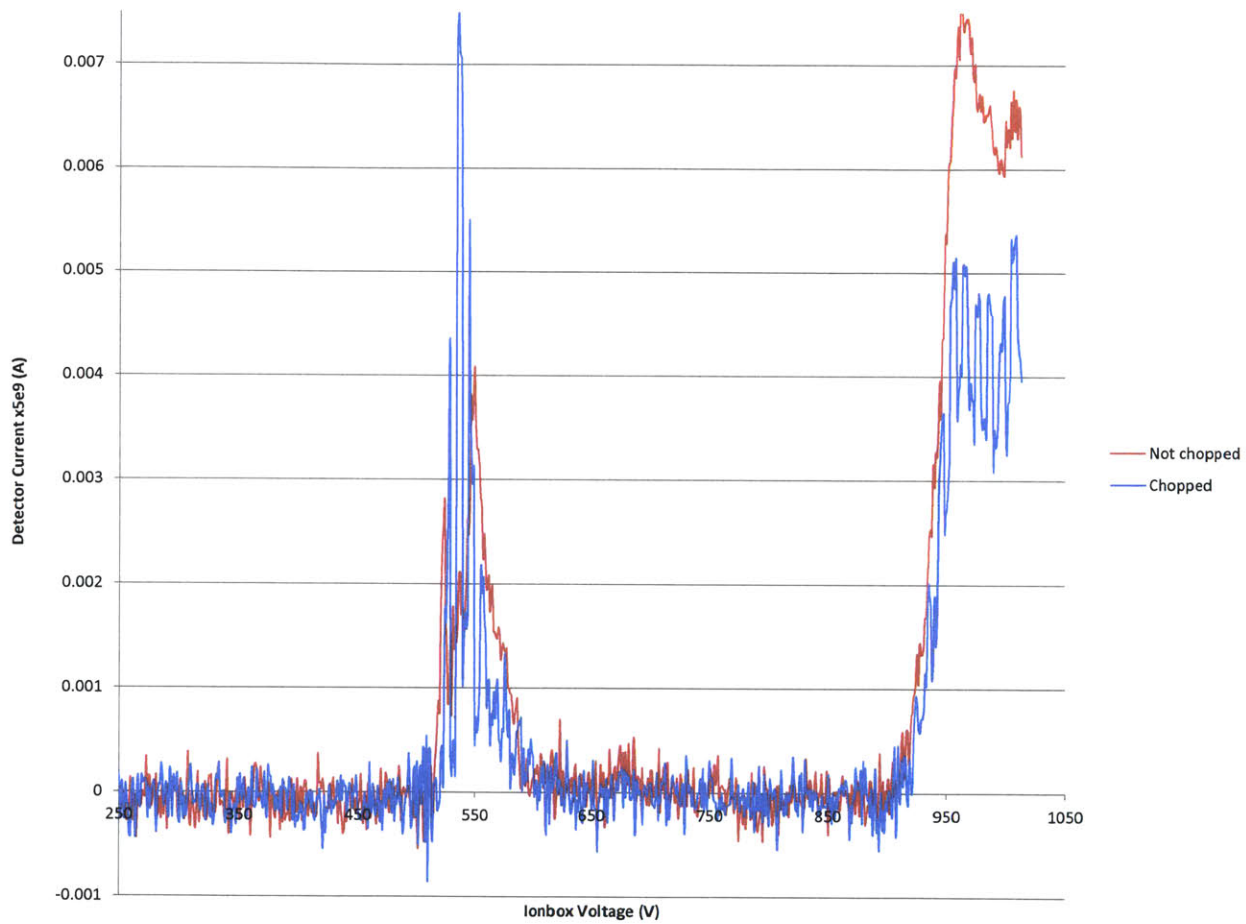


Figure 6-7: A mass spectrograph captured by an early variant of the miniature mass spectrometer prototype.

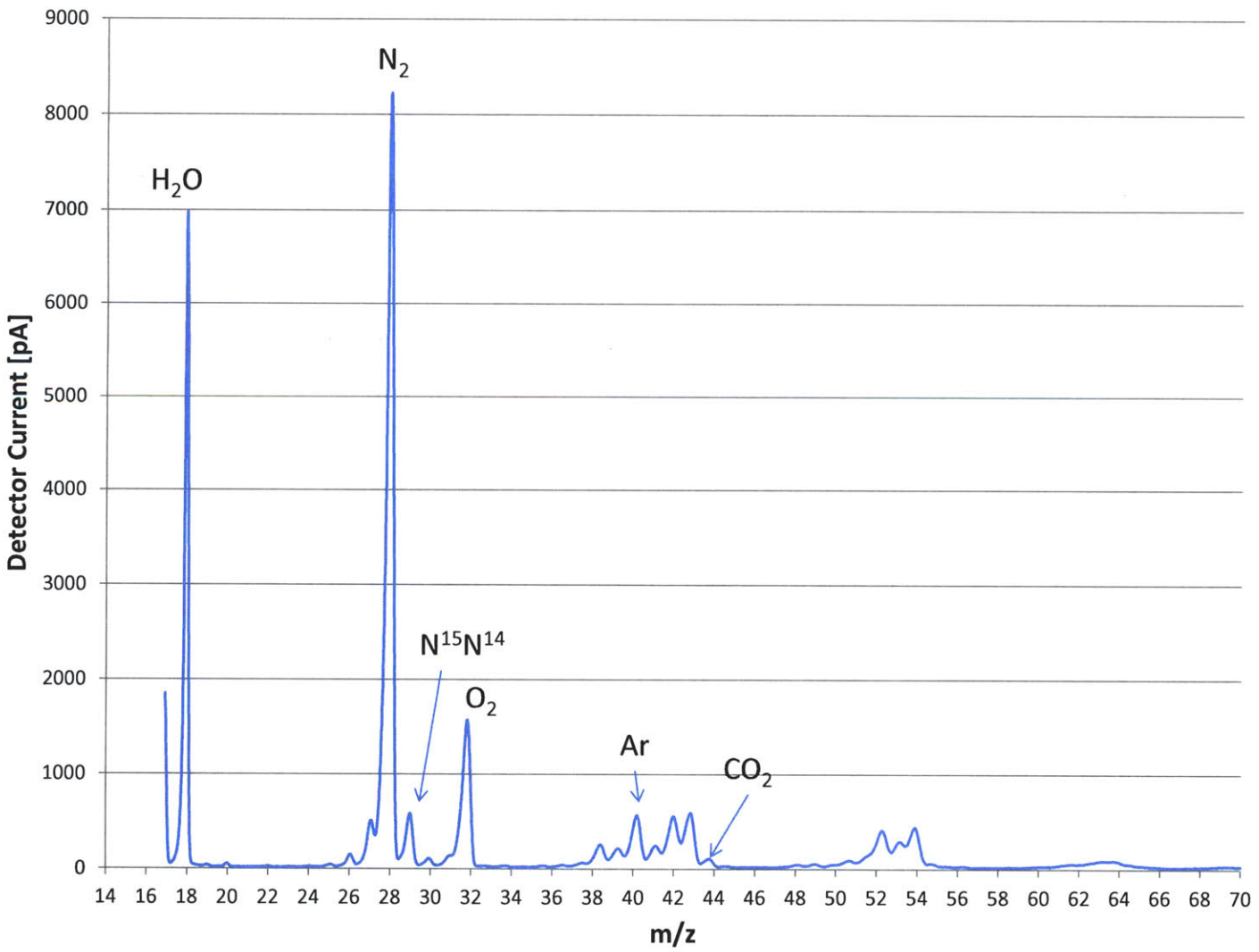


Figure 6-8: A mass spectrograph of air captured by the instrument described in this thesis.

ions were tuned and the resultant curve fitted with a linear interpolation.

Figure 6-10 is a mass spectrum of air indicating the effectiveness of the variable geometry slits. Although several other factors have changed, including the overall gain of the system, the salient features of this comparison are visible at the bases of the peaks. The peak for m/z 27 and 26 are both visible in the red curve, with narrower slits, while they are completely invisible in the blue curve, made with wider slits.

6.7 Introduction of New Species

The real test of a mass spectrometer, however, is whether or not it is capable of detecting a new species entered into the inlet. Figure 6-11 is a test of the mass spectrometer's detection capabilities. A sample of nitrous oxide (N_2O) was injected into the inlet and the mass spectrum sweep run. The control run, in blue, shows the standard spectrum; water, nitrogen, oxygen. The run containing nitrous oxide shows several new peaks. N_2O shows up quite clearly at m/z 44, and another species, the fragmentary ion NO shows up between oxygen and nitrogen, at m/z 30.

6.8 Ion Source Modulation

The grid of the ion source was used to remove the background drift, or $1/f$ noise, of the electrometer. Figure 6-12 is a series of spectra generated using the grid as a modulation source. The blue curve is the baseline curve, generated when the grid is biased such that the ion beam is cut off. The red curve is the signal curve, generated with the ion beam enabled. The green curve is a subtraction of the two, the signal with the baseline offset and drift removed.

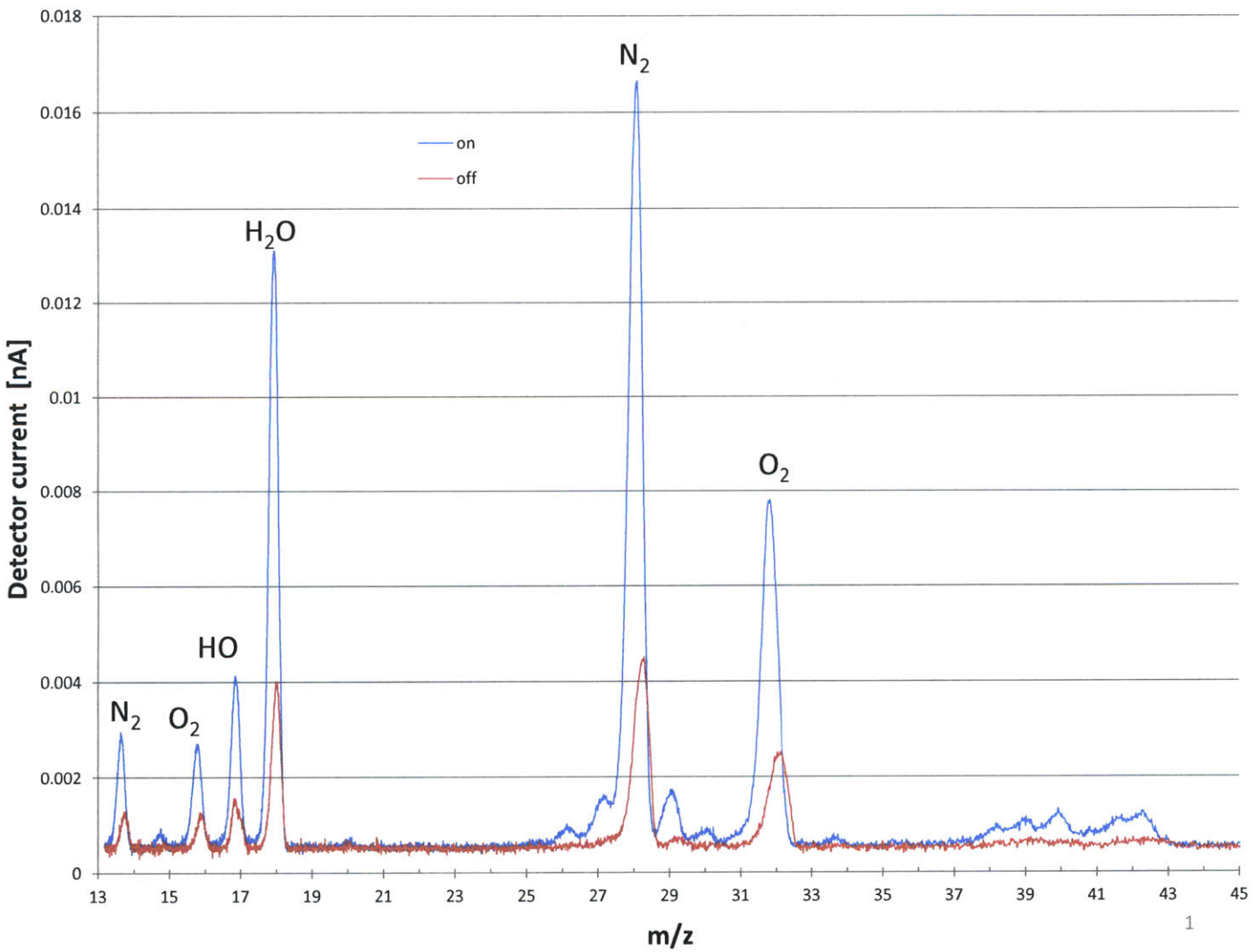


Figure 6-9: A mass spectrograph indicating the value of capturing and using a larger fraction of the ions generated by the electron beam. The signal displayed in the blue curve, in which the electrostatic lenses are active, is nearly an order of magnitude higher than the red curve, in which the lenses were disabled.

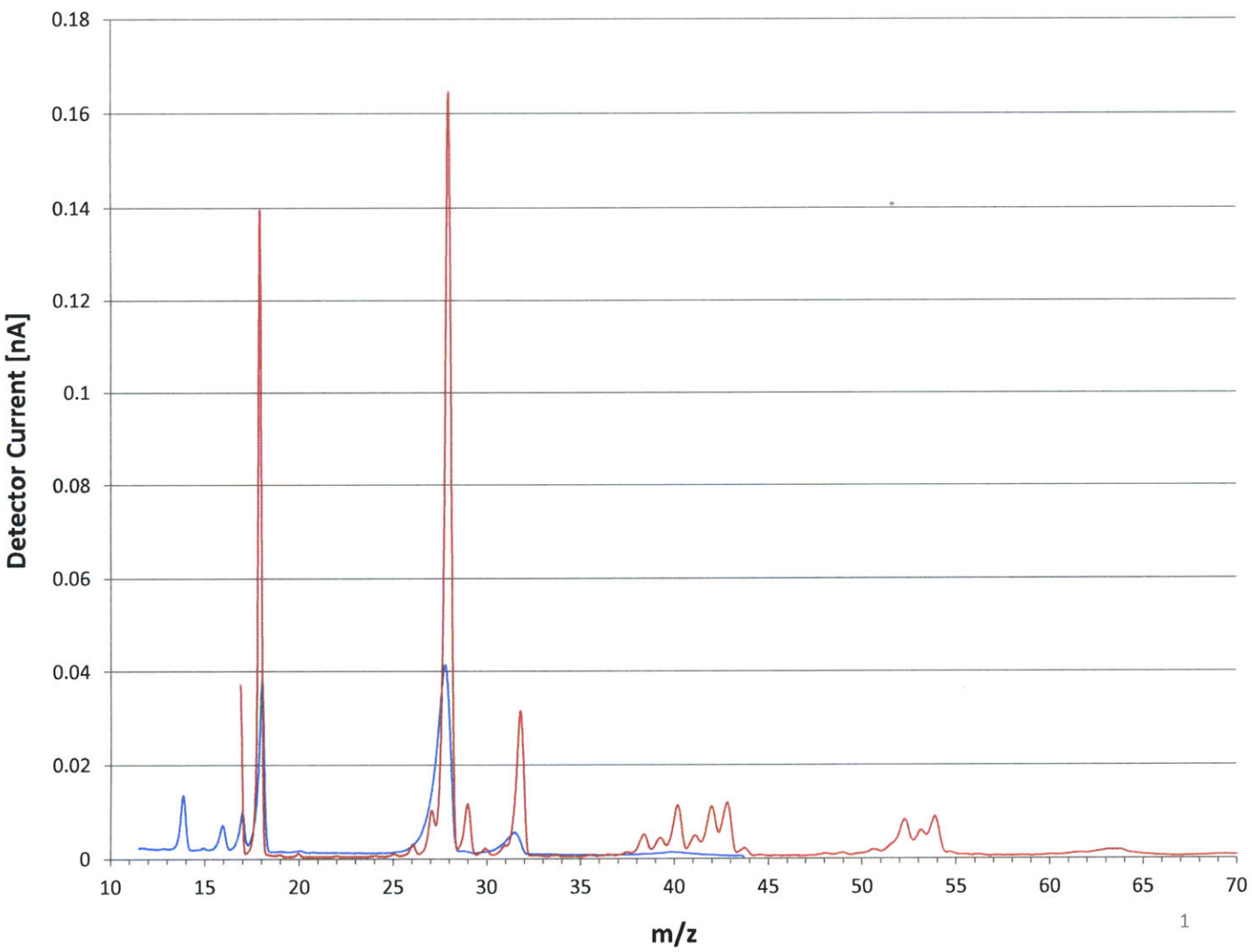


Figure 6-10: A mass spectrograph indicating the effectiveness of narrowing the slits that filter the ion beam. Peaks such as m/z 27 and 26 are invisible with wider slits, as shown in the blue curve, but readily visible in the red curve, with narrow slits.

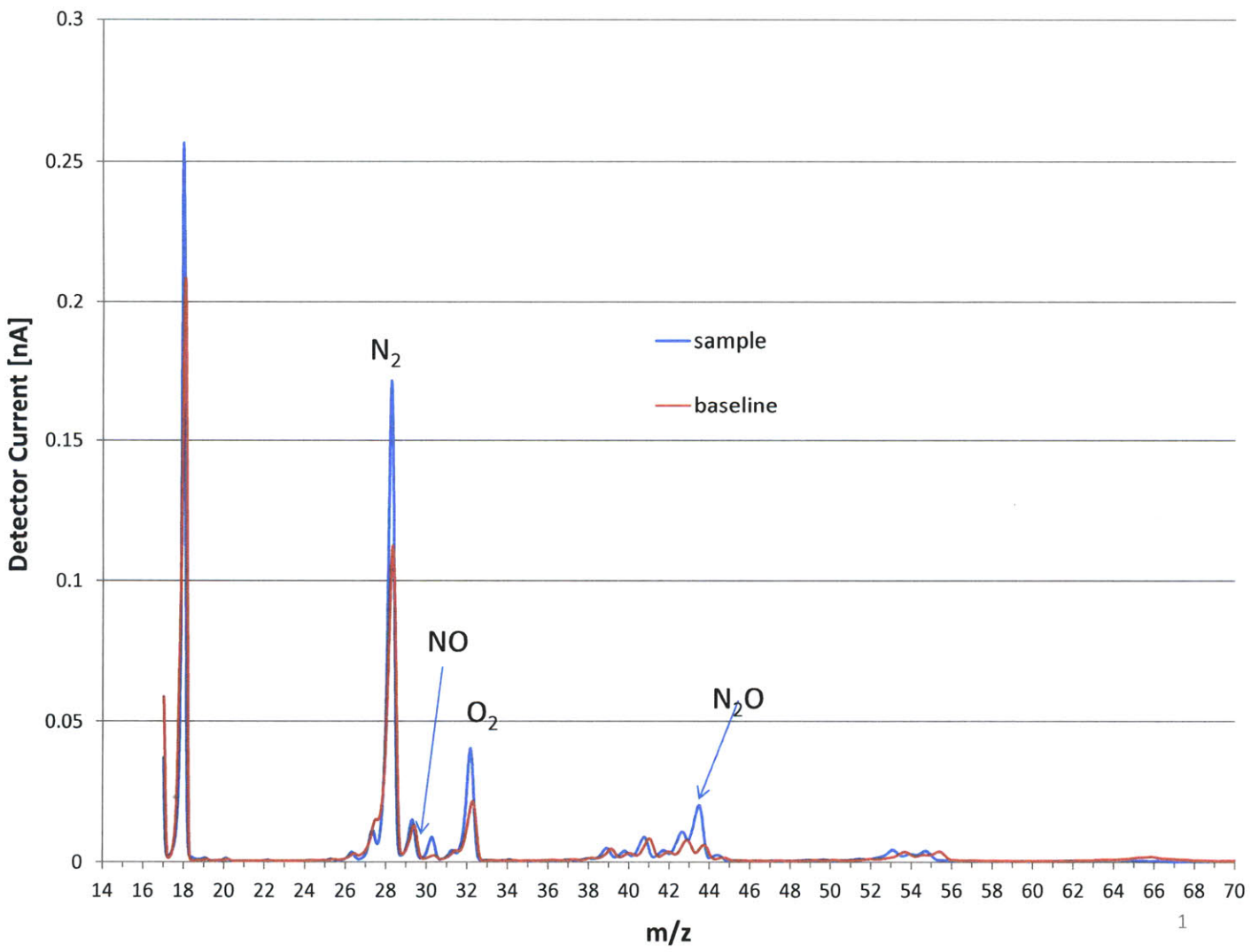


Figure 6-11: A mass spectrograph showing the detection of a new species, nitrous oxide or N₂O, and its fragmentary component NO.

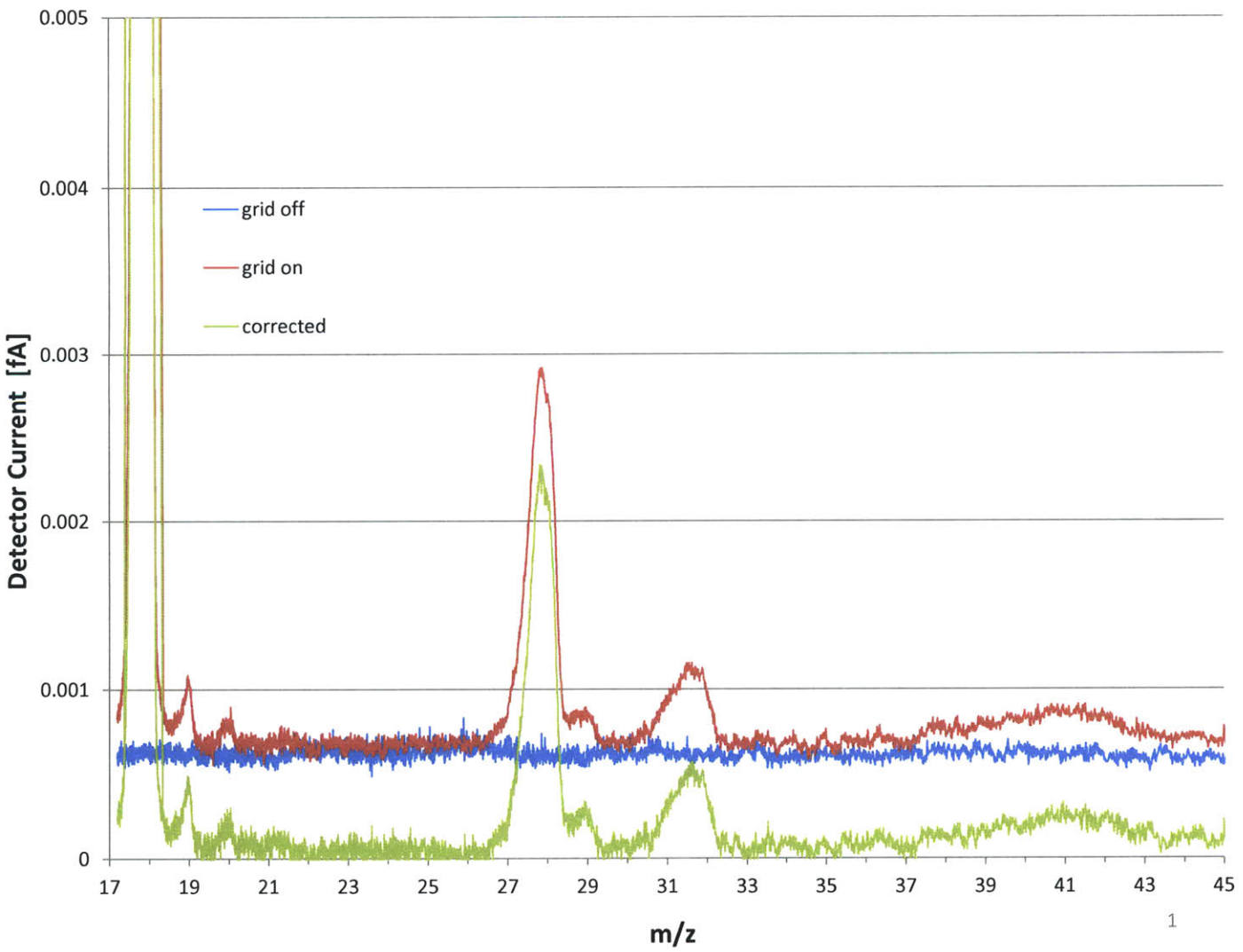


Figure 6-12: A mass spectrum indicating the usefulness of a modulatable grid. In this spectrum, the mass spectrometer's ion source grid was used to generate a trace that could be subtracted from the signal to remove the electrometer offset and drift.

6.9 Results

From the data presented, it is clear that the mass spectrometer works, and that the resolution is sufficient for many tasks. The noise floor is extremely low, below 10 fA, as indicated on the graph in Figure 6-8. Deconvolution with an appropriate function would yield even narrower spectra, however, it is always prudent to produce the best signal possible before relying on signal processing techniques.

THIS PAGE INTENTIONALLY LEFT BLANK

Chapter 7

Conclusions

A miniature mass spectrometer has been designed, constructed, and tested. The resolution and sensitivity of the mass spectrometer are high enough for this instrument to be useful as a medical, environmental, or industrial tool.

The mass spectrometer was designed specifically with low cost and manufacturability in mind. The mass spectrometer can be built with a combination of standard PCB fabrication and assembly for the electronics and substrate, as well as wire EDM for the electrodes, and the total bill of materials is on the order of \$1000.

While wire EDM may not be the most inexpensive machining process, all of the components of the mass spectrometer are symmetric through the vertical access and may be built, possibly with a change of materials, as an extrusion. The extrusion could then simply be chopped into segments, leading to a very economical method of construction.

All of the electrical components may be purchased from any major electronics distributor, and the tolerances of the printed circuit board design are low enough so that it can be built by any major PCB fabricator. Most printed circuit board assembly houses could subsequently fit the components to the board.

Experimental results indicate that the mass spectrometer is sensitive enough to detect species comprising less than 0.5% of the inlet sample gas, and with a mass resolution of 1 AMU.

The design proves that it is feasible to cofabricate an onboard ion pump, using

the same magnetic circuit used in the mass analyzer.

The software reconfigurability makes the instrument extremely versatile.

7.1 Further Work

This mass spectrometer is by no means a finished product; it is the prototype that verifies the concept. The design can be vastly improved from this point forward.

The electronics can be updated and simplified, probably by switching to a different method of measuring the high voltage biased parameters (e.g. filament current, trap current). Tighter tolerances on the closed loop feedback control systems for the electrode drivers would allow less variation in individual units and less customization of the software on each unit.

From here, there are even more exciting possibilities.

An innovation that was dropped early on in favor of getting the instrument as a whole online could be added; a four or five stage discrete-dynode electron multiplier, appropriately placed, could give a signal to noise ratio boost of just over 16 - 32, while the low dynode count would minimize the dark current.

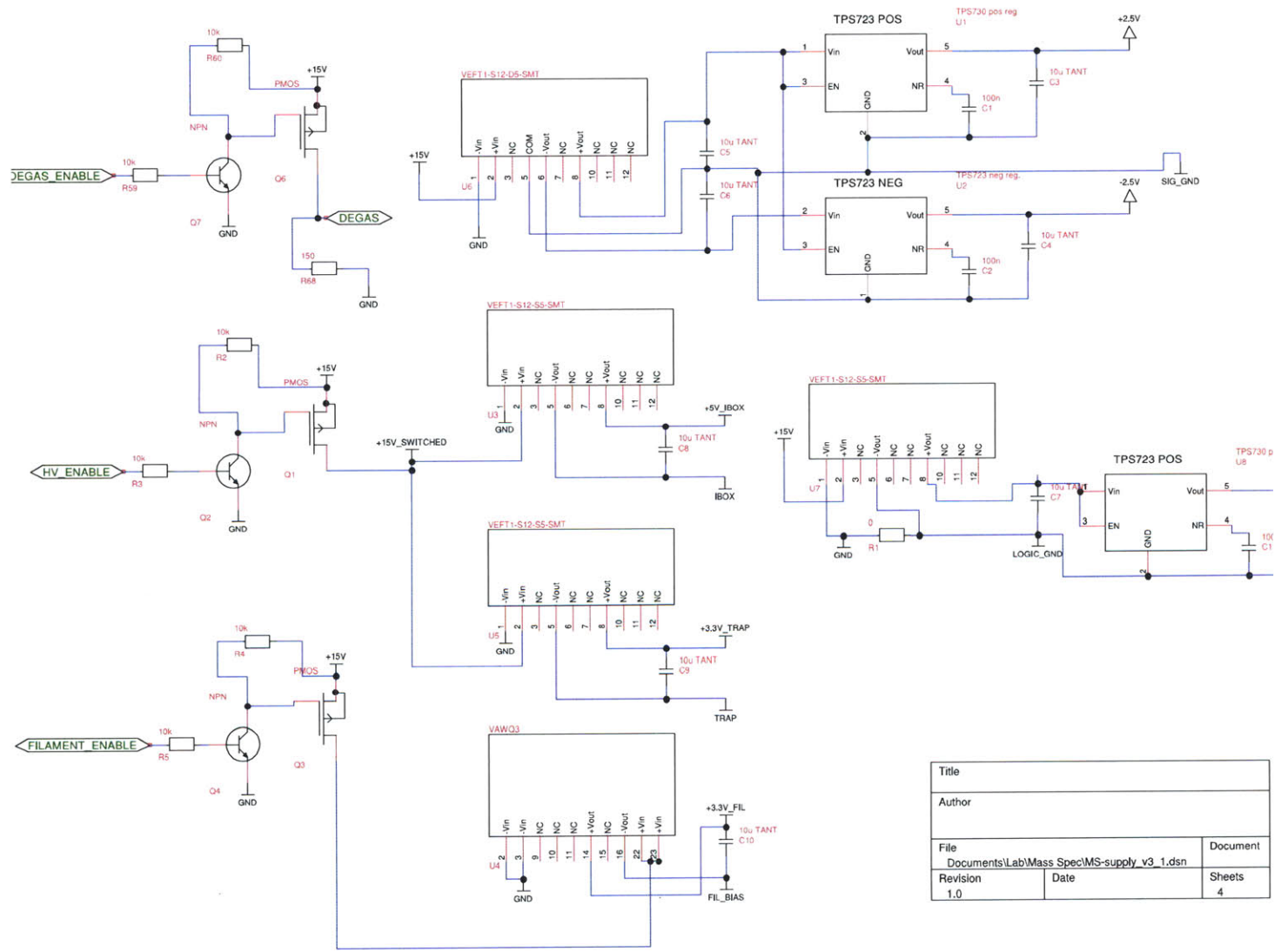
The upper and lower mass analyzer PCBs could be easily modified to include an electric sector, changing the overall mass spectrometer topology to that of a Niel-Johnson double-focusing mass spectrometer, possibly more than doubling the mass resolution.

A stronger magnetic field, possibly employing a more expensive vanadium permendur yoke or possibly a Hallbach array of neodymium-iron-boron magnets would increase the resolution at low masses, while the higher voltages already achievable with the existing design would preserve the upper, light mass resolution.

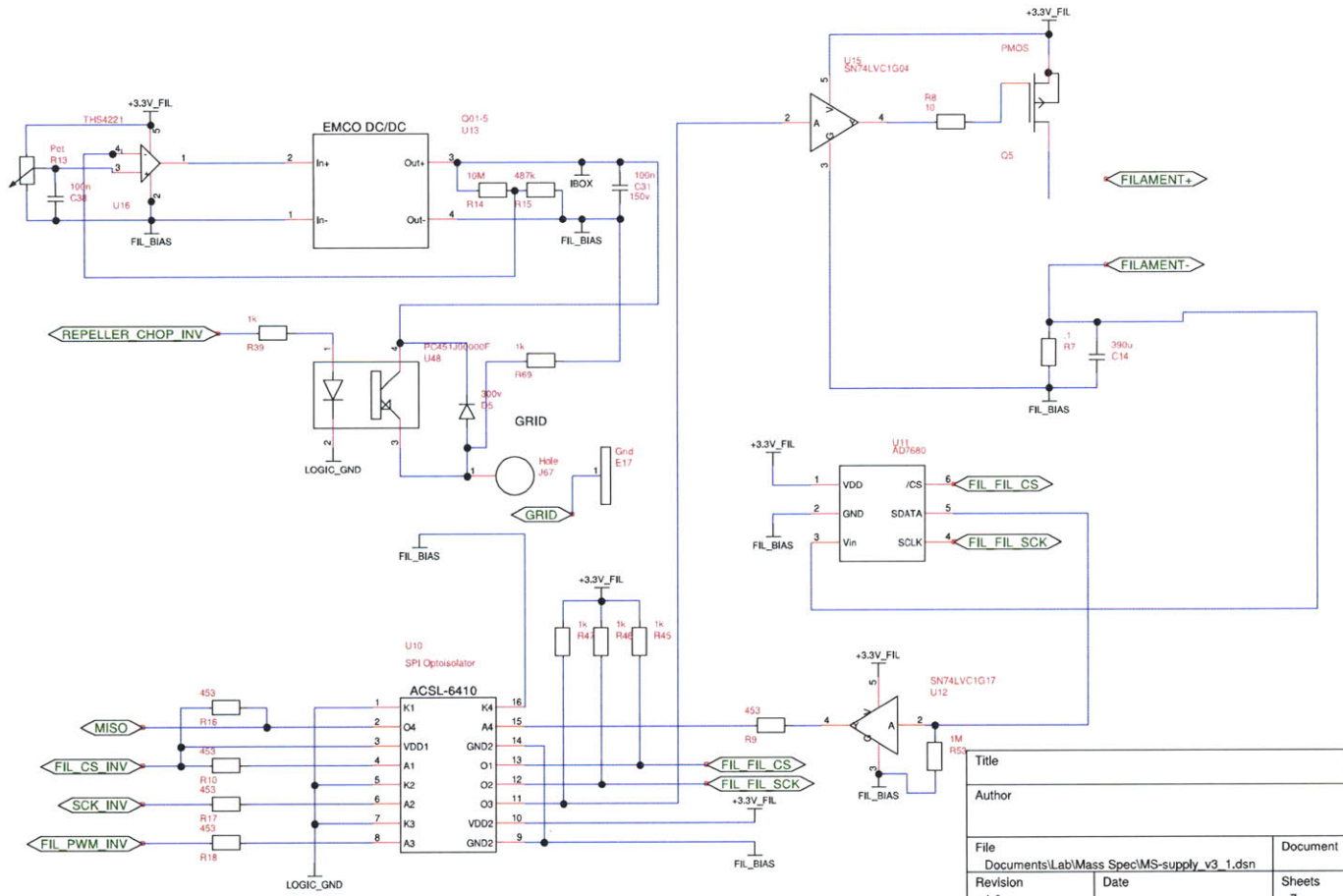
All of these improvements, however, are beyond the time available and scope for this doctoral thesis.

Appendix A

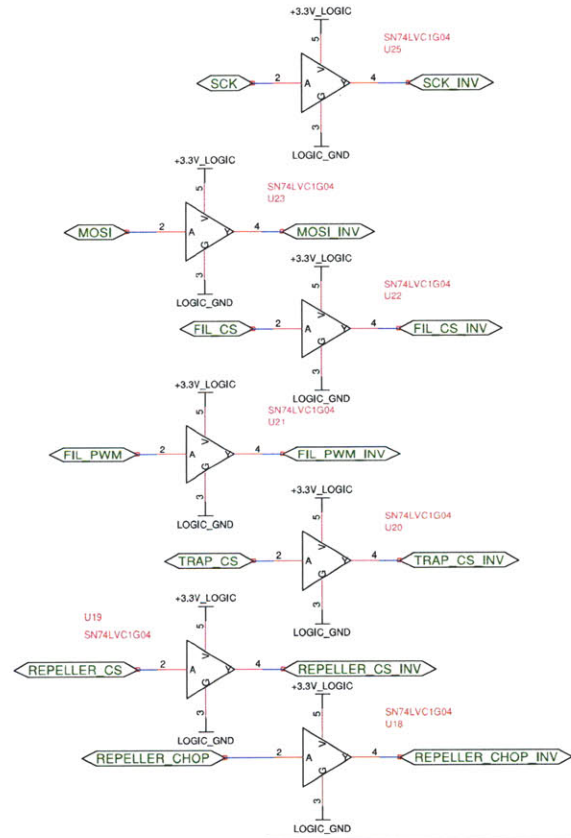
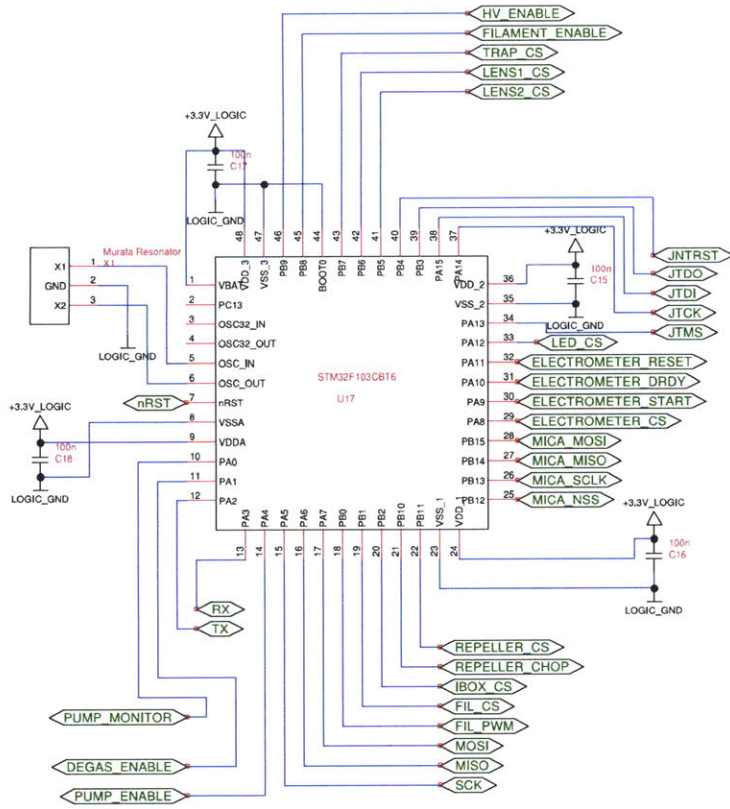
Controller Schematic



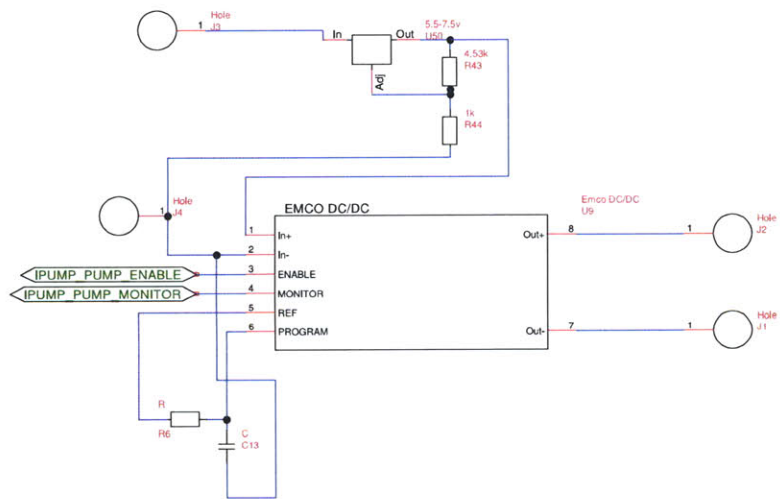
Title		
Author		
File	Documents/Lab/Mass Spec/MS-supply_v3_1.dsn	
Revision	Date	Document
1.0		Sheets 4



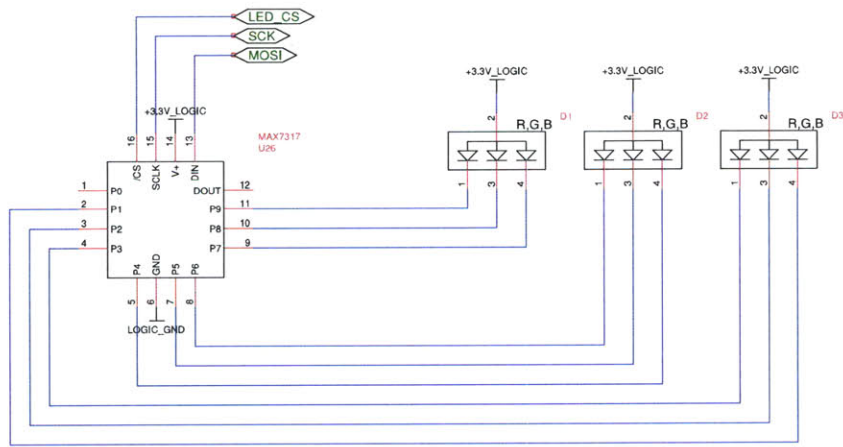
Title		
Author		
File	Documents\Lab\Mass Spec\MS-supply_v3_1.dsn	
Revision	Date	Sheets
1.0		7



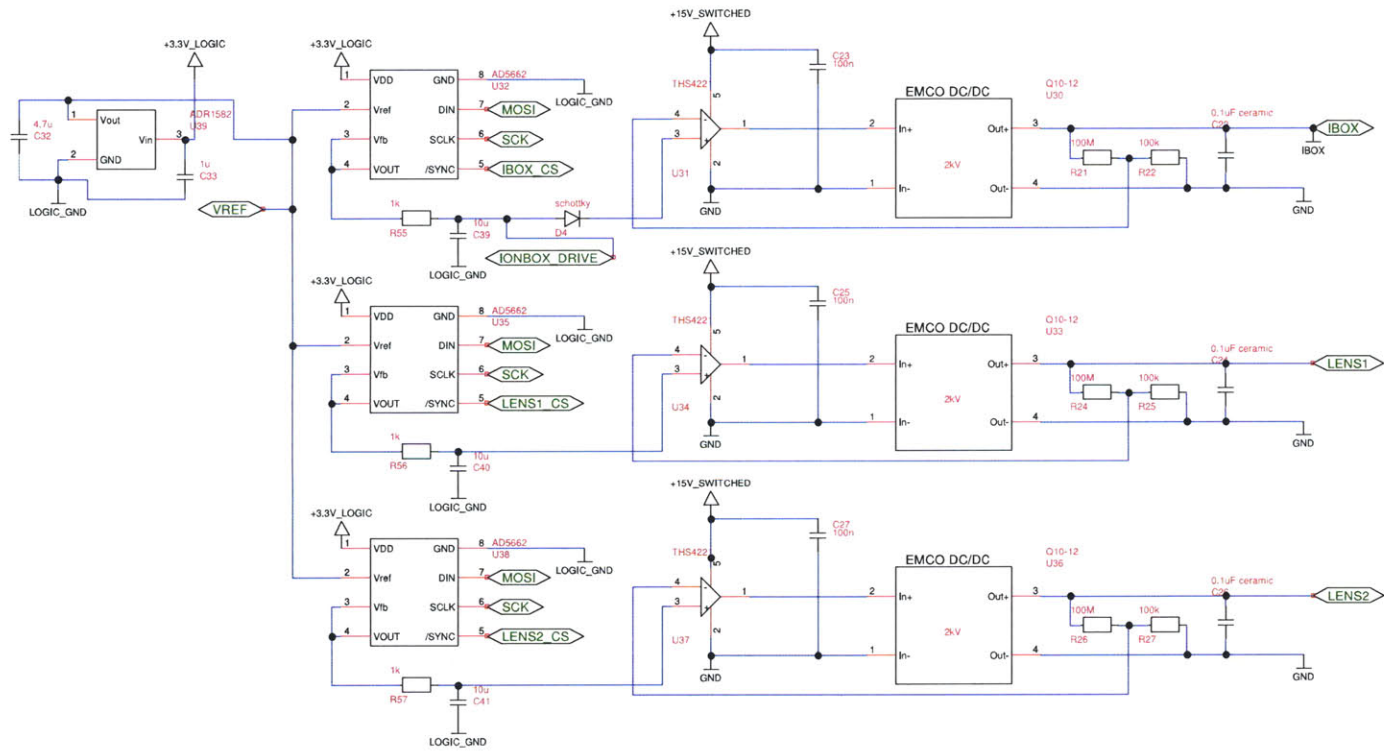
Title		
Author		
File	Document	
D:\My Documents\Lab\Mass Spec\sch-mcu.dsn		
Revision	Date	Sheets
1.0		6



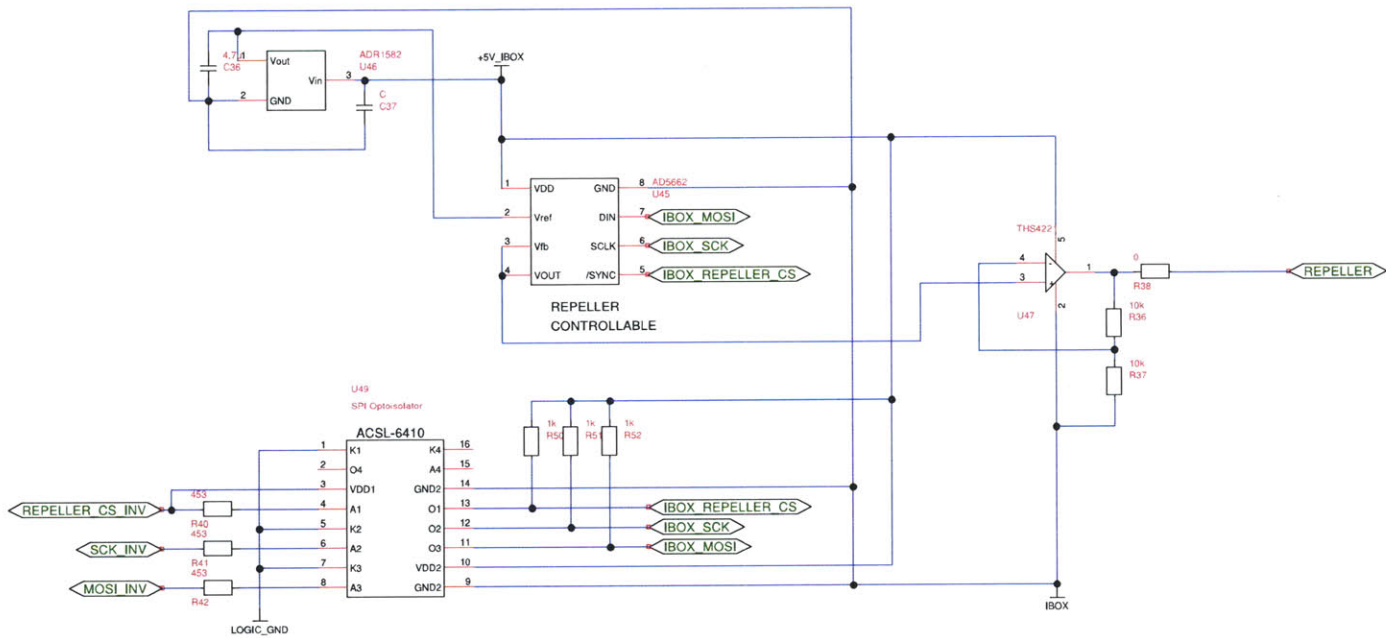
Title		
Author		
File Documents\Lab\Mass Spec\MS-supply_v3_1.dsn		Document
Revision 1.0	Date	Sheets 11



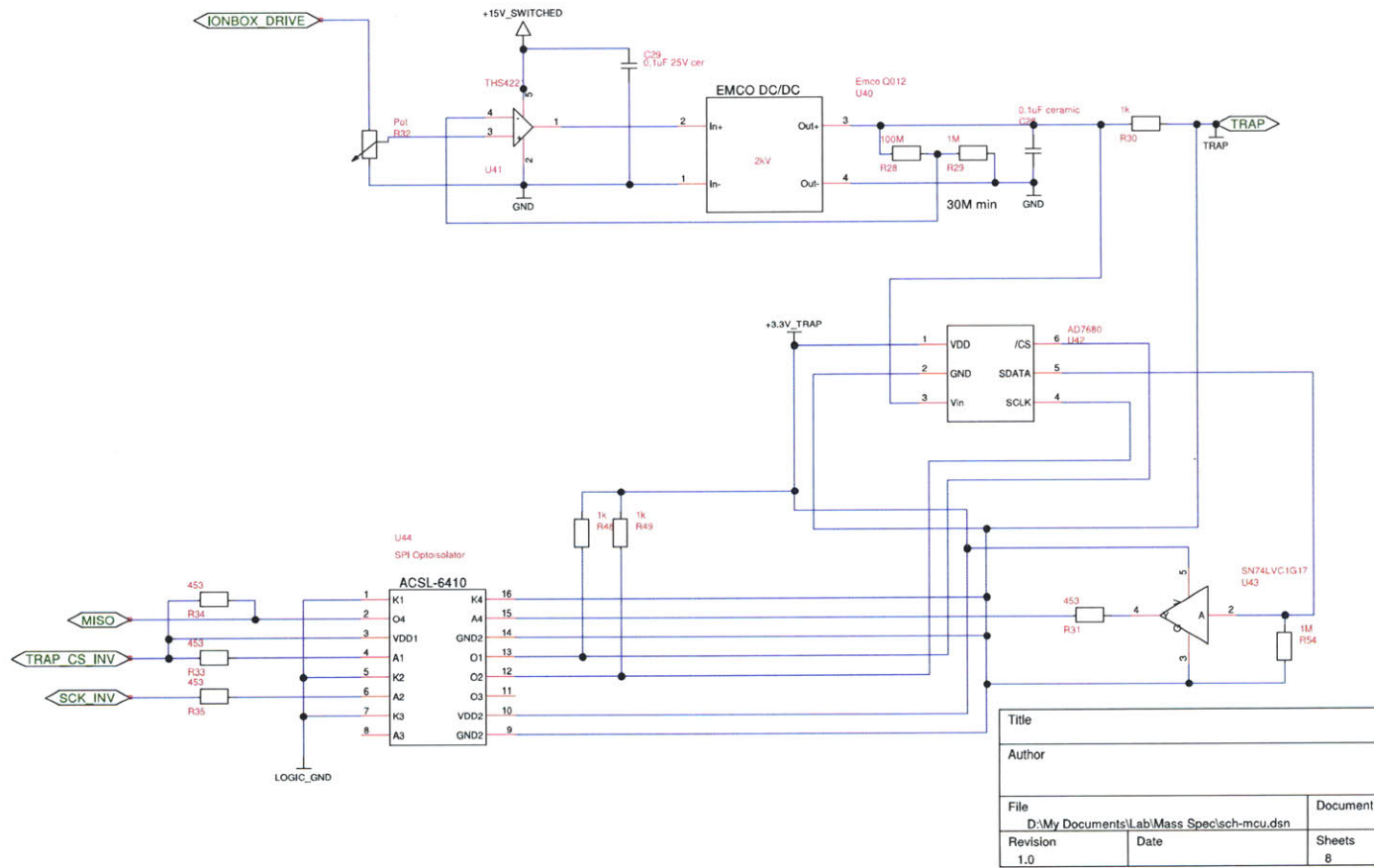
Title		
Author		
File D:\My Documents\Lab\Mass Spec\sch-mcu.dsn		Document
Revision 1.0	Date	Sheets 10



Title		
Author		
File D:\My Documents\Lab\Mass Spec\sch-mcu.dsn		Document
Revision 1.0	Date	Sheets 7

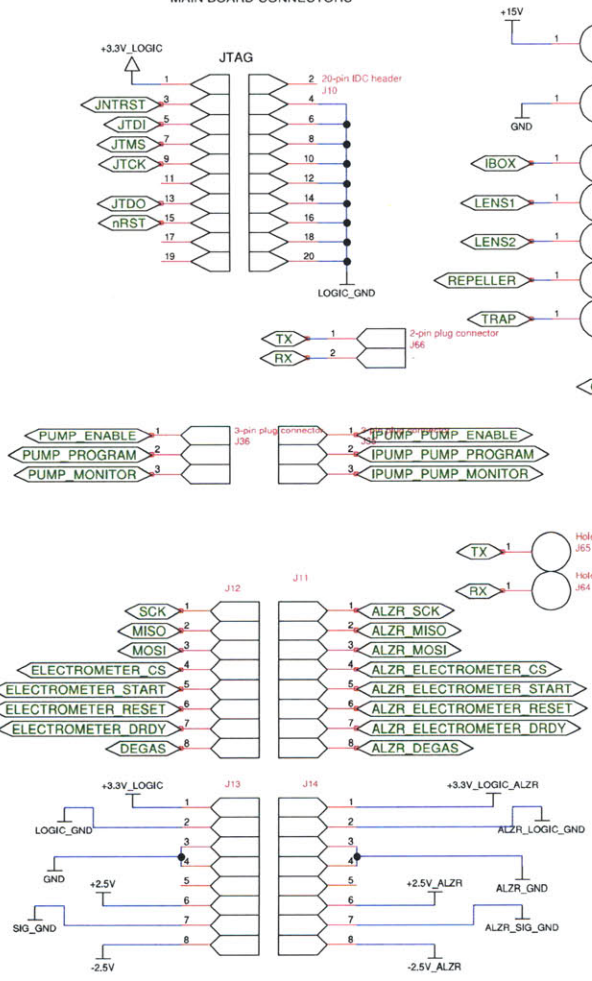


Title		
Author		
File	Document	
D:\My Documents\Lab\Mass Spec\sch-mcu.dsn		
Revision	Date	Sheets
1.0		9

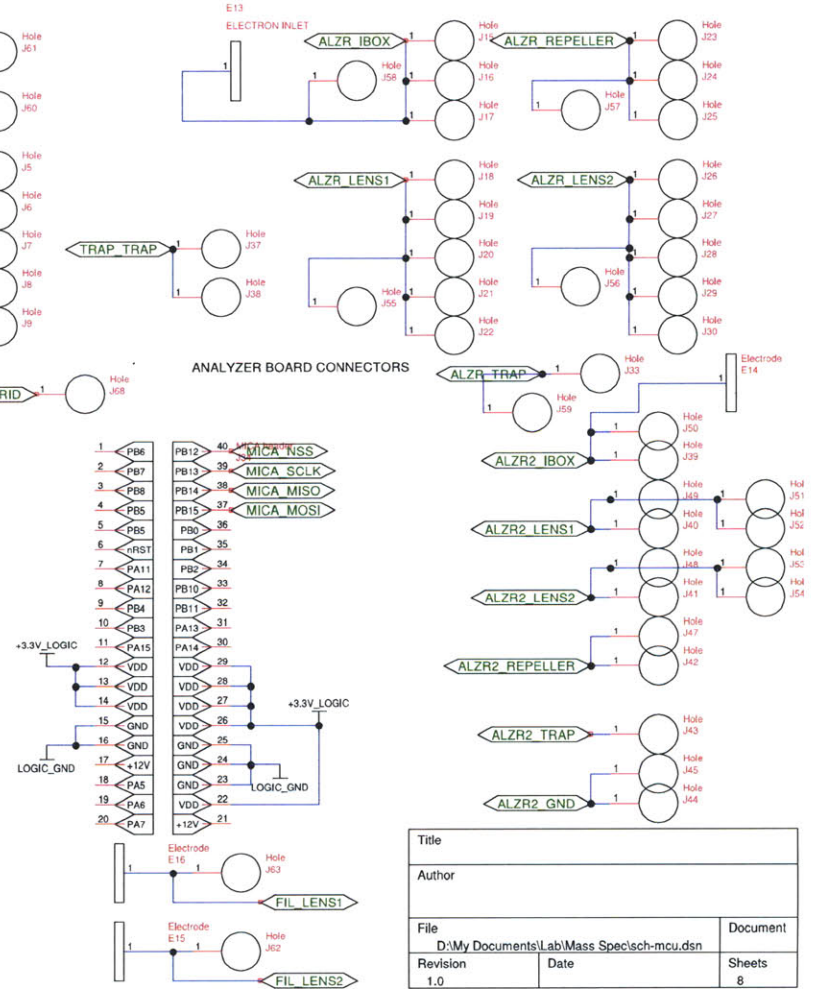


Title		
Author		
File D:\My Documents\Lab\Mass Spec\sch-mcu.dsn		Document
Revision 1.0	Date	Sheets 8

MAIN BOARD CONNECTORS



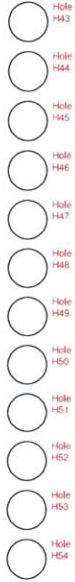
ANALYZER BOARD CONNECTORS



Title		
Author		
File	Document	
D:\My Documents\Lab\Mass Spec\sch-mcu.dsn		
Revision	Date	Sheets
1.0		8

Power Analyzer Standoff

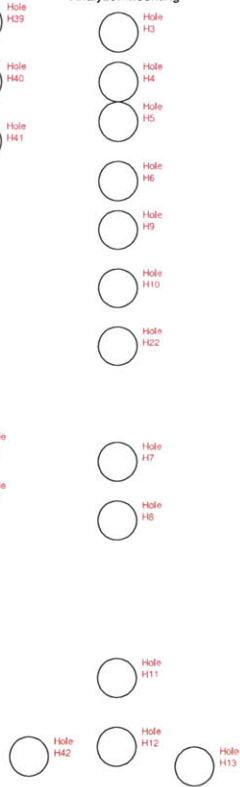
Ion Pump Mount



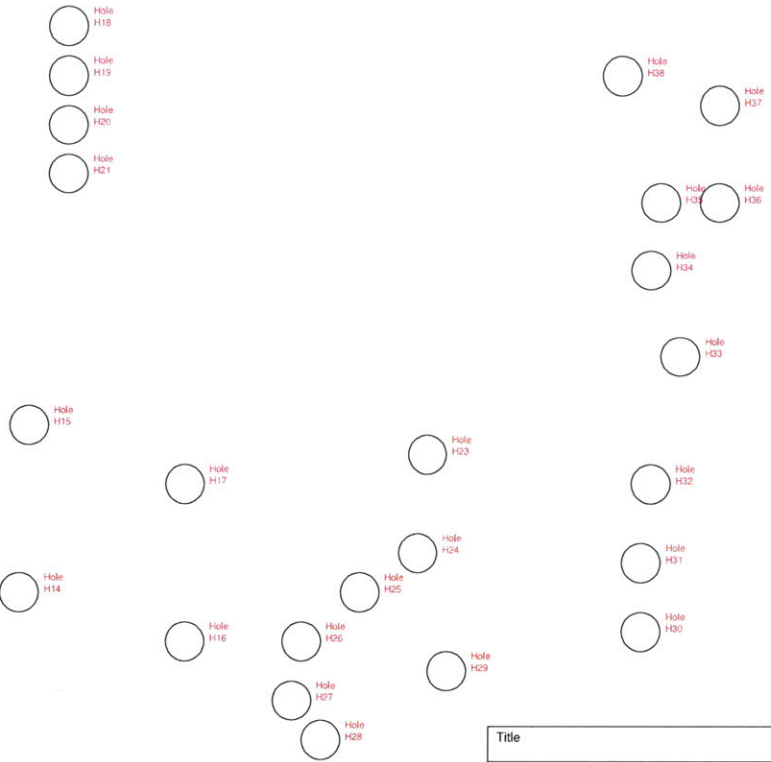
Magnet Mount



Analyzer Mounting



Top Access Holes



Title		
Author		
File D:\My Documents\Lab\Mass Spec\sch-mcu.dsn		Document
Revision 1.0	Date	Sheets 9

THIS PAGE INTENTIONALLY LEFT BLANK

Bibliography

- [1] N. A. Holmberg, "Nasa reference publication 1027: Viking '75 spacecraft design and test summary. volume 1 - lander design," 1980.
- [2] H. B. Niemann, "The gas chromatograph mass spectrometer experiment on the cassini-huygens probe," 2010.
- [3] J.S.Vogel, N. Palmblad, T. Ognibene, M. Kabir, B. Buchholz, and G. Bench, *Biochemical paths in humans and cells: Frontiers of AMS bioanalysis*, vol. 259, 2007.
- [4] W. H. Griest, M. B. Wise, K. J. Hart, S. A. Lammert, C. V. Thompson, and A. A. Vass, "Biological agent detection and identification by the block ii chemical biological mass spectrometer," *Field Analytical Chemistry and Technology*, vol. 5, no. 4, pp. 177–184, 2001.
- [5] R. Camilli, C. M. Reddy, D. R. Yoerger, B. A. S. V. Mooy, M. V. Jakuba, J. C. Kinsey, C. P. McIntyre, S. P. Sylva, and J. V. Maloney, "Tracking hydrocarbon plume transport and biodegradation at deepwater horizon," *Science*, vol. 330, no. 6001, pp. 201–204, 2010.
- [6] W. Potter, "Mass spectrometry for innovative techniques of respirator care, ventilator weaning and differential ventilation in an intensive care unit.," *Critical Care Medicine*, vol. 4, no. 5, pp. 235–238, 1976.
- [7] G. Huang, L. Gao, J. Duncan, J. D. Harper, N. L. Sanders, Z. Ouyang, and R. G. Cooks, "Direct detection of benzene, toluene and ethylbenzene at trace levels in ambient air by atmospheric pressure chemical ionization using a handheld mass spectrometer," *Journal of the American Society of Mass Spectrometry*, vol. 21, pp. 132–135, 2010.
- [8] A. Malcolm, S. Wright, R. R. A. Syms, N. Dash, M.-A. Schwab, and A. Finlay, "Miniature mass spectrometer systems based on a microengineered quadrupole filter," *Analytical Chemistry*, vol. 82, no. 5, pp. 1751–1758, 2010.
- [9] E. de Hoffman and V. Stroobant, *Mass Spectrometry, Principles and Applications, 3rd ed.* Wiley and Sons, 2007.
- [10] J. H. Moore, C. C. Davis, and M. A. Coplan, *Building Scientific Apparatus.* Addison-Wesley, 1983.

- [11] E. Lassner and W.-D. Schubert, *Tungsten: Properties, Chemistry, Technology of the Element, Alloys, and Chemical Compounds*. Kluwer Academic / Plenum Publishers, 1999.
- [12] M.I.T. Research Laboratory of Electronics, "Tube laboratory manual." MIT Libraries, Cambridge, Mass, 1951.
- [13] D. S. Corp., "Ion pumps-operation and applications," 2006.
- [14] S. L. Rutherford, "Miniature sputter-ion pump design considerations," *1999 NASA/JPL Miniature Vacuum Pumps Workshop - July 20-21, 1999*, 1999.
- [15] M. Audi and M. de Simon, "Ion pumps," *Vacuum*, vol. 37, no. 8, pp. 629–636, 1987.
- [16] M. Audi, "Pumping speed of sputter ion pumps," *Vacuum*, vol. 38, no. 8, pp. 669–671, 1987.
- [17] M. Malev and E. Trachtenberg, "Built-in getter-ion pumps," 1973.
- [18] D. Manura and D. Dahl, "Simion (r) 8.0 user manual." Scientific Instrument Services, Inc., Ringoes, NJ 08551, 2008.